

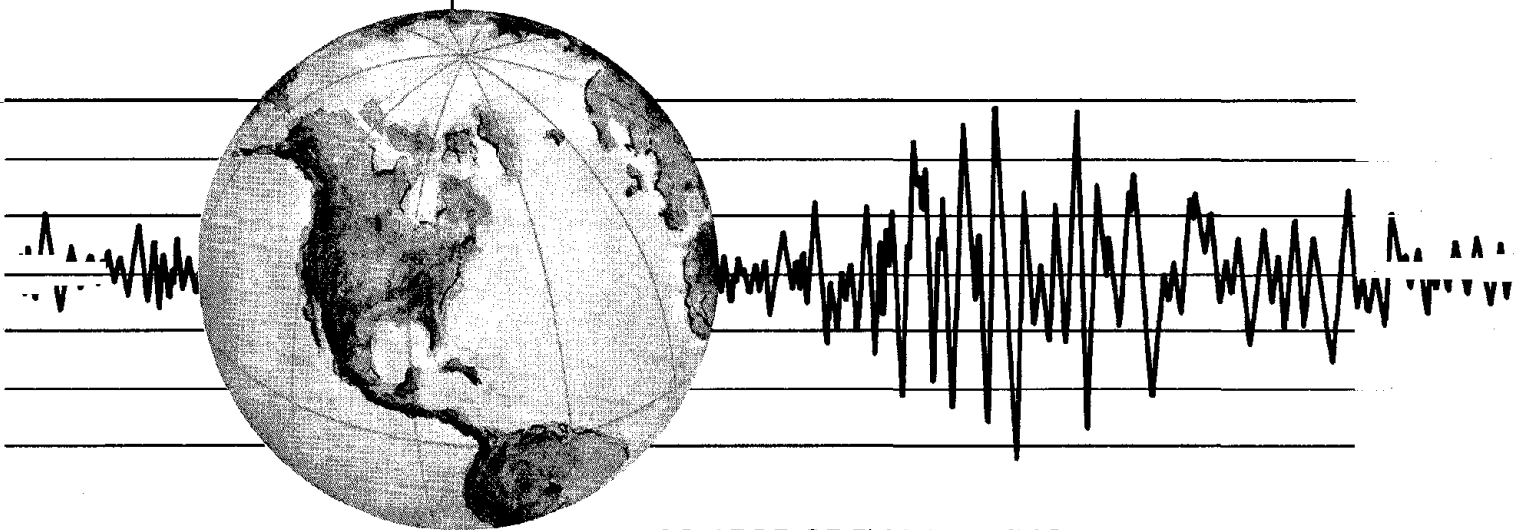
REPORT NO.
UCB/EERC-78/16
SEPTEMBER 1978

EARTHQUAKE ENGINEERING RESEARCH CENTER

SEISMIC RISK STUDIES FOR SAN FRANCISCO AND FOR THE GREATER SAN FRANCISCO BAY AREA

by
CARLOS S. OLIVEIRA

Report to National Science Foundation



COLLEGE OF ENGINEERING

UNIVERSITY OF CALIFORNIA · Berkeley, California

REPRODUCED BY
NATIONAL TECHNICAL
INFORMATION SERVICE
U.S. DEPARTMENT OF COMMERCE
SPRINGFIELD, VA 22161

REPORT DOCUMENTATION PAGE		1. REPORT NO. NSF/RA-780765	2.	3. Recipient's Accession No. PBM 120115	
4. Title and Subtitle Seismic Risk Studies for San Francisco and for the Greater San Francisco Bay Area				5. Report Date September 1978	
7. Author(s) Carlos S. Oliveira				6.	
9. Performing Organization Name and Address Earthquake Engineering Research Center University of California, Richmond Field Station 47th and Hoffman Blvd. Richmond, California 94804				8. Performing Organization Rept. No. UCB/EERC-78/16	
12. Sponsoring Organization Name and Address National Science Foundation 1800 G Street, N.W. Washington, D.C. 20550				10. Project/Task/Work Unit No.	
15. Supplementary Notes				11. Contract(C) or Grant(G) No. (C) (G) ENV77-20667	
16. Abstract (Limit: 200 words) Three aspects of seismic risk for the greater San Francisco Bay Area are considered here: First, an evaluation of the overall properties of parameters characterizing the seismicity of the San Francisco region; secondly, an evaluation of methods for computing seismic hazard at a site; and finally, an evaluation of seismic risk in terms of population exposure. For the first item, available data concerning (i) geotectonic evolution during the last twenty million years, (ii) historical seismicity of the Bay Area, and (iii) characterization of earthquake mechanisms, of propagation of seismic waves and of geological features to obtain a four-dimensional space-time-energy-source continuum model, are studied thoroughly Then, for the second item, a review is given of mathematical modelling proposed by different authors to obtain probability distribution functions for the site parameters. Distributions of peak ground motion parameters, such as acceleration, velocity and displacement as well as duration, are obtained for a point-source and for a line-source model using either an experimental method or an analytical method. Emphasis is given to a two-parameter source model (magnitude and stress drop), to the direct development of seismic hazard in terms of response spectra, and to a joint probability distribution function of duration and one peak ground motion parameter. The influence of some uncertainties on the final probability distributions is analyzed. Finally, overall seismic risk for the Bay Area is briefly characterized by including the interaction between seismic action and the geographic location of population. Spatial correlation with earthquake action is taken into consideration in developing a probability distribution for the number of people affected by a given level of seismic acceleration.				13. Type of Report & Period Covered	
18. Availability Statement: Release Unlimited				14.	
19. Security Class (This Report)			21. No. of Pages 138		
20. Security Class (This Page)			22. Price		

SEISMIC RISK STUDIES FOR SAN FRANCISCO AND FOR THE GREATER
SAN FRANCISCO BAY AREA

by

Carlos S. Oliveira

Visiting Assistant Research Engineer
University of California, Berkeley
and
Research Engineer
Laboratório Nacional de Engenharia Civil,
Lisboa, Portugal

Report to
National Science Foundation

Report No. UCB/EERC-78/16
Earthquake Engineering Research Center
College of Engineering
University of California
Berkeley, California

September, 1978

ABSTRACT

Three aspects of seismic risk for the greater San Francisco Bay Area are considered here: First, an evaluation of the overall properties of parameters characterizing the seismicity of the San Francisco region; secondly, an evaluation of methods for computing seismic hazard at a site; and finally, an evaluation of seismic risk in terms of population exposure.

For the first item, available data concerning (i) geotectonic evolution during the last twenty million years, (ii) historical seismicity of the Bay Area, and (iii) characterization of earthquake mechanisms, of propagation of seismic waves and of geological features to obtain a four-dimensional space-time-energy-source continuum model, are studied thoroughly.

Then, for the second item, a review is given of mathematical modelling proposed by different authors to obtain probability distribution functions for the site parameters. Distributions of peak ground motion parameters, such as acceleration, velocity and displacement as well as duration, are obtained for a point-source and for a line-source model using either an experimental method or an analytical method. Emphasis is given to a two-parameter source model (magnitude and stress drop), to the direct development of seismic hazard in terms of response spectra, and to a joint probability distribution function of duration and one peak ground motion parameter. The influence of some uncertainties on the final probability distributions is analyzed.

Finally, overall seismic risk for the Bay Area is briefly characterized by including the interaction between seismic action and the geographic location of population. Spatial correlation with earthquake action is taken into consideration in developing a probability distribution for the number of people affected by a given level of seismic acceleration.



ACKNOWLEDGMENTS

The work described herein was initiated during a two month study leave (October-December, 1976) at the Earthquake Engineering Research Center, under the sponsorship of the National Science Foundation. Professor Joseph Penzien acted as Principal Faculty Investigator.

My thanks to the Director of the Seismographic Station of the University of California, Berkeley, Dr. B.A. Bolt, who provided the seismicity data used in this work. The computer facilities at the Laboratório Nacional de Engenharia Civil-Lisboa, were used for the numerical computations.

I am deeply indebted to Dr. Beverley Bolt for her efforts in editing and supervising the final draft of this report. Ruth Horning typed the manuscript.

DISCLAIMER

The contents of this report reflect the views of the author but not necessarily those of the Earthquake Engineering Research Center, University of California, Berkeley and/or the Sponsor.

TABLE OF CONTENTS

	<u>Page</u>
ABSTRACT	i
ACKNOWLEDGMENTS	iii
DISCLAIMER	iii
TABLE OF CONTENTS	v
LIST OF TABLES	vii
LIST OF FIGURES	ix
NOTATION	xiii
1. INTRODUCTION	1
2. GEOLOGIC AND GEOTECTONIC FEATURES IN THE VICINITY OF SAN FRANCISCO	9
2.1 Generalities	9
2.2 Historical Evolution of Plate Configurations	9
2.3 Present Geotectonic Features	11
2.4 Geotectonic Interpretation using Earthquake Source Mechanisms	15
2.5 Influence of the Geology of the San Francisco Bay Area on Earthquake Wave Amplification	17
3. EXISTING DATA	27
3.1 Seismographic Network. Reliability of Data	27
3.2 Major Historical Shocks	29
3.3 Statistical Analysis of Data	29
3.3.1 On Spatial Location of Earthquakes	30
3.3.2 On Time of Occurrence	32
3.3.3 On Magnitude	37
3.3.4 On Elastodynamics of Earthquake Source Mechanism	40

	<u>Page</u>
3.3.5 On Wave Propagation	45
4. COMPUTER MODELLING FOR RISK ANALYSES	69
4.1 Seismic Hazard Analysis	69
4.1.1 Definition of Source Models	74
4.1.2 Further Studies on Uncertainties	75
4.1.3 Joint Densities of Peak Acceleration and Duration Research Needs	79
4.1.4 Comparison between Different Methods of Analysis of Seismic Hazard	81
4.2 Risk Analysis	83
4.2.1 Generalities	83
4.2.2 How to Handle the Problem	84
5. SEISMIC HAZARD ANALYSIS FOR A SITE IN DOWNTOWN SAN FRANCISCO .	91
5.1 Main Results	91
5.2 Comparison with Previous Works	95
6. POPULATION EXPOSURE TO SEISMIC HAZARD IN THE GREATER SAN FRANCISCO BAY AREA	105
7. CONCLUSIONS	111
REFERENCES	113

LIST OF TABLES

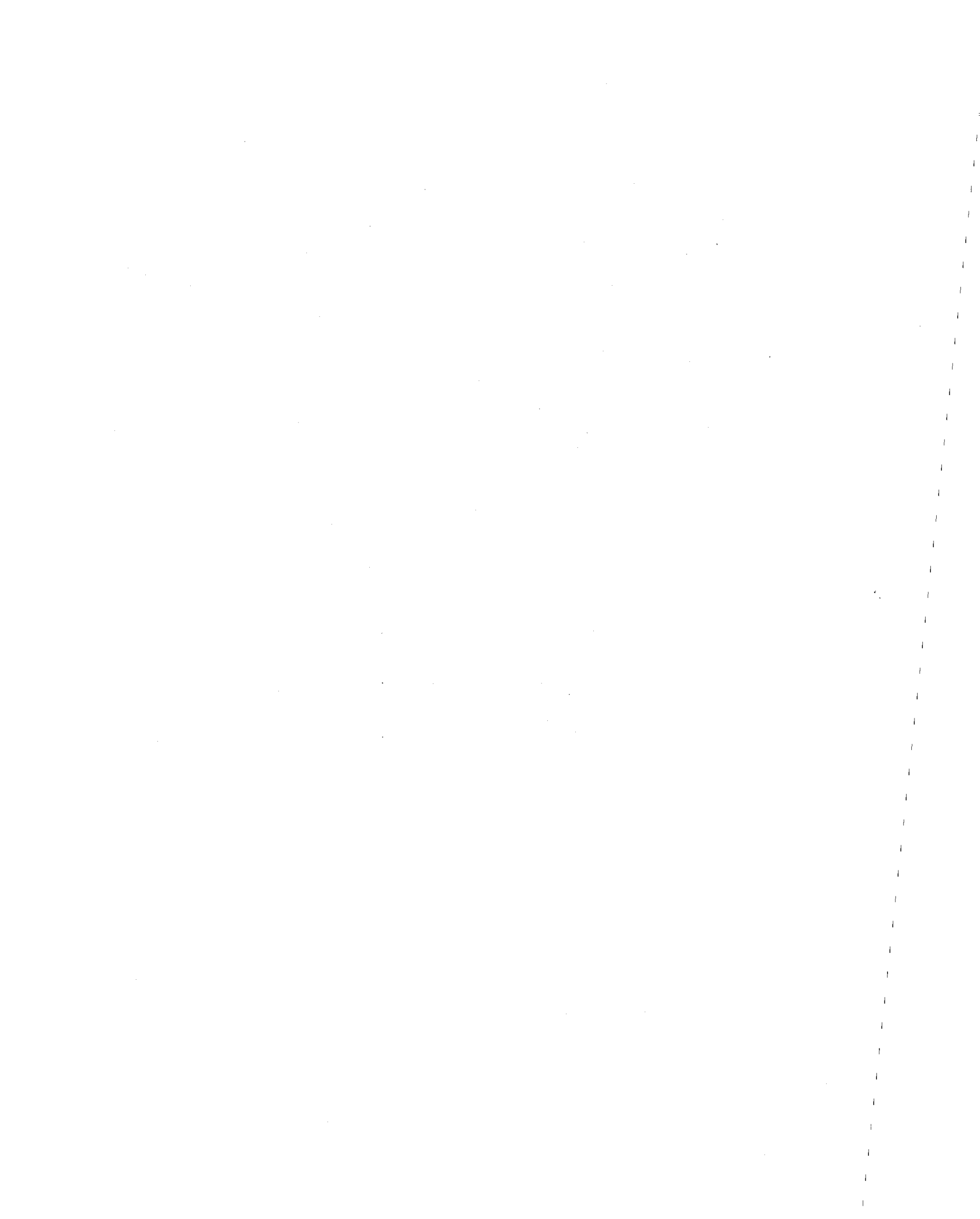
<u>Table</u>		<u>Page</u>
I	The Main Earthquakes Reported in the San Francisco Vicinity since 1800	1
II	Percentage Contribution of the Four Most Damaging Earthquakes to the Total Accumulated Damage in a 168-Year Period	2
III	Seismicity Parameters Suggested by Wallace (1970) for the San Francisco Area	15
IV	Stationarity of Earthquake Generation in Time	33
V	Seismic Characteristics of Earthquake Source-Areas	39
VI	Attenuation Formulae with Distance	49
VII	Sensitivity of Final Distribution to a 10% Change in Para- meters	72
VIII	Proposed Values for Seismic Hazard Parameters	94
IX	Résumé of Sensitivity Studies Analysed	110

LIST OF FIGURES

<u>Figure</u>	<u>Page</u>
1. Major Regional Geotectonic Structures Related to California Seismicity	7
2. Evolution of Plate Configuration in the Last 40 x 60 ⁶ Years.	19
3. San Andreas Fault System in the Vicinity of San Francisco. .	20
4. Earthquake Recurrence Intervals on the San Andreas Fault based on Strain Accumulation and Creep Measurements.	21
5. Crustal Model for the San Francisco Vicinity	22
6. Fault Plane Solutions in the Central Coast Ranges of California	22
7. General Geology of the San Francisco Bay Area.	23
8. Isoseismals Showing the Geographical Distribution of Damage.	24
9. U.S.G.S Strong Motion Accelerometer Recordings of Surface Accelerations at Four Different Sites During the 1957 San Francisco Earthquake	25
10. Number of Seismographic Stations Operating Since 1887 . . .	51
11(a). Map of Epicenters for the San Francisco Region of Earthquakes with $M > 4$ for the Period 1807-1969.	52
11(b). Map of Epicenters for Northern California for all Earthquakes Felt in the Decade 1960-1969	53
11(c). Microearthquakes Recorded During 1970.	54
12. Statistical Analysis of Focal Depths	55
13. Earthquake Source Areas.	56
14. Historical Data of Recorded Earthquakes Within 100 km of San Francisco	57
15. Testing the Poisson Model for Time Events.	58

<u>Figure</u>	<u>Page</u>
16. Testing the Time Interval between Consecutive Events for the Periods 1934-1973 and 1850-1933	59
17. Interpretation for the Time Interval between Consecutive Events	60
18. Hazard Function for the Gamma and Weibull Distributions ($\lambda=1$)	60
19. Values of the Poisson Dispersion Coefficient (Variance/ Mean) as a Function of Increasing Time Interval	61
20. Probability Distributions of Magnitude.	62
21. Probability Distribution of b/b_0	63
22. Earthquake Elastodynamic Model of Fault Mechanism	64
23. Interrelations among the Five Most Important Parameters Characterizing the Elastodynamics of Earthquake Generation.	65
24. Two Parameter Model for the Mechanism of Earthquake Genera- tion at the Source	66
25. Comparison between Different Attenuation Formulae	67
26. Significant Duration of Ground Motion as a Function of Dis- tance to Source, Site Conditions and Magnitude for the Bay Area	68
27. Sketch for Line-Source Model	87
28. Linear Earthquake Source Zone. Correction to Account for the Line-Source Model	87
29. Comparison between the Markov, Poisson and Gamma Models of Time Generation	88
30. Correlation between Peak Ground Acceleration and Duration of Motion	89

<u>Figure</u>	<u>Page</u>
31. Location of a Single Rectangular Source Representing Bay Area Conditions with Normal Distribution of Epicenters in the Transverse Direction	96
32(a). Annual Probability Distribution of Duration using the Experimental Method with a Point-Source Generating Process .	96
32(b). Annual Probability Distributions of Ground Motion Parameters using the Experimental Method for the Period 1800-1973 . . .	97
33. Influence of Sampling Interval for the Point-Source Model using the Experimental Method	98
34. Comparison between Experimental and Analytic Models	99
35. Sensitivity Studies of the Influence of Uncertainties . . .	100
36. Annual Probability Distribution Function for Response Spectra ($T_0 = 0.1$ sec, $\eta = 5\%$)	101
37. Seismic Hazard Analysis in Terms of Response Spectra for 10, 100 and 1000 years mean return periods	102
38. Maximum Accelerations Expected along a Transverse Profile to the San Andreas Fault, for 100 and 1000 year mean return periods	102
39. Proposed Annual Probability Distribution Function of Peak Acceleration for San Francisco	103
40(a). Boundaries of the Area Studied for Population Exposure . . .	107
40(b). Population Distribution for the Study Case	108
41. Probability Distribution Function of People Experiencing the Threat of Peak Accelerations Greater than a_{\max} during a Reference Time Interval $T_r = 10$ years	109



NOTATION

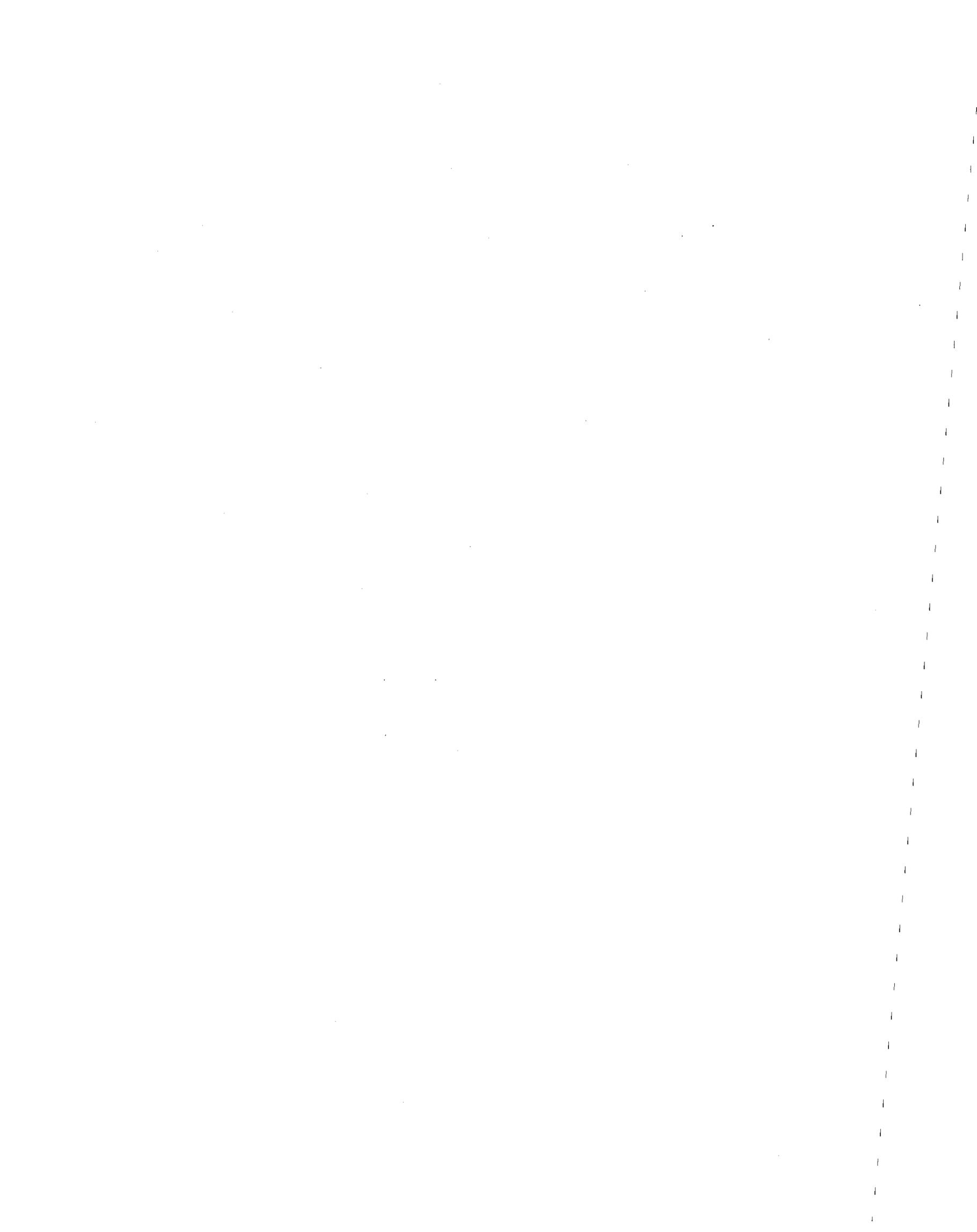
M, m	Richter magnitude
m_s	surface wave magnitude
I_o	maximum Modified Mercalli Intensity
MM	Modified Mercalli Intensity
h	focal depth
m_o	lower magnitude threshold
m_1	upper magnitude
R	hypocentral distance
T	waiting time between consecutive events-interarrival time
T_1	waiting time of first passage
E_T	expected value of random variable T
σ_T^2	variance of random variable T
r.v.	random variable
M, m	random variable M with argument m
$f_M(m)$	probability density function of M
$F_M(m)$	probability distribution function of M
$G_M(m)$	probability distribution function of extreme values of M
pdf	probability density function
cdf	cumulative probability distribution function
$h(t)$	hazard function
N_m, λ	number of earthquakes with magnitude $\geq m$
α, β	parameters of the Richter law of magnitude
r	equivalent source dimension connected to the earthquake or source dimension connected to the earthquake mechanism
L	fault length
w	fault width
\bar{D}	fault offset
s	fault area

Notation - continued

$A(f)$	source excitation-Fourier amplitude spectra of ground acceleration
$\Omega(f)$	displacement amplitude spectrum
f	frequency (in Hertz)
ω	circular frequency (in rad sec^{-1})
f_c	corner frequency
M_0	seismic moment
μ	shear modulus
$1/Q$	specific attenuation
$R_{\theta\phi}$	radiation pattern
$\Delta\sigma$	static stress drop
Y, y	maximum acceleration, velocity or displacement of earthquake ground motion
ϵ	random error in attenuation
s	duration of ground motion
a_{max}	peak ground acceleration
v_{max}	peak ground velocity
d_{max}	peak ground displacement
S_v	pseudo-spectral response
ξ	damping ratio
T_p	predominant period of ground motion
SHA	seismic hazard analysis
SRA	seismic risk analysis
$\Phi(\cdot) \equiv \text{erf}(\cdot)$	cumulative distribution function of the standardized Gaussian distribution
$\Phi^*(\cdot) = \text{erfc}(\cdot)$	complementary distribution function of the standardized Gaussian distribution
PGA	peak ground acceleration

Notation - continued

d	epicentral distance
P_Y, ν	mean number of occurrences of the Poisson Process $Y(t)$
T_r	reference time-interval
AD	accumulative damage



1. INTRODUCTION

The San Francisco Bay Area has a high degree of earthquake threat. During the last two centuries there have been some large earthquakes in the area; Table I summarizes the most important events that occurred in that period of time. The total material losses since 1865 add to more than 500 million dollars, and more than 700 lives have been lost. It has been estimated that a major earthquake nowadays in San Francisco could cause property losses of approximately 50 billion dollars (Borcherdt, 1975).

TABLE I

The Main Earthquakes Reported in the San Francisco Vicinity since 1800.

Year	Location	\$ Loss at the time of the earthquake	Lives Lost
1836	San Francisco Bay		
1838	San Francisco		
1865	San Francisco	500,000	0
1868	Hayward	350,000	30
1898	Man Island	1,400,000	0
1906	San Francisco	500,000,000	700
1955	Oakland	1,000,000	1
1957	San Francisco	1,000,000	0
	TOTAL	\$ 504,250,000	731

Damage from these earthquakes was spread not only throughout the city of San Francisco but also in metropolitan San Francisco. Table II presents the contributions of the four most damaging earthquakes to the total accumulated damage from all earthquakes in the 168-year period, considering separately the city and metropolitan San Francisco (Friedman, 1975).

TABLE II

Percentage Contribution of the Four Most Damaging Earthquakes to the Total Accumulated Damage in a 168-Year Period

Earthquake	City of San Francisco	Metropolitan San Francisco
1836, San Francisco Bay	6%	13%
1838, San Francisco	24%	21%
1868, Hayward	12%	17%
1906, San Francisco	44%	33%
TOTAL	86%	84%

With this seismic history it would be of interest to be able to quantify the parameters of future seismic activity in terms of location of focus, origin time and size of the earthquake.

Seismic risk* studies are the fundamental tools needed to analyze the effects of earthquakes on buildings and over metropolitan areas. The object of analysis could be a single structure, a group of structures, a

* The difference between seismic risk and seismic hazard analyses is discussed in Chapter 4.

lifeline, a large housing project. The input to the study is the set of seismic parameters characterizing the seismicity of the area surrounding the object, the geometry of the object and its intrinsic seismic resistance. The output of the study depends on the problem. For point objects, the output is, in general, the maximum acceleration or the maximum velocity expected during a reference time-interval while for line objects or area objects it is the maximum loss or the number of people that can collectively suffer from earthquake activity.

Research in prediction of earthquakes has increased in the last decade but there is still not a practical method of prediction. When this becomes a reality it will be possible to control injury to human life from earthquakes, and to reduce other losses. However, material losses will not be avoided for buildings and the design of structures to withstand seismic loads will still be necessary.

The great variability in the characteristics of ground motion and the uncertainty in assessing expected intensity levels during a given interval of time justify the use of the probabilistic model in the seismic formulation.

Different levels of risk are considered for the design of different types of structures. Structures which require a high safety standard are usually designed to withstand seismic actions with very low probabilities of occurrence (Prob $< 10^{-8}$). Modern structures should be designed to meet the following two basic requirements:

a) The structure should perform during a moderate earthquake in such a way as to minimize total inflicted costs (initial + repair + maintenance) (Prob $< 2 \times 10^{-2}$).

b) The structure should not collapse during a major to catastrophic earthquake (Prob $< 10^{-2}$ to 10^{-3}).

In this study, probability distributions will be considered for given seismic parameters during a reference time interval, using all available information concerning (i) the geotectonic evolution during the last one million years, (ii) the historical seismicity of the Bay Area Region and (III) studies on the characterization of earthquake mechanisms, propagation of seismic waves and geological features. The full characterization of earthquake threat involves a knowledge of earthquake action at any single site and the quantification of overall risk for the entire region. In other words, the probability distributions for a group of sites or for an area should be examined as well as the probability distributions for a single site.

Not many studies on seismic risk for San Francisco and for the Greater San Francisco Bay Area have been made. Studies concerning the former include the following:

Dalal (1972) used a Poisson model to represent the spatial distribution and time sequence of earthquake occurrence.

Vagliente (1973) used a Markov chain model for the occurrence of earthquakes after analyzing the phenomenon of "elastic rebound theory".

Kiremidjian and Shah (1975) studied the seismic risk of California and the influence of uncertainties in some parameters.

Kiureghian and Ang (1975) used San Francisco in an example to illustrate a method of seismic risk analysis including a line-source model.

Algermissen and Perkins (1976) in their study of maximum acceleration maps for the contiguous United States also give results for San Francisco.

All the above studies refer to seismic risk at a point. Studies

dealing with seismic risk for the entire Bay Area have also been done. In particular, O.E.P. (1972) and Friedman (1975) both study earthquake losses that could occur during a large earthquake in the Bay Area, but do not consider the spatial correlation of earthquake action.

The present study contains the following: an evaluation of the overall properties of seismicity characteristics; an evaluation of methods of computing seismic risk for both point and area elements; comparisons with previous work; ways of presenting results and an analysis of the sensitivity of the final result to a particular parameter. Furthermore, a detailed discussion of the methods used in each section of the analysis is given.

The next chapter of this report presents the geologic and tectonic features of the San Francisco vicinity in order to summarize all the up-to-date relevant information that could throw light onto the geotectonic evolution near San Francisco in the last one million years. In the following chapter, data since the nineteenth century on the elastodynamic properties of the San Andreas fault are characterized. Particular emphasis is given to the form of attenuation of ground motion in the region close to the fault. This form is critical when studying seismic hazard and seismic risk in the Bay Area. Earthquake parameters for engineering planning and design are also discussed. Chapter 5 presents a seismic hazard analysis for a site in downtown San Francisco and studies the effects of uncertainties of some parameters on the final probability distributions. Some of the uncertainties are directly incorporated into the mathematical models. The influence of site location within the Bay Area is also analyzed. In Chapter 6 population exposure to seismic threat in the Greater San Francisco Bay Area is considered. The main conclusions are summarized in Chapter 7.

Most of the work presented here is a compilation of results obtained from different areas of the earth sciences and earthquake engineering together with a critical discussion of seismic risk methods. The basic mathematical developments of the subjects covered herein are presented elsewhere. A list of references is given in Oliveira (1974), (1975).

The main innovations are

- a) a definition of hazard risk in terms of response spectra,
- b) a study of the influence of uncertainties in particular parameters on the final distributions, and
- c) global earthquake risk for a region in terms of population exposure.

In the course of the work some modifications are made with the aim of improving the models; in particular the use of

- d) stochastic point processes with memory for occurrence of earthquakes, and
- e) a two-parameter model to simulate the mechanism of earthquake generation at the source.

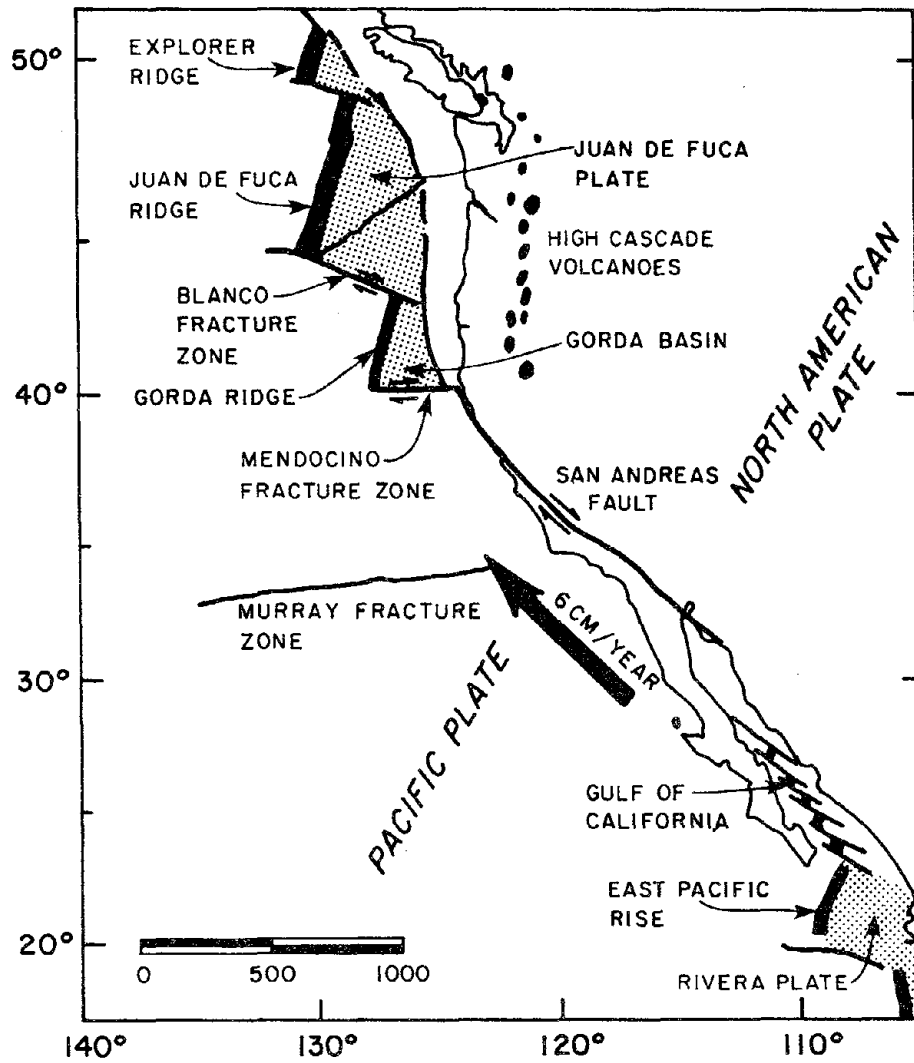


FIGURE 1 MAJOR REGIONAL GEOTECTONIC STRUCTURES RELATED TO CALIFORNIA SEISMICITY

After Atwater (1970)

2. GEOLOGIC AND GEOTECTONIC FEATURES IN THE VICINITY OF SAN FRANCISCO

2.1 Generalities

The historical record of the seismicity of the west coast of the United States started as early as 1780 although, as is shown in the next chapter, only since 1930 has a fairly complete record of earthquake activity in the State of California been kept.

In particular, for studies of risk analysis dealing with low risks ($<10^{-3}$) this record is very short. A time history analysis of geologic and geotectonic features that covers the last million years however, can supplement the above information and throw some light on the origins of the present state of stresses, of recurrence intervals of large earthquakes, of clustering of events in time and space, migration, etc. Studies of young fault scarps and fault traces (Wallace, 1977), together with the evolution of the geotectonic features can help in refining seismic zoning and in understanding the origin and mechanical behavior of large tectonic blocks and provinces.

2.2 Historical Evolution of Plate Configurations

Some of the major regional features which may be brought into a genetic relationship with Californian seismicity are the East Pacific rise, which appears to cause the opening of the Gulf of California, and the Murray and Mendocino fracture zones, two large oceanic scarps which intersect the American continent somewhere along the 35th and 40th parallels (see Fig. 1). Linking the spreading rises in the Gulf of California and the East Pacific rise with the spreading rises of the Gorda and Juan de Fuca ridges, just north of the Mendocino fracture, off the coast of Oregon, is a 1500 km long continental fault system known as

the right lateral strike-slip San Andreas fault.

Different studies have shown that the San Francisco region, since the Early Tertiary period (40×10^6 years ago), has been dominated by the conjugation of movements of the Pacific, the Farallon and the American plates (Atwater, 1970). The Farallon plate is a small plate moving away from the rigid Pacific plate.

In Early Tertiary the Farallon plate moved towards the American plate at a rate of 10 cm/year, while the American plate moved at 6 cm/year to the south creating an oblique subduction (see Fig. 2). The Farallon plate went underneath the American plate and the mid-ocean ridge approached the American plate. Because most of the Farallon plate no longer exists, there probably was a trench which consumed it at its boundary with the American plate. Subsequently the American plate has continued to move south relative to the Pacific plate, giving rise to transcurrent motion on the San Andreas system.

Figure 2 shows what is thought to be the evolution of plate tectonics in the last 40 million years. Figure 3 is another scheme for the same evolution. Even though Fig. 3 is an interpretation of the past evolution since the Early Tertiary, it is almost certain that the San Andreas fault began activity in its present role not earlier than 30×10^6 years ago. Strike-slip activity in San Francisco may have begun $(5 \text{ to } 10) \times 10^6$ years ago.

The overall displacement measured by surveyed triangulation along the San Andreas fault system as a whole, about 6 cm/year, is consistent with the transcurrent motion of the Pacific plate obtained from sea floor spreading measurements.

2.3 Present Geotectonic Features

The San Andreas fault system in the vicinity of San Francisco is made up of three major faults: on the western side lies the San Andreas fault; parallel to it and located some 15 miles to the east is the Hayward fault; further to the east lies the third major fault, the Calaveras fault (see Fig. 3). The San Andreas fault zone varies considerably in width. In some places it may be less than 100 meters wide and made up of a few entangled lines of rupture. Its actual edges are imprecise because of many lines of activity that are now hidden under recent gravel deposits or alluvium, and because of land sliding that has covered several miles at a stretch. Other smaller faults can also be identified, such as the Healdsburg-Rodgers fault in the northern continuation of the Hayward-Calaveras system; the Pleasanton fault, east of Calaveras; and a large number of small fault traces that can be found on a large-scale geological map. Recently, Herd (1978) proposed that the shaded zone in Fig. 3 be considered as the Humboldt plate which moves independently of the Pacific and North American plates.

According to studies of differential movements across the San Andreas fault using surveyed triangulation analysis of earthquake records and surface rupture associated with historical earthquakes there are three different zones that should be considered for the San Andreas fault system. The first zone is the section of the San Andreas fault between Cape Mendocino and San Francisco Bay which is relatively inactive. North of San Francisco Bay, the Hayward and Calaveras faults are no longer mapped as separate entities. The Coast Ranges are much wider and many faults, mostly of short extent, are mapped. Here the seismicity is much more dispersed, with small earthquakes occurring throughout the region.

The relatively large Santa Rosa earthquake of April 25, 1968 near the southern end of the mapped Healdsburg fault did not show any surface rupture.

In contrast with the frequent occurrence of earthquakes in the Coast Ranges, only one earthquake was detected during the last 20 years along the San Andreas fault from Bolinas north of San Francisco to Point Arena. The largest offset in the San Andreas fault zone was due to the 1906 San Francisco earthquake with movement between San Juan Bautista and southern Humboldt County. The maximum horizontal right lateral ground offset at the fault was 5.25 meters, near the head of Tomales Bay; vertical movement was not more than 7.5 cm.

The second zone is the section of the San Andreas fault from the northern end of San Francisco Bay to north Los Gatos, which has periods with high activity alternating with periods which are relatively inactive. Surveyed triangulation shows movements across the fault in the periods 1866-1874 and 1892-1906; the first were possibly due to the Hayward earthquake of 1868 and the second to the 1906 San Francisco earthquake. No creep was detected along the fault system from Cape Mendocino to Los Gatos, for the period between 1876 and 1906.

There is little indication of slippage on the San Andreas fault north of Los Gatos since 1906. Triangulation in the San Francisco Bay Area despite somewhat contradictory results, shows a general trend of northward transcurrent motion of the coast with respect to the continent, particularly west of the Hayward Fault.

In this zone, strong earthquakes (Mercalli Modified Intensity MM=X) occurred on the Hayward fault in 1836 and 1868, and fractures were reported along the fault after the 1868 earthquake. Surface rupture,

probably along the Calaveras fault, accompanied a moderate earthquake in 1861. These two faults can be considered moderately active although only one earthquake with magnitude in the range 5.5-5.9 was recorded between 1931 and 1965. Creep has been reported at several points along the Hayward fault and the average rate of displacement ranges between 0.4 and 0.6 cm/year. Possible creep has been reported on the Calaveras fault and the subsidiary Pleasanton fault (Wallace, 1970).

South of San Francisco, epicenters of small earthquakes form a cluster near, but somewhat to the west of, the Hayward fault; further south there is a quiet zone for 30 km. Directly to the east, a similar cluster has been located a kilometer or so to the east of the mapped Calaveras trace. The third section of the San Andreas fault, south of Los Gatos, has been one of its most active parts, although it has been characterized by earthquakes of magnitude about 5 or less, (McNally, 1976). From 1959 to 1967 the average annual fault movement on the fault was greatest just south of Hollister, about 4.4 cm/year (Hofmann, 1968). North of Hollister, where the Calaveras and Hayward Faults have splintered off from the San Andreas fault, an annual total slip of about 4 cm/year is distributed among the three faults. The portion of movement carried by each fault changes with time. The accumulation of this displacement is observed to be a combination of fault creep or slippage and strain or distortion of the Earth's surface.

The high seismic area between Hollister, Watsonville and Mount Hamilton (as well as the Calaveras displacement which averages 1 cm/year) may be due to the northward compressional stresses which have arisen from the movement of the Pacific plate to its present position. The change in strike of the San Andreas fault to the north is also possibly associated with this granitic mass. The additional activity at the Hayward-

Calaveras bifurcation is similar, but on a smaller scale, to that of the San Andreas and Calaveras faults between Bear Valley and Hollister.

The effect of creep is of crucial importance. If the rate of accumulation of strain energy is relatively constant, appreciable loss of elastic strain energy by tectonic creep might preclude a great earthquake as long as creep continues. However, creep need not be constant as has been observed near Hollister. At the moment, however, there is little evidence of any drastic changes in the average rate of elastic strain accumulation; indeed, historic rates of slip are of the same order as the long term geologic slip rates. This suggests that tectonic driving mechanisms are continuing to work at the same average rate at which they have for the last 25×10^6 years. However, on a smaller time scale, of the order of a century, (from the last two centuries of historical seismic knowledge) earthquake activity has not been stationary as far as large events are concerned (see next chapter). For instance, along the San Andreas fault the period from 1836 to 1906 suggests a clustering of events. The possible clustering that has been assigned to the earthquake activity may be due to changes in the driving force which shows periodicities of tens of thousand years, and to changes in the release mechanism.

Values for recurrence intervals for the three main sections of the San Andreas system are given by Wallace (1970); however, his recurrence interval may be incorrect by a factor of two depending on the values estimated for the secular slip rate. His results are presented in Table III. Tectonic creep is believed to increase the recurrence interval for earthquakes of a given magnitude and to have a greater effect on lower magnitude earthquakes and little or no effect on earthquakes of magnitude greater than 8.

TABLE III

Seismicity Parameters Suggested by
Wallace (1970) for the San Francisco Area

	MENDOCINO- LOS GATOS	SOUTH LOS GATOS	HAYWARD- CALAVERAS
MAXIMUM MAGNITUDE	7 → 8 ⁺	5 → 6	6 → 7
MAXIMUM STRIKE SLIP (meters)	1.2 → 10	0.1 → 0.3	0.3 → 1.2
CREEP RATE (% OF SECULAR)	<10	30 → 50	10 → 30
RECURRENCE INTERVAL (years)	100 → 1000	<10	10 → 100

If the rate of accumulation of strain energy is extrapolated backwards into the Tertiary, displacements of the order of hundreds of miles can be inferred. Indeed, the geological evidence implies that the accumulated lateral motion since the Early Tertiary totals more than 250 km for central California. These conclusions are based on geological correlations involving considerable uncertainty but are now generally accepted by most California geologists. Even though these are large movements when compared with those in other regions of high seismicity, much of the total motion may take place by continuous slippage or fault creep. The missing part may be released over a time scale of centuries with episodes of large and sudden ruptures.

2.4 Geotectonic Interpretation Using Earthquake Source Mechanisms

Refraction studies of seismic waves have shown that the crustal model in the region of San Francisco is approximately as shown in Figure 5.

The Earth's crust is about 25 to 30 km thick. The average focal depth for California is less than 10 km (see Section 3.3.1). This confirms that the elastic strain energy stored appears to be restricted mainly to the upper part of the crust at a depth between 2 and 15 km. Estimates of depth of faulting in the San Francisco 1906 earthquake are within the upper 10 to 20 km of the Earth. Since displacements of at least 100 km (and probably 300 to 500 km) have occurred along the San Andreas Fault, it is almost certain that deformation by creep without observable earthquake activity must be occurring at a depth greater than 20 km. Thus, an upper layer in which earthquakes occur should be associated with a zone of low strength below.

Fault plane solutions have been systematically determined for recorded earthquakes. The focal mechanisms confirm, in general, the right lateral strike-slip behavior of the San Andreas system, derived through geological evidence as well as from surveillance measurements (see Fig. 6).

2.5 Influence of the Geology of the San Francisco Bay Area on Earthquake Wave Amplification

The San Francisco Bay region includes a variety of geological units ranging from granitic rocks to semi-consolidated and unconsolidated alluvium to recent water-saturated mud deposits, as shown in Fig. 7. San Francisco Bay is located in a northwest trending valley. The Bay is bounded mostly by marshlands, alluvial plains (1 to 15 km wide) and beyond by ridges of the Coast Ranges. The active San Andreas and Hayward fault zones trend northwestward about 5 km apart along the western and eastern margins of the bay, respectively. The geological units are broadly characterized as bedrock, alluvium and bay mud. In general, the

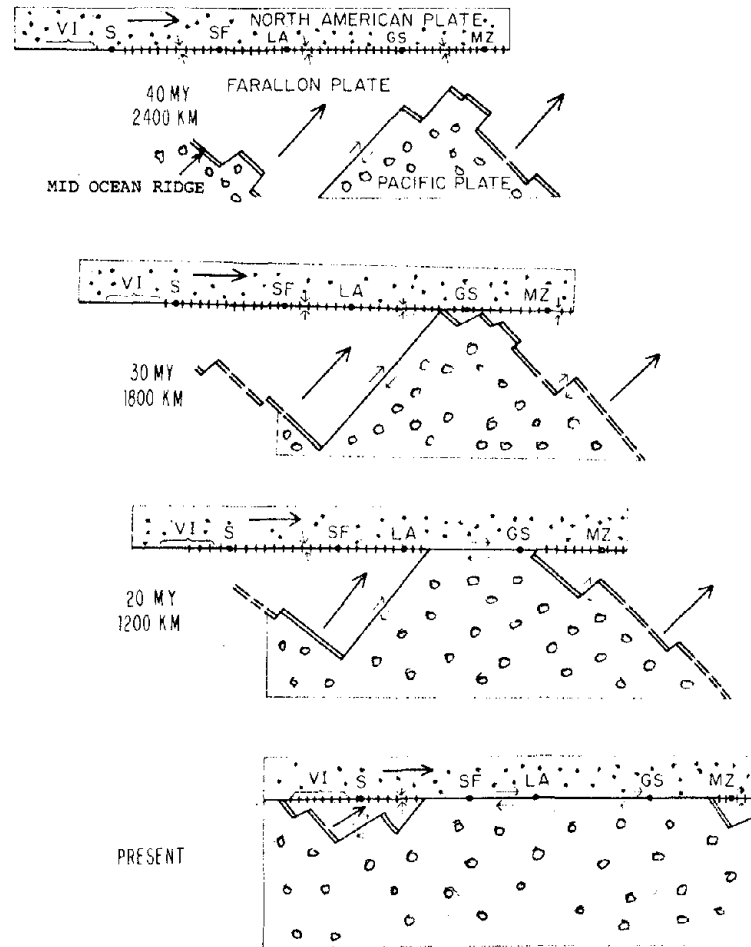
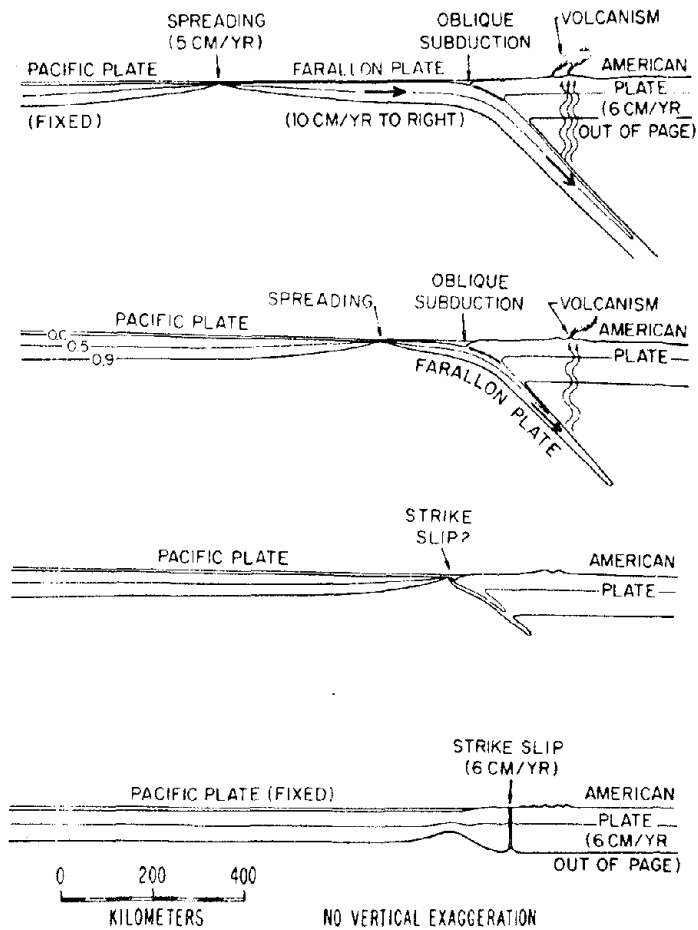
bedrock is exposed with ridge systems and forms the irregular floor of a trough containing the alluvium which, where not exposed at the surface, is overlain by bay mud.

Local geological conditions can substantially change the characteristics of seismic waves. In particular, waves of certain frequencies can be amplified considerably by thick sections of unconsolidated near-surface deposits. Overall damage potential is likely to be greater in soft grounds than on rock because of possible ground failures, extended duration of shaking and amplification at lower frequencies. Although weak foundation materials, such as the Bay mud and the Holocene alluvium, may be expected to reduce the peak levels of acceleration due to attenuation in these formations during transmission of intense motion from bedrock to the ground surface, the predominance of soft alluviums in San Francisco Bay makes the area more hazardous than areas where the soil is "firm". Thus the damage expected in this area, particularly along the shore of the Bay, is much larger. During the San Francisco 1906 earthquake structures located on bedrock suffered little or no damage while those on bay fill were heavily damaged. Figure 8(a) shows the California isoseismals for the 1906 San Francisco earthquake and Fig. 8(b) the damage caused by the 1957 San Francisco earthquake. Studies done with data collected during the latter earthquake (Idriss and Seed, 1968), and from ground motion measurements at 99 points in San Francisco Bay caused by nuclear explosions in Nevada (Borcherdt and Gibbs, 1976) show that the average spectral amplifications observed for vertical and horizontal ground motions are approximately constant in the frequency range of 0.25 to 3 Hz and are respectively equal to 1.0 and 1.0 for granite,

1.5 and 1.6 for the Franciscan Formation, 3.0 and 2.7 for the Santa Clara Formation, and 3.7 and 11.3 for the Bay mud formations more than 10 meters thick. Figure 9 presents surface accelerations recorded during the San Francisco 1957 earthquake at four different sites.

Liquefaction of sand is another important problem which may arise for certain water levels due to high pore pressures and extended duration of ground motion.

In this research only the average "firm" conditions are considered. The probable effect of soil strata will be indicated. A detailed study of specific sites, including the geology, within metropolitan San Francisco or the Bay Area is however, outside the scope of this report.



Initials represent cities on the west coast from Vancouver Island (VI) to Mazatlan (MZ). Single lines are transform faults, double lines are spreading centers and hatched lines are zones of subduction. Large arrows show motion of plates with respect to the Pacific Plate which is arbitrarily held fixed. Small arrows show relative motions at points along plate boundaries.

(a) CROSS SECTION

(b) HORIZONTAL PROJECTION

FIGURE 2 EVOLUTION OF PLATE CONFIGURATION IN THE LAST 40×10^6 YEARS

After Atwater (1970)

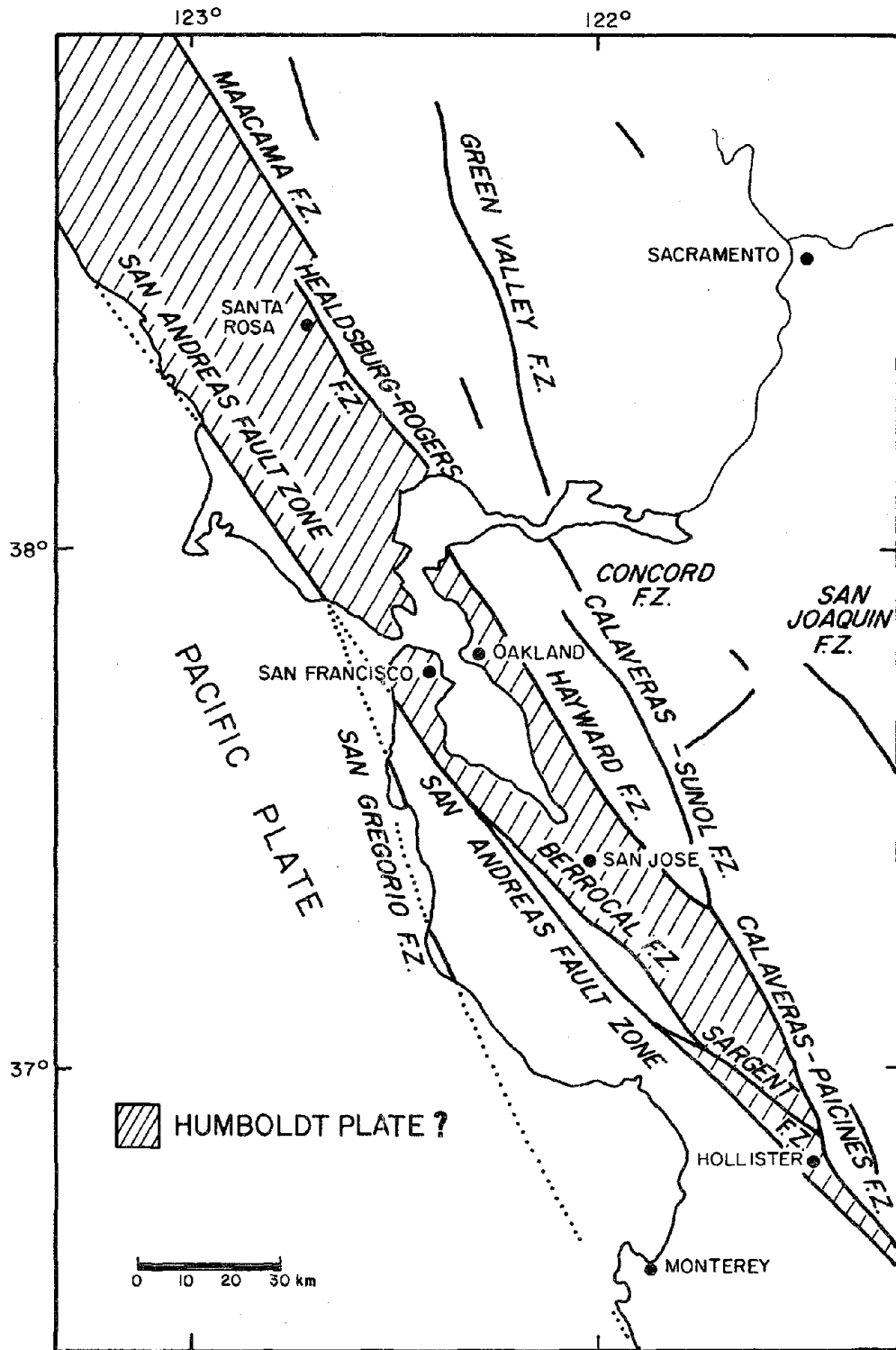
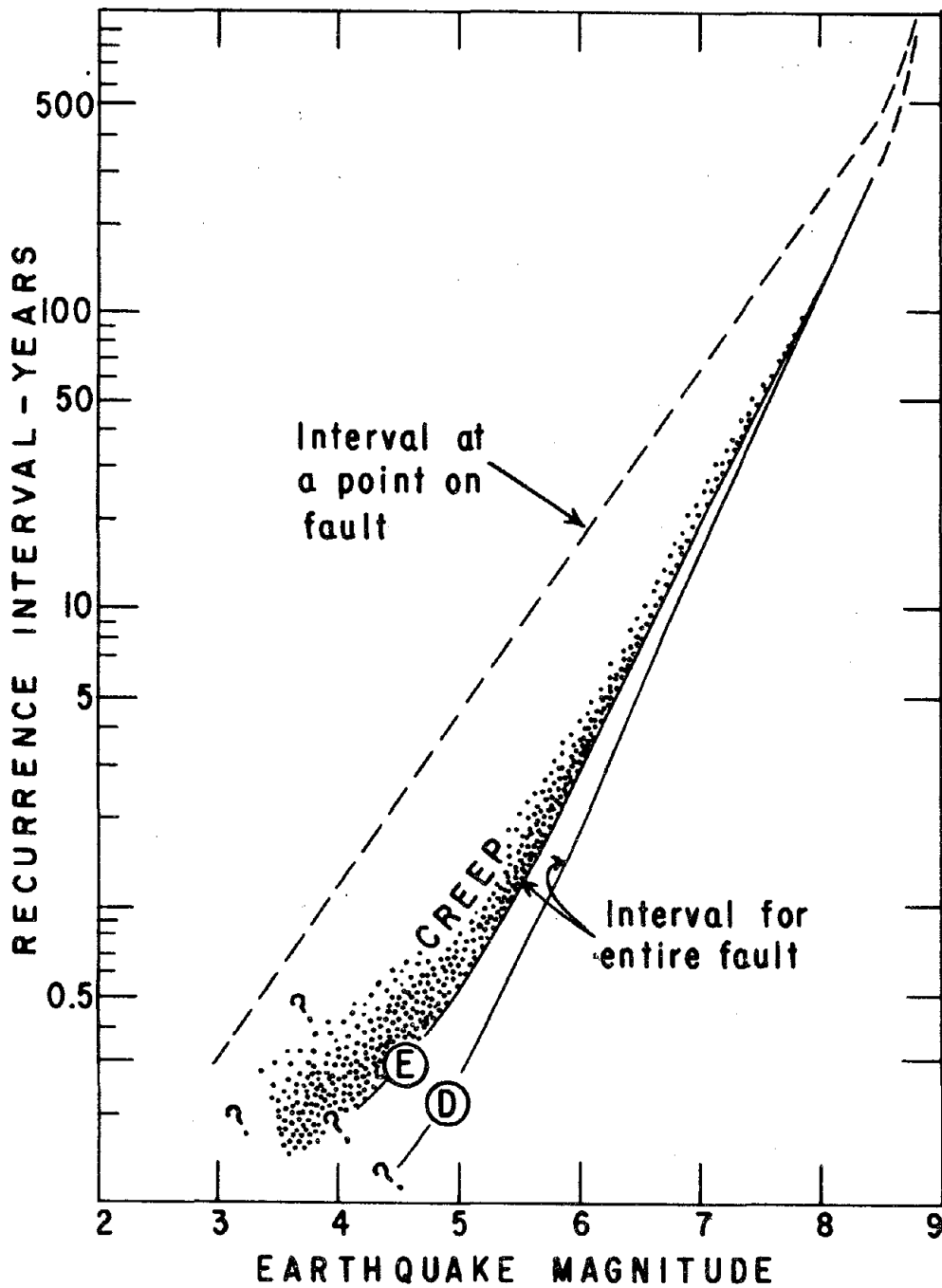


FIGURE 3 SAN ANDREAS FAULT SYSTEM IN THE VICINITY OF SAN FRANCISCO



Curve D considers no creep effect.

Curve E considers 50% of secular strain for generation of earthquakes with $M \geq 5$ and 50% released as creep.

FIGURE 4 EARTHQUAKE RECURRENCE INTERVALS ON THE SAN ANDREAS FAULT BASED ON STRAIN ACCUMULATION AND CREEP MEASUREMENTS

After Wallace (1970)

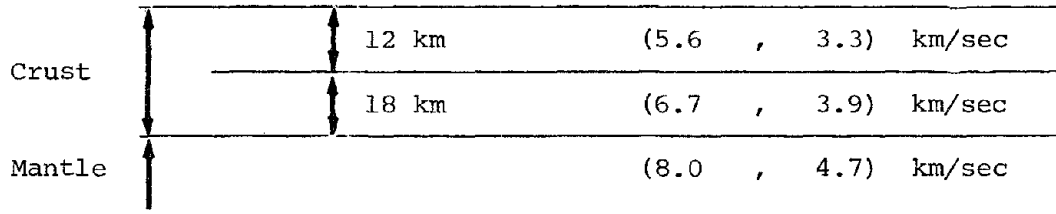


FIGURE 5 CRUSTAL MODEL FOR THE SAN FRANCISCO VICINITY
(P AND S WAVE VELOCITIES ARE GIVEN IN PARENTHESES)

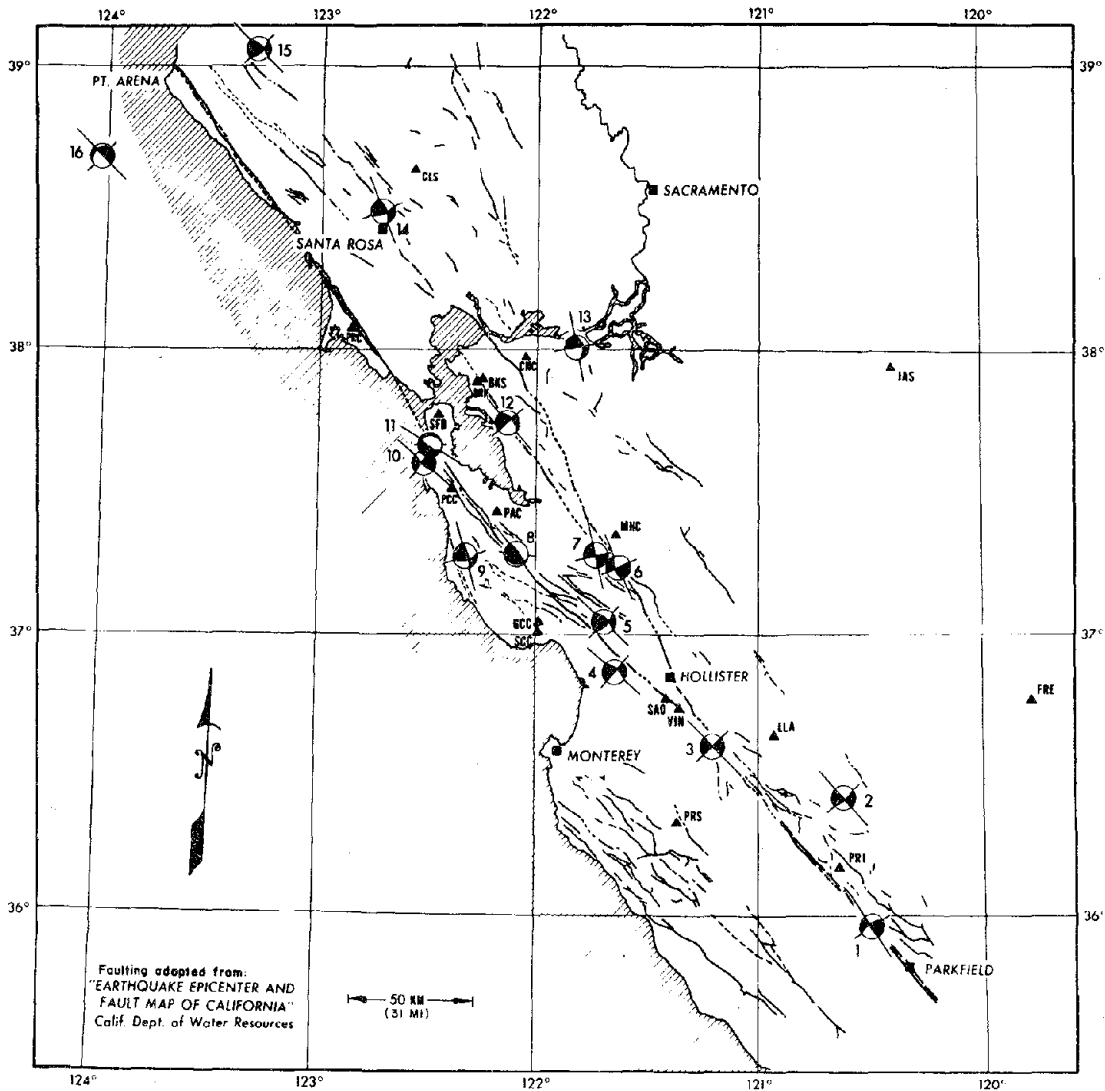


FIGURE 6 FAULT PLANE SOLUTIONS IN THE CENTRAL COAST RANGES OF CALIFORNIA

After Bolt et al. (1968)

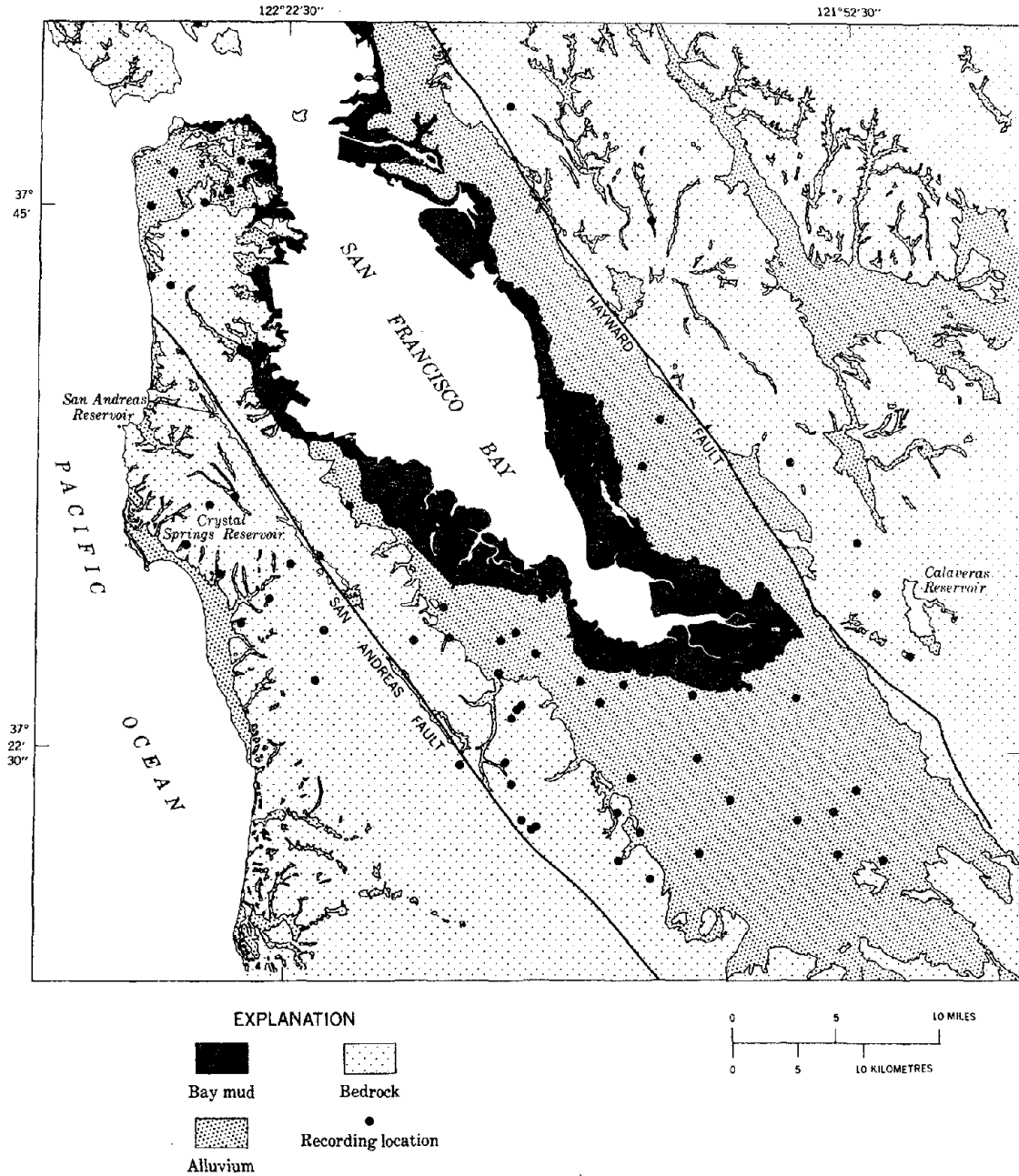
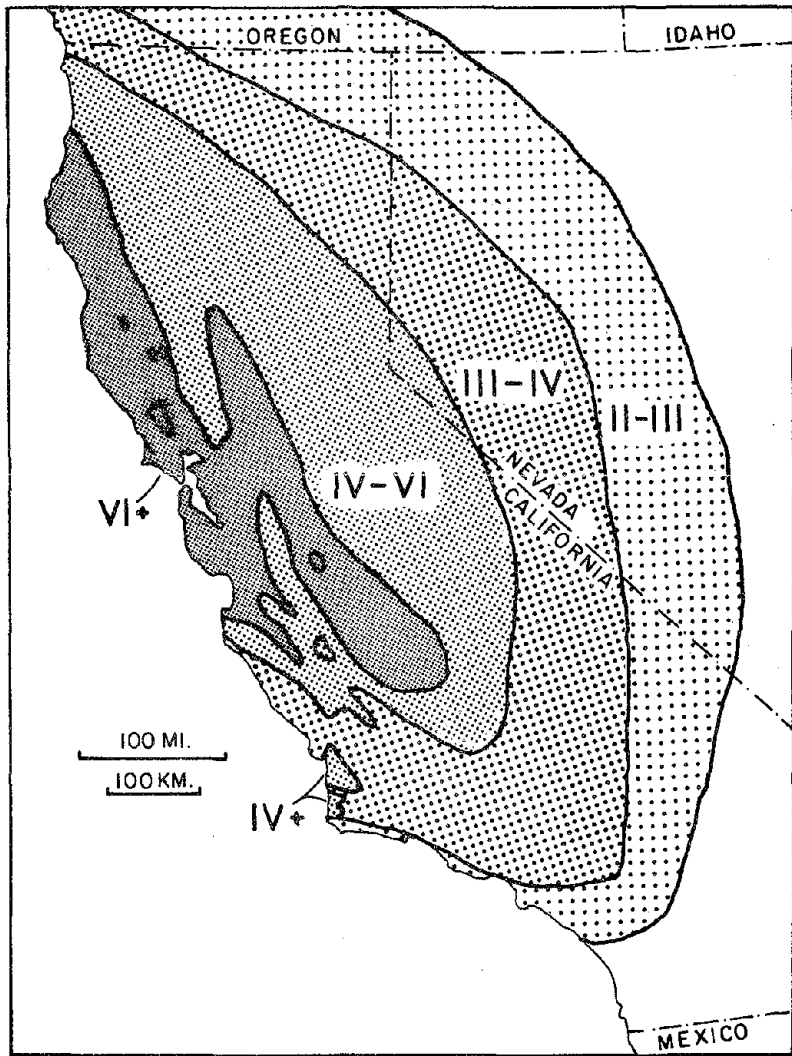
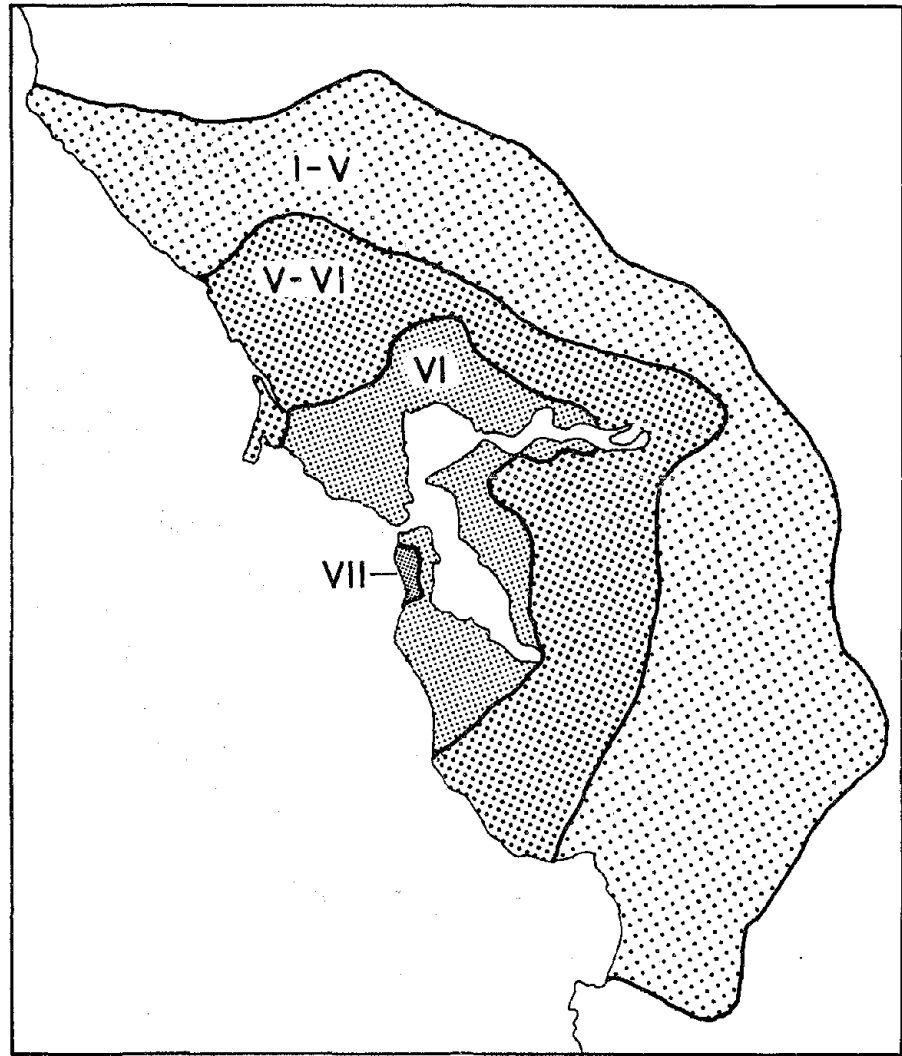


FIGURE 7 GENERAL GEOLOGY OF THE SAN FRANCISCO BAY AREA

After Borchardt (1975)



(a) THE 1906 SAN FRANCISCO EARTHQUAKE



(b) THE 1957 SAN FRANCISCO EARTHQUAKE

FIGURE 8 ISOSEISMALS SHOWING THE GEOGRAPHICAL DISTRIBUTION OF DAMAGE

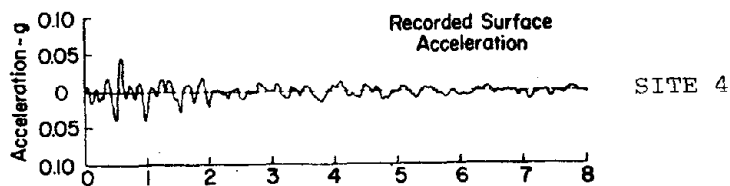
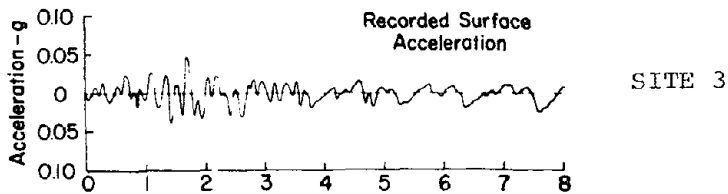
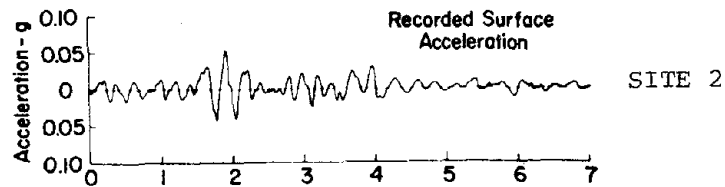
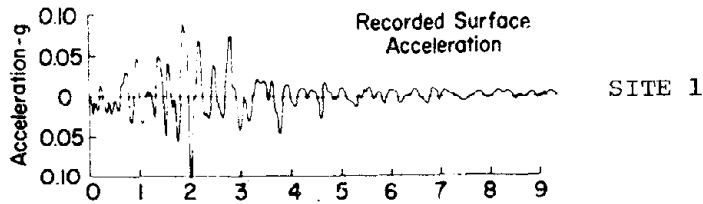
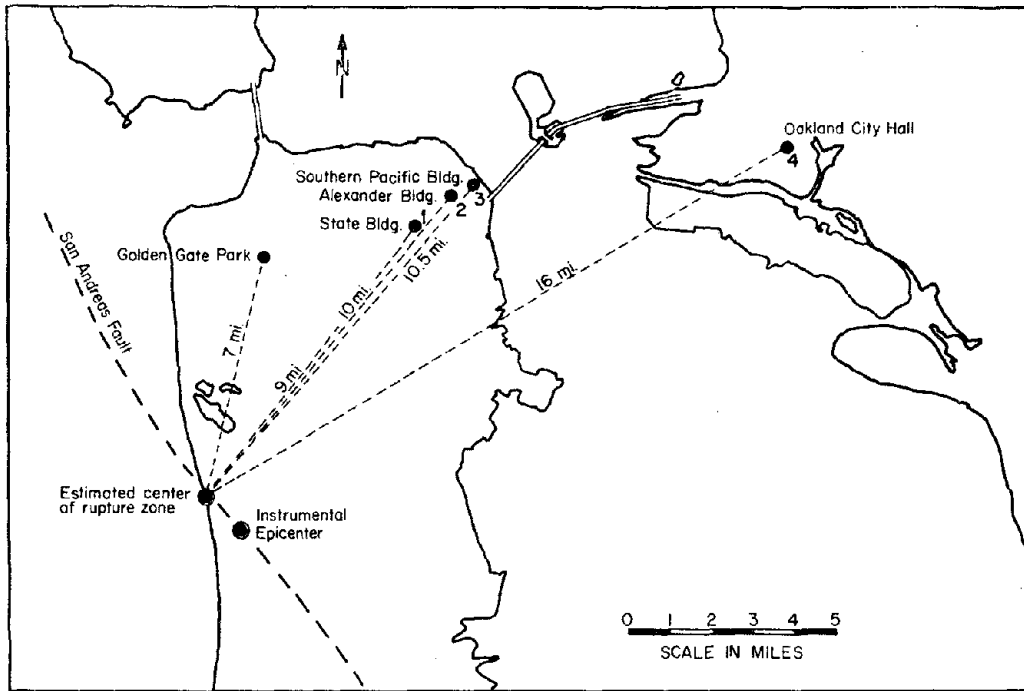


FIGURE 9 U.S.G.S. STRONG MOTION ACCELEROMETER RECORDINGS OF SURFACE ACCELERATIONS AT FOUR DIFFERENT SITES DURING THE 1957 SAN FRANCISCO EARTHQUAKE

After Idriss and Seed (1968)

3. EXISTING DATA

3.1 Seismographic Network. Reliability of Data

The historical record of seismicity in the San Francisco region started as early as 1780 when the first immigrant arrived. The earliest records are non-instrumental. The first seismographs were installed in 1887 but the results obtained were not very precise. Only since 1933 has a fairly complete record of earthquake activity in the State of California been kept. Figure 10 shows the number of seismographic stations in service within a 300 km radius from San Francisco, and the year in which they began operating.

As seen in the figure the number of seismographic stations increased substantially in the late sixties. Consequently the quality of hypocentral determination which depends on the number of stations, as well as on the types of seismographs in use at the time of recording, and on the method of location, has increased considerably. By 1975 a telemetry network of fifteen stations in Central California was operated by the University of California.

From 1910 through 1941 the error in location of epicenters could be many tens of kilometers; whilst in the last decade the average uncertainty has been 5 km. Focal depths are generally less precise but a major step was the discovery about 1963 that depth does not exceed 15 km in this region. The error in determination of Richter magnitude, M , was 30% to 37% in the early periods, because most of the determinations were based on felt intensity. Nowadays magnitude determinations are based upon the surface wave energy, m_s , and then transformed into M . Errors are now less than 10%. (Rarely is the error more than 0.2 to 0.3 on the Richter scale.)

In addition to the seismographic stations, there is a network of strong motion accelerometers installed at different sites and structures. Data covering the period 1910-1972 are published in the "Catalogue of Earthquakes in Northern California and Adjoining Areas" (Bolt and Miller, 1975), with the following information:

- a) time of occurrence;
- b) epicentral location;
- c) quality of determination;
- d) Richter magnitude rating;
- e) number of recording stations;
- f) felt or not felt;
- g) maximum intensity in different towns. Comments.

Data for earthquake activity before 1933 can be considered in three periods: 1780-1850, 1850-1906 and 1906-1933. A great deal of caution should be exercised in the evaluation of historical records prior to 1933, especially for small earthquakes. However there are enough data to conclude that since 1910 the catalogue of earthquakes is complete for magnitudes above 3.5. For those earthquakes for which the Richter magnitude is not included in the catalogue, it was generated from the maximum Modified Mercalli Intensity, I_0 , using the transformation formula suggested by Richter (1955) for California

$$M = 0.6 I_0 + 1.3 .$$

This transformation creates an additional uncertainty. Earthquakes without information regarding epicentral location were disregarded and no critical study was made to test the validity and reliability of data.

For the studies presented here, all earthquakes with $M > 3.5$ and lying within a circle of 200 km centered at San Francisco (37.75°N , 122.45°W)

were selected from the computer tape provided by the University of California, Berkeley Seismographic Station. There were 945 such earthquakes.

3.2 Major Historical Shocks

The consequences of historical shocks felt in the San Francisco region since 1800 are thoroughly described by Tocher (1959). The two shocks of greatest energy release were the Hayward earthquake of October 21, 1868 and the San Francisco earthquake of April 18, 1906. Figure 8(a) presents the isoseismals of the latter, which show how far the accelerations were felt as well as the radiation pattern. Figures 11(a) and (b) show the location of earthquakes with $M > 4$ for the period 1807-1969, and the location of all shocks felt in the decade 1960-1969, respectively.

3.3 Statistical Analysis of Data

Earthquake generation can be represented by stochastic point processes in a three-dimensional space-time-energy continuum (L_i, T_i, M_i) , where L_i is the location of focus, which itself is a three component vector characterized by latitude, longitude and depth, T_i is the time of occurrence, M_i the magnitude. For small epicentral distances the characterization of the size of an earthquake requires a vector quantity that represents the mechanism of generation and the radiation pattern, adding one more dimension to the problem. To complete the earthquake representation it is necessary to describe the ground motion generated by the earthquake and felt at any given distance. Earthquake ground motion can be considered as a continuous time parameter stochastic process that attenuates with distance.

The complex phenomenon of seismic wave propagation from fault to site, is taken care of by the use of attenuation formulae which transform

the seismic action at the focus into the seismic action at the site.

A complete statistical analysis of earthquakes must consider the distribution and correlations of these four parameters. This involves the handling of a four-dimensional continuum which generally constitutes a very complicated model. Furthermore, each parameter has to be analyzed in turn to see how much can be inferred from data. To be able to do this, boundaries in space, time and magnitude have to be fixed initially. At this time the influence of the mechanism of rupture will be disregarded. In the following an attempt has been made to collate all available information and results from analyses of data made by several authors, and to make statistical inferences whenever possible.

3.3.1 On Spatial Location of Earthquakes

It is well-known that earthquakes are related to the presence of faults. Chapter 2 demonstrated the presence of active faults in California, the existence of mechanisms for the accumulation of strain and the occurrence of earthquakes. Using these elements, the spatial location of epicenters, and recent geodetic studies of fault movement it is possible to define zones of homogeneous seismicity, although this is not easy on a very fine scale. Figure 11(b) shows the general seismic pattern in Northern California, indicating a high density of seismic events concentrated around the San Andreas fault system. This concentration is not uniform over its length, however, and depends on the minimum magnitude threshold. This means, as discussed in Chapter 2, that sections of the faults are not moving and consequently are not generating earthquakes. Microearthquakes recorded recently along the San Andreas system, shown in Fig. 11(c), confirm the fault pattern of Fig. 3 and can be used to define more precisely the location of earthquake source zones. As can be seen from Figs. 11(a),

(b) and (c) the uncertainty existing in the correlation between active known faults and the location of epicenters increases when higher magnitudes are considered. To account for this problem different types of source areas have been used in hazard analysis.

In this area earthquakes are quite shallow. Indeed, Bolt and Miller (1971) in a sample of 99 earthquakes with $M > 3$, which occurred between San Francisco and Priest Valley in the period 1965-1969, showed that these California earthquakes in the Central Coast Ranges have focal depths less than 15 km (Fig. 12). The same conclusions were obtained by McNally (1976) for the Bear Valley-Stone Canyon Region. Hence, the observed seismic activity along the San Andreas system is confined to the upper 20 km of the Earth and much of its activity is confined to the upper 5 or 10 km. Estimates of the depth of faulting in the San Francisco earthquake of 1906 are within the upper 10 to 20 km of the Earth (see section 2.4).

The simplest model of the distribution of seismic sources for the San Francisco area would be an homogenous single zone representing the Central Coast Ranges, with uniform seismic properties. More detailed representations have been proposed by (i) Kiremidjian and Shah (1975) who only consider seismic source lines that coincide with main fault lines as in Fig. 13(a); (ii) Algermissen and Perkins (1976) who define several seismic source areas which have the main fault lines as longitudinal axes as in Fig. 13(b); and (iii) Kiureghian and Ang (1975) who consider both seismic source lines for known faults and seismic source areas in zones of unknown fault systems as shown in Fig. 13(c).

These three models of seismic source areas are representative of the types that have been suggested; but other models with non-uniform source areas could be explored as well.

3.3.2 On Time of Occurrence

The most widely used model to represent the occurrence of large earthquakes has been the Poisson model. Many studies of Southern California including those by Knopoff (1964) and Gardner and Knopoff (1974), have been made to check the validity of this model. However for the Bay Area the only known study was made of a segment of the San Andreas fault zone near Hollister by McNally (1976), and for micro-activity by Udias and Rice (1975). The validity of the Poisson assumption for a set of events of magnitude greater than a given lower bound can be tested by the following methods: (i) direct analysis of the number of earthquakes occurring during a given period of time; (ii) statistical analysis of interarrival times; (iii) the hazard function; (iv) the variance-time curve; and (v) the autocovariance function, (Esteva, 1977; Knopoff 1971; and Lomnitz, 1974). The first four techniques will be considered here.

It is of particular interest to examine the data for the San Andreas fault to determine if, for large earthquakes, there is any memory-type behavior. Vagliante (1973) used a first order Markov Process to consider the salient features of the "elastic rebound theory" and he applied it to seismicity in the Bay Area. He did not, however, compare his results with a Poisson process. Esteva (1975) and Kelleher et al. (1973) refer to deviations from the Poisson process as observed on the Mexican Coast where seismic activity migrates along the region in such a manner that large earthquakes tend to occur at seismic gaps; this implies that the hazard function grows with time since the last earthquake.

The data used are shown in Fig. 14 which presents the number of events per year, with magnitude greater than 4, within a 100 km of

San Francisco, as a function of time. As can be seen the mean number of events changes with time in the 200 year period of observation. (The catalogue of earthquakes is supposed to be complete for $M > 3.5$ since 1910.) Table IV shows the mean number of events as a function of the interval of time considered in the analysis.

TABLE IV

Stationarity of Earthquake Generation in Time ($M > 4.0$, $R < 100$ km)

INTERVALS	PERIOD	NO. EARTHQUAKES	AVERAGE
50 YEARS INTERVALS	1800 - 1850	10	0.5
	1850 - 1900	143	2.86
	1900 - 1950	79	1.58
20 YEARS INTERVALS	1800 - 1820	5	0.20
	1820 - 1840	4	0.25
	1840 - 1860	30	1.50
	1860 - 1880	58	2.90
	1880 - 1890	56	2.80
	1900 - 1920	41	2.05
	1920 - 1940	24	1.20
	1940 - 1960	31	1.55

The time analysis made herein treats all earthquakes within 100 km radius independently of their seismic zone.

To establish the first order Markov chain model, consider the events (Vagliente, 1973; Oliveira, 1974)

1. - no earthquake occurs
2. - an earthquake occurs

and the transition probability matrix

$$P = \begin{bmatrix} 1-a & a \\ b & 1-b \end{bmatrix}, \quad (1)$$

where $(1-a)$ is the probability of having an earthquake in this current period of time given that one earthquake occurred during the last period; and b is the probability of having one earthquake in this current period of time given that no earthquake occurred during the last period.

The n^{th} step transition probability matrix is

$$\phi(n) = \frac{1}{a+b} \begin{bmatrix} b & a \\ b & a \end{bmatrix} + \frac{(1-a-b)^n}{a+b} \begin{bmatrix} a & -a \\ -b & b \end{bmatrix}. \quad (2)$$

During the period 1807-1977 there are four earthquakes with $M \geq 7.0$ and eleven (with three consecutive events) with $M \geq 6.5$ in the San Francisco region, yielding the following values for a and b .

$$M \geq 7.0 \rightarrow a = 1.0, b = 0.02352$$

$$M \geq 6.5 \rightarrow a = 0.98823, b = 0.06470$$

The mean, E_{T_1} , and standard deviation, σ_{T_1} , of waiting time of first passage, T_1 , were computed from

$$E_{T_1} = \frac{a+b}{b} \quad \text{and} \quad \sigma_{T_1} = \frac{b(2-a-b)}{a^2} \quad (3)$$

and are equal to

$$M \geq 7.0 \begin{cases} E_{T_1} = 43.52 \text{ years} \\ \sigma_{T_1} = 42.01 \text{ years} \end{cases} \quad M \geq 6.5 \begin{cases} E_{T_1} = 16.27 \text{ years} \\ \sigma_{T_1} = 14.95 \text{ years} \end{cases}.$$

The chi-squared distribution was used to test the validity of the Poisson model of occurrence of earthquakes with $M > 3.5$ for the period 1934-1972. If the Poisson model holds and x is the number of events occurring

in time interval t at a constant rate μ .

$$f(x/t, \mu) = \frac{(\mu t)^x}{x!} e^{-\mu t} \quad (4)$$

Several selections of cells for data grouping were considered and the results are presented in Fig. 15. The influence of the aftershocks was also studied. In every case analyzed, the Poisson fitting was poor and the significance values were always below 0.1%. A drawback to this test is precisely its dependence upon selection of cells for data grouping.

The generation process can be analysed by considering tribution of time between consecutive events, i.e. the interarrival times T . The distribution of interarrival times for a Poisson model is exponential so that

$$F_T(t) = 1 - \exp(-\mu t) \quad (5)$$

For this case the hazard function $h(t)$, (Barlow and Proschan, 1975) defined by

$$h(t) = \frac{f(t)}{1-F_T(t)} \quad (6)$$

is constant and equal to μ . Figure 16 shows $1-F_T(t)$ for interarrival times plotted on semi-log paper for the periods 1850 - 1933 and 1933 - 1972. The exponential distribution would yield from Eq. (5) a straight line representation on this paper. It can be seen however, from Fig. 16 that for the smaller intervals the distribution deviates considerably from a straight line demonstrating the existence of a much larger number of small intervals than expected, as previously shown by Udias and Rice (1975). The hazard function is largest for small T and indicates greater probability than predicted by the exponential model, thus perhaps indicating clustering of events. For a large interarrival time, corresponding

to the occurrence of large earthquakes, the memory-type feature should become dominant. The data do not cover a period of time long enough to allow positive conclusions to be drawn on the subject. Figure 16 shows increasing fluctuations for the large interarrival times. Figure 17 presents a sketch for the interpretation of the model discussed before. The hazard function is a decreasing function of T for small interarrival times. It should grow with the time elapsed since the last event and not remain constant as the Poisson assumption implies. Periodicities should also show up for the large waiting times.

Gamma and Weibull probability distributions differ slightly from the exponential model but have a hazard function that varies with the elapsed time. For the Gamma distribution, the density and distribution functions are, respectively,

$$f_{\lambda, \alpha}(t) = \frac{\lambda^\alpha t^{\alpha-1}}{\Gamma(\alpha)} e^{-\lambda t} \quad (7)$$

for $t \geq 0$ and $\lambda, \alpha > 0$, and

$$F_{\lambda, \alpha}(t) = 1 - \sum_{i=0}^{\alpha-1} \frac{(\lambda t)^i}{i!} e^{-\lambda t}$$

where $\Gamma(\alpha)$ is the gamma function of α ;

and for the Weibull distribution

$$F_{\alpha}(t) = 1 - e^{-(\lambda t)^\alpha}, \quad t \geq 0 \text{ and } \lambda, \alpha > 0.$$

Figure 18 shows the variations of the hazard function with elapsed time for different values of α . The Gamma distribution for $\alpha < 1$ represents the cluster zone of the distribution, for $\alpha = 1$ represents the exponential distribution and for $\alpha > 1$ the zone of large events. The Weibull distribution for $\alpha = 1$ represents the exponential distribution. For $\alpha > 1$ it shows a

hazard function monotonically increasing with T ; hence, it can be used to simulate the behavior at large waiting times. Another index of deviation from the Poisson model called the Poisson dispersion coefficient is the ratio of the variance to the mean. From the variance-time curve one can measure how long the dependence between events lasts. For the Poisson model this index has the value of one. Figure 19 shows the Poisson dispersion coefficient as a function of the time interval, T .

No further studies were made to reduce the deviations from the Poisson model by making use of cluster effects, migration, or to use the spectral techniques of analysis. More data are needed to approve or reject the Poisson model in favor of other models. So at present just two simple hypotheses are being considered; a Poisson process, which shows no memory and a Gamma Process which takes memory into account.

3.3.3 On Magnitude

The linear relation

$$\log N_m = a - bm, \quad m_0 < m < m_1 \quad (8)$$

or

$$\ln N_m = \alpha - \beta m \quad (\alpha = a \ln 10; \beta = b \ln 10),$$

which is generally assumed between m and the logarithm of N_m , where N_m is the number of earthquakes of magnitude $\geq m$, can be used in the Central Coast Ranges. The above expression holds for the interval (m_0, m_1) where m_0 is a constant defined by the lower limit of magnitude for which the data are complete and m_1 is another constant representing the upper bound of possible magnitudes; a and b can be determined using standard fitting linear regression techniques. Equation (8) leads to a double truncated exponential distribution for M . Under the hypothesis that b is essentially the same for the entire region, Bolt and Miller (1975) calculated

$\beta = 2.30 \pm 0.09$ for $3 \leq M \leq 4.4$, Kiureghian and Ang (1975) obtained $\beta = 1.22$ to 1.39 for $M \geq 4$, Dalal (1972) calculated $\beta = 0.87$ to 0.94, and Galanopoulos (1968) found $\beta = 2.1$.

On the other hand, Kiremidjian and Shah (1975) and Algermissen and Perkins (1976) computed b independently for each earthquake source area. Figure 20 presents the data fitting for four source areas of Kiremidjian and Shah's model and also shows the interval of confidence for the linear fitting using a Student-t test for a 95% level. Estimates of the parameters α , β , m_0 and m_1 for each of the above models is presented in Table V, as well as variances in the estimates of α and β . The estimate of m_1 is not made from a statistical analysis but is based on geotectonic information compiled in Chapter 2. The uncertainty in the estimate of b , and hence β , is large with a coefficient of variation of 0.24 for a San Andreas source and 0.51 for a Middland. The coefficient of variation of a , and hence α , is smaller than that of b , and varies from 0.19 to 0.41.

Utsu (1966) derived the exact probability distribution function of b when there is no upper limit on M as

$$f(b) = \frac{n^n}{\Gamma(n)} \left(\frac{b_0}{b}\right)^{n+1} \exp\left(-\frac{nb_0}{b}\right) \frac{1}{b_0} \quad (9)$$

where n is the sample size and b_0 is the central value of b equal to

$$b_0 = \frac{\log e}{\bar{M} - m_0} \quad (10)$$

(\bar{M} is the expected value of M)

The value b_0 is in fact the maximum likelihood estimate of b (Aki, 1965). Steward (1974) observed that b_0 is preferable to least square fitting in the case of data showing curvature or truncation in the high magnitude range. Figure 21 shows the cdf of b as a function of the sample size n .

TABLE V

Seismic Characteristics of Earthquake Source Areas

AUTHOR	ZONES	β	$\alpha_{m=4}$	m_0	m_1	σ_β	σ_α
KIREMIDJIAN AND SHAH	11 A	1.337	0.322	4.0	7.0	0.500	2.294
	12 A	1.167	0.595	4.0	8.3	0.282	1.638
	13	1.308	0.162	4.0	7.0	0.561	2.455
	14	1.735	0.701	4.0	7.7	0.529	2.603
	15	2.822	0.178	4.0	7.0	1.445	5.696
ALGERMISSEN AND PERKINS	2	1.382	1.10	4.3	8,5		
	3	1.554	0.272	4.3	7.9		
	5	1.727	0.149	4.3	7.3		
	6	1.554	0.444	4.3	7.9		
	7	1.830	2.996	4.3	6.1		
KIUREGHIAN AND ANG	1	1.30	3.220	4.0	8.5		
	2	1.30	0.147	4.0	7.3		
	3	1.30	0.220	4.0	7.3		

For $n > 50$ the distribution approaches the normal distribution. For small n the distribution is quite asymmetric. Furthermore α and β are not independent random variables; their correlation coefficient can be computed as

$$\text{cov}(\alpha, \beta) = \sigma^2 \frac{m_\alpha - \bar{M}}{\sum (m_\alpha - \bar{M})^2}, \quad (11)$$

where

$$\text{var} \hat{\beta} = \frac{\sigma^2}{\sum (m_\alpha - \bar{M})^2} \quad (12)$$

and

$$\text{var} \hat{\alpha} = \sigma^2 \left(\frac{1}{n} + \frac{\bar{M}}{\sum (m_\alpha - \bar{M})^2} \right) \quad (13)$$

An estimation of m_1 the upper value of M , for each source area can be made from a statistical analysis using an extreme value type III distribution and geotectonic information; MM intensity as presented by Brazee (1976) can also be used or it can be obtained in terms of energy released (Lomnitz 1974). Results from different authors agree well with the values presented in Table V; hence, m_1 requires no further discussion at present.

3.3.4 On Elastodynamics of Earthquake Source Mechanism

In the preceding sections earthquake generation has been characterized in terms of time of occurrence, epicentral location and magnitude. It is still necessary, however, to quantify the earthquake action over a structure located at a given distance from the focus. When the dimensions of the surface rupture are of the same order as the distance to the location of interest (near field), the magnitude is not enough to characterize the earthquake at the source. The effect of other parameters connected with the elastodynamics of the system, can be very significant. For epicentral distances large in comparison with the dimensions of the surface rupture (far field), the magnitude becomes dominant. In studying the San Francisco Bay Area the importance of the generating mechanism cannot be ignored.

The mechanism of generation for both the near field and far field in terms of spectral ordinates and in terms of peak ground motion parameters*, is reviewed in this section with regard to the source term, and in Section 3.3.5 with regard to curve attenuation with distance; i.e., the propagating term.

* There is a direct correspondence between Fourier spectrum and response spectrum and peak ground motion parameters (Pereira et al, 1977).

Source details of the rupture mechanism are not yet clear because of the limited data available in the near field. However, it is accepted that shallow focus earthquakes which are the most damaging in California, are the result of shear dislocations in the Earth's crust under the stress field imposed by interplate movements. While no exact solutions exist for shear dislocations, there is extensive research in progress into approximate source models. Several elastodynamic models have been developed, which allow computation of the displacement, velocity and acceleration power spectra of the near and far field solutions. They all agree (e.g. Brune 1977) in the following as shown in Fig. 22: the state of stress near the fault increases gradually as a long-term process; failure occurs when the static friction is insufficient to contain the high stresses stored. The potential elastic energy is then transformed into kinetic energy of wave propagation, followed by a readjustment of the state of stress in the vicinity of the source. This phenomenon of rupture may spread along the fault.

The main parameters describing the geometry and the mechanics of the strick-slip fault are

L	- rupture length	}	geometry
A	- fault area		
h	- fault depth		
w	- rupture width		
ρ	- density	}	material
μ	- shear modulus		
\bar{D}	- average displacement		
r	- equivalent source dimension		
σ	- effective dynamic stress		

$R_{\theta\phi}$	- radiation pattern	
$\Delta\sigma$	- stress drop	} global dynamic measure
M_o	- seismic moment	
m	- magnitude (Richter magnitude M , body magnitude m_b or surface magnitude m_s)	
v_R	- rupture velocity along the fault	} source time function
τ	- rupture duration (rising time)	

The five most critical parameters are the magnitude, the seismic moment, the fault rupture, the average displacement and the stress drop.

For the 1906 San Francisco earthquake they were estimated as:

$$m = 8.3, \quad M_o = 5.4 \times 10^{27} \text{ dyne-cm}, \quad L = 300 \text{ km}$$

$$\bar{D} = 4\text{m}, \quad \Delta\sigma \approx 130 \text{ bar.}$$

The five parameters are related in the following way:

$$M_o = \mu A \bar{D} \quad (14)$$

$$\Delta\sigma = \frac{c \mu \bar{D}}{L} \quad (15)$$

and

$$L = a_1 \exp(a_2 M - a_3), \quad (16)$$

where c , a_1 , a_2 and a_3 are constants. Thus the complex elastodynamic model depends only upon two parameters. Figure 23 illustrates an example of the interrelations among the five parameters (Dieterich, 1973).

The Fourier amplitude ground displacement, recorded at distances from the fault such that $\frac{\beta}{\omega R} \ll 1$ (i.e. the far field spectrum) is typically fairly flat in the frequency range 0.1 to 1 Hz. At frequencies below 0.1 Hz, the spectrum is much more variable. Beyond about 2 Hz spectra from different earthquakes show a pronounced decrease with increasing frequency, which is fairly linear on a log (- log) plot and typically has a slope of about -2 to -3. The horizontal portion of the spectrum is usually

called Ω_0 and can be estimated from M in the following way:

$$\Omega_0 = \frac{1}{4\pi R} \frac{M_0}{\mu} \frac{1}{\beta} R_{\theta\phi}^* \quad (\text{for S waves}) \quad (17)$$

where R is the focal distance, β the shear velocity and $R_{\theta\phi}$ the radiation pattern. For the other waves the formulae are identical $R_{\theta\phi}$ depends on the mechanism of generation, on the type of wave and is very much influenced by the propagating rupture. The four-lobe representation for the overall performance is still not well documented. Thus the use of $R_{\theta\phi} = 1$ is strongly recommended for all circumstances.

The intersection of the two lines defines the so-called corner frequency f_c , which is generally connected with the geometry of faulting, the magnitude and the azimuth. f_c can be computed from the formula

$$f_c = \frac{2.34 \beta}{2\pi r} \quad (18)$$

where r represents an equivalent source dimension obtained from

$$r = \left(\frac{M}{\Delta\phi}\right)^{1/3}.$$

The slope γ of the asymptote depends on the details of propagation of rupture, rising time, etc.. In Central California, Johnson and McEvilly (1974) observed that corner frequencies are only weakly dependent on magnitude. In fact, data from earthquakes are surprisingly similar in regard to the fundamental source parameters with only the seismic moment showing strong dependence on magnitude. Johnson and McEvilly propose the following expressions to relate M_0 and f_c with m

$$\begin{aligned} \log M_0 &= (17.60 \pm 0.28) \pm (1.16 \pm 0.06) m \\ \log f_c &= (0.48 \pm 0.12) \pm (0.079 \pm 0.030) m. \end{aligned} \quad (19)$$

* To get the spectral acceleration the relation $A_0 = (2\pi f_0)^2 \Omega_0$ should be used.

The high frequency asymptote of the spectrum is typically about -2. For the San Andreas fault the following relation between L and m has been proposed

$$L = \exp(0.836 m - 1.08)$$

although some authors prefer a function of L^2 or L^3 instead of L (see Tocher et al., 1977).

For very short epicentral locations, just in the vicinity of the fault, the Fourier amplitudes for the lower frequencies do not show the features of the far-field spectrum. In fact, the near-field solution exhibits an asymptote proportional to ω^{-1} in the low frequency range (Fig. 22). Figure 24 shows the influence of the mechanism of rupture on the acceleration source spectrum. Data were obtained from Berrill's analysis (1975) of the San Fernando earthquake. In both situations the seismic moment is $M_0 = 10^{26}$ dyne-cm; the full line corresponds to $r = 12$ km and the dotted spectrum corresponds to $r = 6$ km which is the hypothesis of a massive initial rupture over a much smaller area.

As will be seen in the next section, peak ground motion parameters are good indicators to predict the performance of structures. Unfortunately there is little information on strong motion recordings in the near field. There are indications that the intensity of ground motion close to the fault zone, even for moderate earthquakes, is large. An extrapolation into the near field using the far-field data should be exercised with caution (Fig. 24). The curves should become flat close to the fault to reflect the finite limits of motion at the fault surface.

According to the theories of elastodynamics near the source, initial particle velocities depend on the density and rigidity of the material

surrounding the fault and on the stress drop,

$$\dot{u} = \frac{\Delta\sigma}{\mu} \beta ; \quad (20)$$

peak acceleration depends on these parameters and also on the high frequency cut off in the response content

$$\ddot{u} = \frac{2\Delta\sigma}{\rho\beta\tau} \approx \frac{2c\mu}{\rho\beta\tau} \frac{\bar{D}}{L} . \quad (21)$$

High stress drop can induce large initial particle velocities of the order of 100 cm/sec and an upper bound acceleration of 2 g.

These values may be expected on competent rocks but on unconsolidated alluvium the strength may be insufficient to transmit such intense motion to the surface.

There has been a tendency to specify very large values for the ground parameters, such as in the northern San Fernando Valley (Degenkolb, 1975), but there is no reference to the probability associated with such motion.

Uncertainty is still very large in these determinations. Tocher et al. (1977) suggest that a full probabilistic treatment should be exercised over the entire problem.

In resumé, the two-parameter model simulating the earthquake mechanism at the source can be either the seismic moment and the corner frequency or the magnitude and the stress drop. The correspondence between the two models is obvious. In the following chapters attention will mostly be on the latter representation.

3.3.5 On Wave Propagation

The seismic waves generated at the source propagate in all directions obeying two general attenuation features:

- a) geometrical spreading attenuation - P and S waves at large distances compared to the source dimensions are attenuated as R^{-1} ; surface

waves are attenuated as $R^{-1/2}$. At short distances the geometric attenuation is a function of the source parameters and mechanisms of generation, and the amplitudes decay in proportion to R^{-2} (near-field solution).

b) material attenuation - the internal dissipation of energy introduces an attenuation approximately represented by the model

$$A(\omega, R) = A(\omega, 0) \exp[-a(\omega) R] \quad (22)$$

where

$$a(\omega) = \frac{\omega}{2Qc}$$

c is the phase velocity; $1/Q$ is the specific attenuation; $A(\omega, R)$ the Fourier amplitude at distance R and $A(\omega, 0)$ the Fourier amplitude at $R = 0$. The larger Q is, the smaller is the damping. For California $Q \approx 400$.

With this formulation the wave attenuation is a function of the distance, of the earthquake size at the source and of the frequency. The Fourier amplitude at a given location is obtained from the product of the source spectrum and the attenuation (Fig. 24).

Berrill (1975) computed the Fourier amplitude of acceleration $A(\omega, 0)$ at the source from analysis of high frequency strong motion ($0.4 < f < 16$ Hz) in the San Fernando earthquake of 1971, using a two-parameter model and a least squares fitting.

However, the present state of knowledge of seismic loads and their effect on structures suggests that peak ground acceleration (a_{\max}), velocity (v_{\max}), displacement (d_{\max}), and duration of ground motion (s_{\max}) are suitable characteristics to define earthquake ground motion (Newmark and Rosenblueth, 1971). Actually a_{\max} and d_{\max} are fairly good indicators of the response of structures possessing, respectively, very high (>2 Hz) and very low (<0.5 Hz) natural frequencies. In the intermediate range of natural periods v_{\max} correlates better with the response but the correlation is less precise than that of the former parameters.

These parameters are not all independent. ad/v^2 and v/a were proposed as two important parameters controlling the construction of response spectra. They are somehow related to the transitions $a \rightarrow v$ and $v \rightarrow d$ in the spectrum. Without going into details it can be said that ad/v^2 and v/a increase with distance, but while the former decreases with magnitude the latter increases.

Johnson (1973), Lynch (1969) and McGuire (1974) made correlation studies on ground motion parameters and on response spectra. The former used data from nuclear events in Nevada and the latter studied the San Fernando earthquake. In general, better correlations are obtained for intermediate natural periods in terms of spectral response ordinates. Spectral ordinates do not, however, yield better correlations for the low and high range of natural periods (McGuire, 1974; Esteva, 1977).

Peak ground displacement attenuates with distance at a rate less than velocity, and velocity at a rate less than acceleration. The transition between the near field and the far field is fixed by the intersection of the two straight lines.

The above considerations have led to the use of empirical formulae of the following form

$$y = b_1 e^{b_2 m} [f(R)]^{-b_3} \epsilon \Delta \sigma \quad (23)$$

to express the attenuations of the several types of waves present in the ground motion, where

y represents a_{\max} , v_{\max} , d_{\max} or the pseudospectral velocities,

b_1, b_2, b_3 are constants to fit the experimental data,

$f(R)$ is a function of focal distance,

ϵ is a random variable which takes into consideration the dispersion between the experimental data and the computed values using the above

formula, and

$\Delta\sigma$ is a variable representing the effect of stress drop in the case of the near-field solution. As a simplification $\Delta\sigma$ may be taken as a function of the type of faulting (strike-slip, normal or thrust).

Table VI shows the values proposed by different authors for the attenuation formulae considered in this study. Coefficients of dispersion are also given. The dispersion is seen to be very large. The preceding discussion is required to obtain the response spectra for any given M,R (and $\Delta\sigma$ for the near field) in a given region. For the statistical characterization of any parameters defining response spectra it is necessary to have sufficient data and this is available only for a limited number of areas and mainly in terms of acceleration. To obtain response spectra in regions with little data, the shape of spectral densities from other regions has to be adopted and suitably scaled. Figure 25 presents the different formulae of Table VI.

Brazee (1976) studied the area of perceptibility for earthquakes occurring in California and Western Nevada in terms of magnitude. He did not, however, study the effect of radiation. McEvelly and Simla (1972) also studied attenuation of intensity with distance.

Duration of earthquake ground motion* depends mainly on the earthquake parameters, and on focal distance. The type of rupture in the fault zone could also be important. McEvelly and Simla showed that the duration for small magnitude earthquakes occurring near San Francisco was almost independent of distance up to 50 miles. For large magnitudes Dobry et al. (1977) present a curve of significant duration as a function of m and R valid for the Western United States. Here, the geology also plays an important part.

* No single measure of duration has yet been widely accepted. Roughly speaking it corresponds to the intense phase of shaking or to the time for which acceleration is kept above a given threshold.

TABLE VI
Attenuation Formulae with Distance

Ground motion parameters: $y = b_1 \exp(b_2 m) [F(R)]^{-b_3}$							
AUTHOR	y	b_1	b_2	b_3	f(R)	σ	IDENTIF
McGuire	a, cm s ⁻²	472	0.640	1.301	R+25	0.51	a ₁
Donovan	"	1080	0.50	1.32	"	0.707	a ₂
Esteva	"	5000	0.8	2.0	R+40	--	a ₃
McGuire	v, cm s ⁻¹	5.64	0.923	1.202	R+25	0.63	v ₁
Correction $I = \frac{\log 14v}{\log 2}$	"	52.6	0.579	1.32	"	--	v ₂
McGuire	d, cm	0.393	0.999	0.885	"	0.76	d ₁
5% damped spectral pseudo-velocities: $S_v = a' 10^{bm} [F(R)]^{-c}$							
	Period(sec)	a'	b	c	f(R)	σ	
McGuire	0.1	10.09	0.233	1.341	R+25	0.59	
	0.2	31.45	0.226	1.323	"	0.54	
	0.5	5.74	0.356	1.197	"	0.55	
	0.8	1.245	0.415	1.020	"	0.58	
	1.0	0.432	0.399	0.704	"	0.63	
	2.0	0.122	0.466	0.675	"	0.80	
	5.0	0.0706	0.557	0.938	"	0.94	
	8.0	0.1475	0.435	0.767	"	0.82	
Johnson	0.055	2.691	0.303	1.395			$\sigma \equiv$ Standard deviation of $\ln y$
	0.101	7.497	0.327	1.558			Duration in Sec:
	0.248	20.01	0.305	1.396			$s_1 = 10^{(0.435m-1.85)+0.3R}$
	0.609	2.067	0.429	1.135			$s_2 = 0.02 \exp^{(0.74m)+0.3R}$
	1.004	0.831	0.501	1.134			
	2.469	0.405	0.532	1.137			

Soil sites show much more scatter, with durations on rock providing a lower bound. The larger durations recorded at soil formations seem to be caused by long period motions at the end of the record, perhaps associated with surface waves, (see Dobry et al., 1977). In this analysis the following expression, based on the above discussion, was used for duration

$$s = d_1 e^{d_2 m} + d_3 R \quad (24)$$

The values of parameters d_1 , d_2 and d_3 used in the analysis are given in Table VI and Fig. 26.

The effect of duration is of prime importance in the study of cumulative damage in structures, mainly in soil structures. The phenomenon of liquefaction of sands is a typical example where the duration and the acceleration of ground motion play a very important role. In fact, laboratory test data have indicated that the greater the number of applications of a given level of acceleration, the smaller the dynamic strength of sand against liquefaction. For a complete analysis the statistics of both acceleration and duration should be known. Even though a positive correlation would be expected between these two random variables no correlation studies have been done so far in the area.

The predominant period, T_p , of ground motion, connected with the frequency content of the waves, is another characteristic often used in the literature. For California, T_p can be written as

$$T_p = \begin{cases} \frac{m}{27} + m^{2.5} \frac{R}{67000} & R \geq 40 \text{ km} \\ \frac{m}{27} & R < 40 \text{ km} \end{cases} \quad (\text{in sec}) \quad (25)$$

These two last expressions represent mean values of samples with large dispersion.

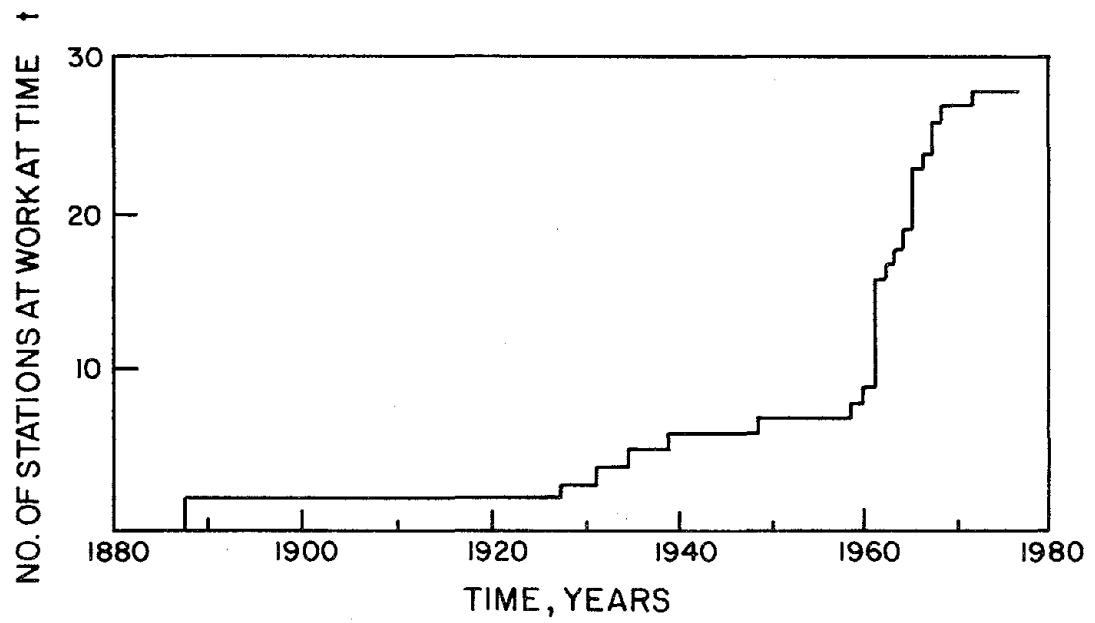


FIGURE 10 NUMBERS OF SEISMOGRAPHIC STATIONS OPERATING SINCE 1887

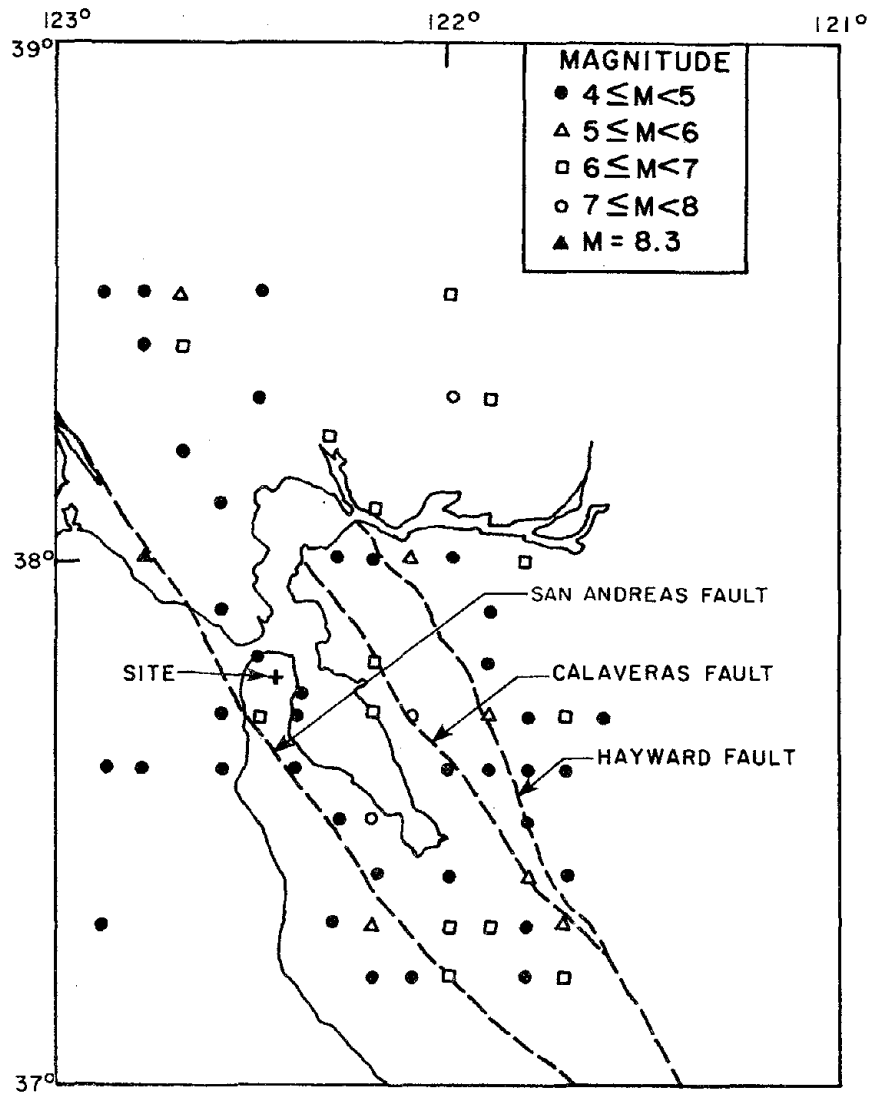


FIGURE 11(a) MAP OF EPICENTERS FOR THE SAN FRANCISCO REGION OF EARTHQUAKES WITH $M \geq 4$ FOR THE PERIOD 1807-1969

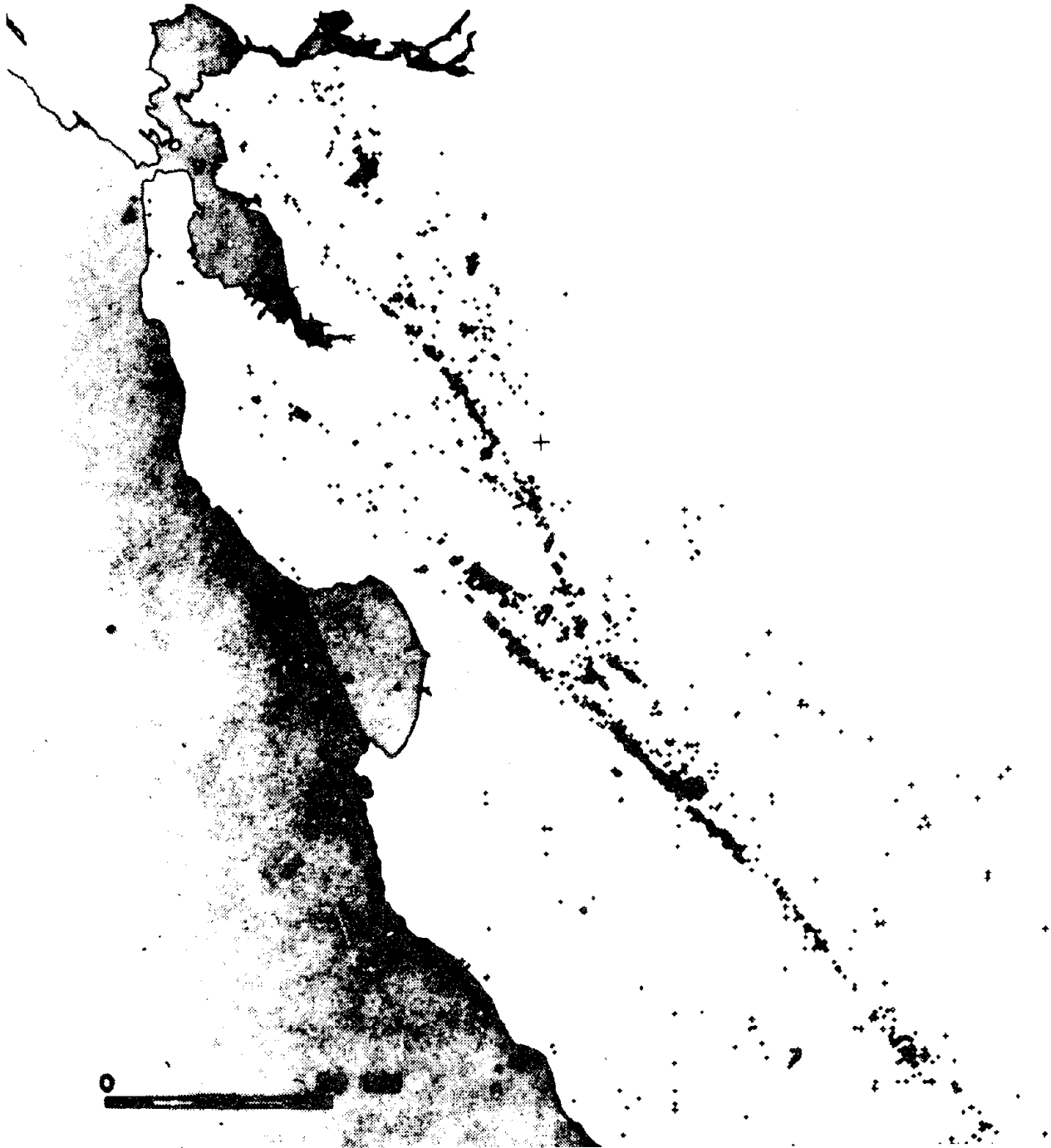


FIGURE 11 (c) MICROEARTHQUAKES RECORDED DURING 1970
(U.S. GEOLOGICAL SURVEY)

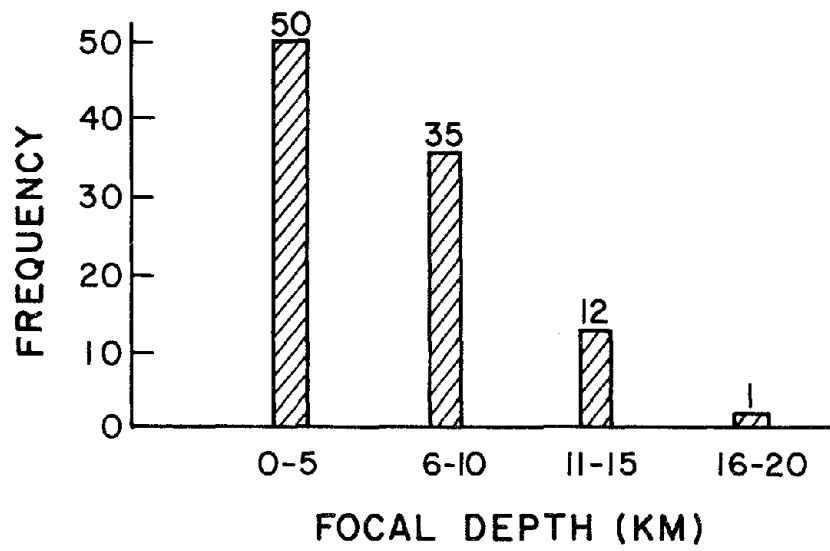
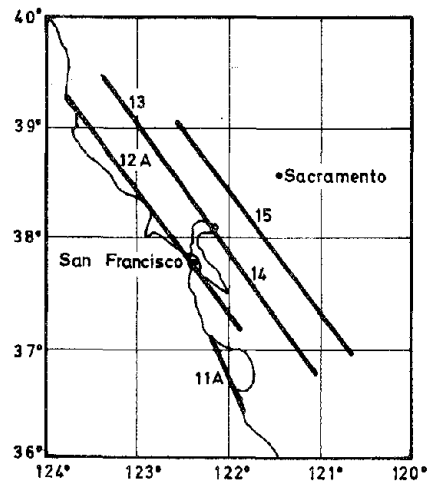
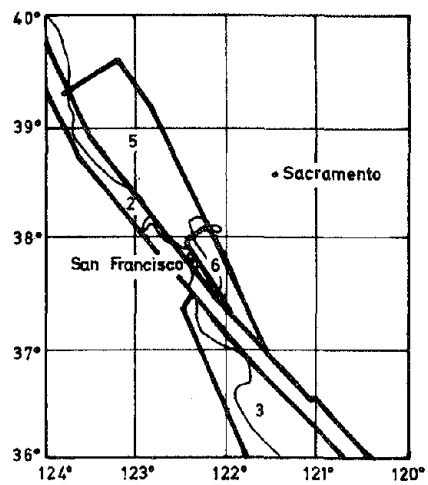


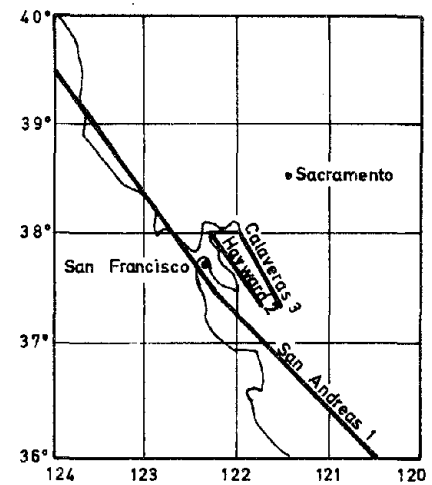
FIGURE 12 STATISTICAL ANALYSIS OF FOCAL DEPTHS



(a) After Kiremidjian and Shah (1975)



(b) After Algermissen and Perkins (1976)



(c) After Kiureghian and Ang (1975)

FIGURE 13 EARTHQUAKE SOURCE AREAS

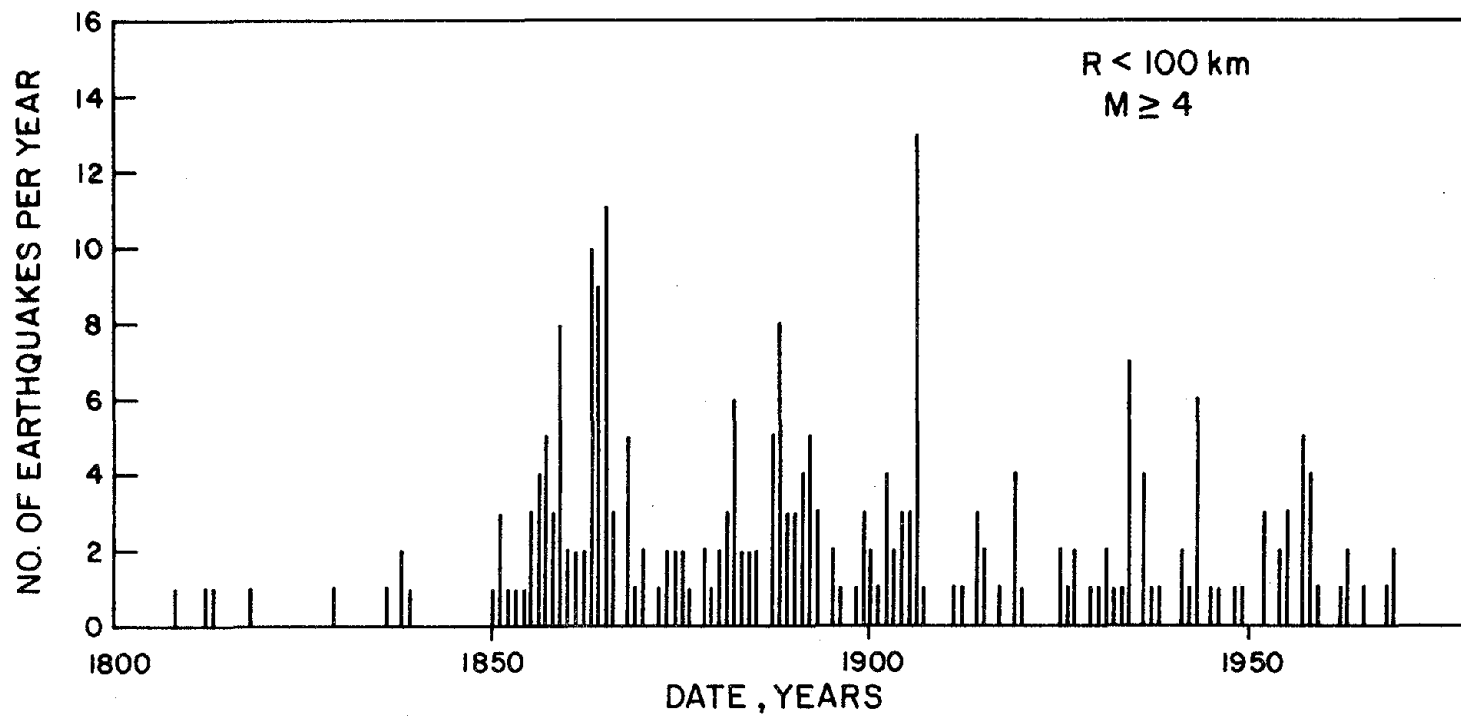
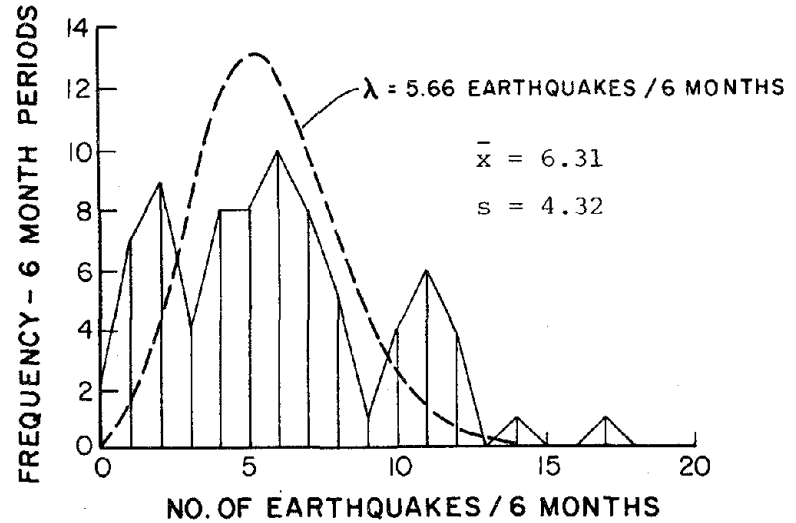
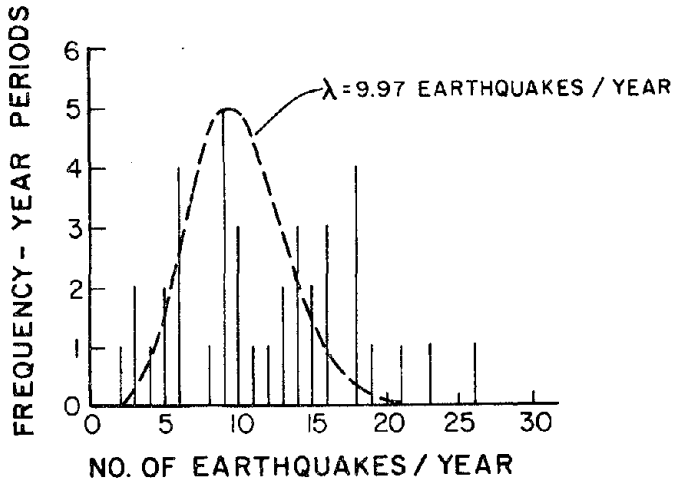
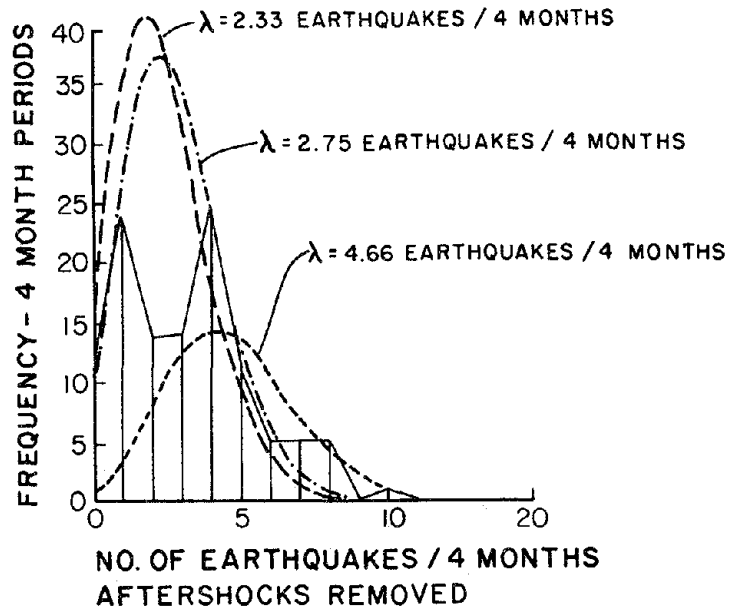
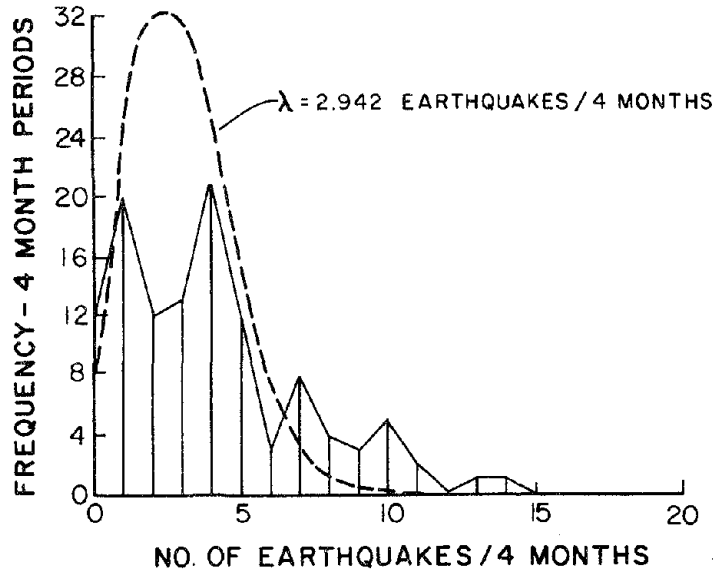


FIGURE 14 HISTORICAL DATA OF RECORDED EARTHQUAKES WITHIN 100 km OF SAN FRANCISCO



χ^2 TEST
 $< 0.1\%$ SIGNIFICANCE

459 EARTHQUAKES WITH $M > 3.5$ FROM 1934 TO 1972

FIGURE 15 TESTING THE POISSON MODEL FOR TIME EVENTS

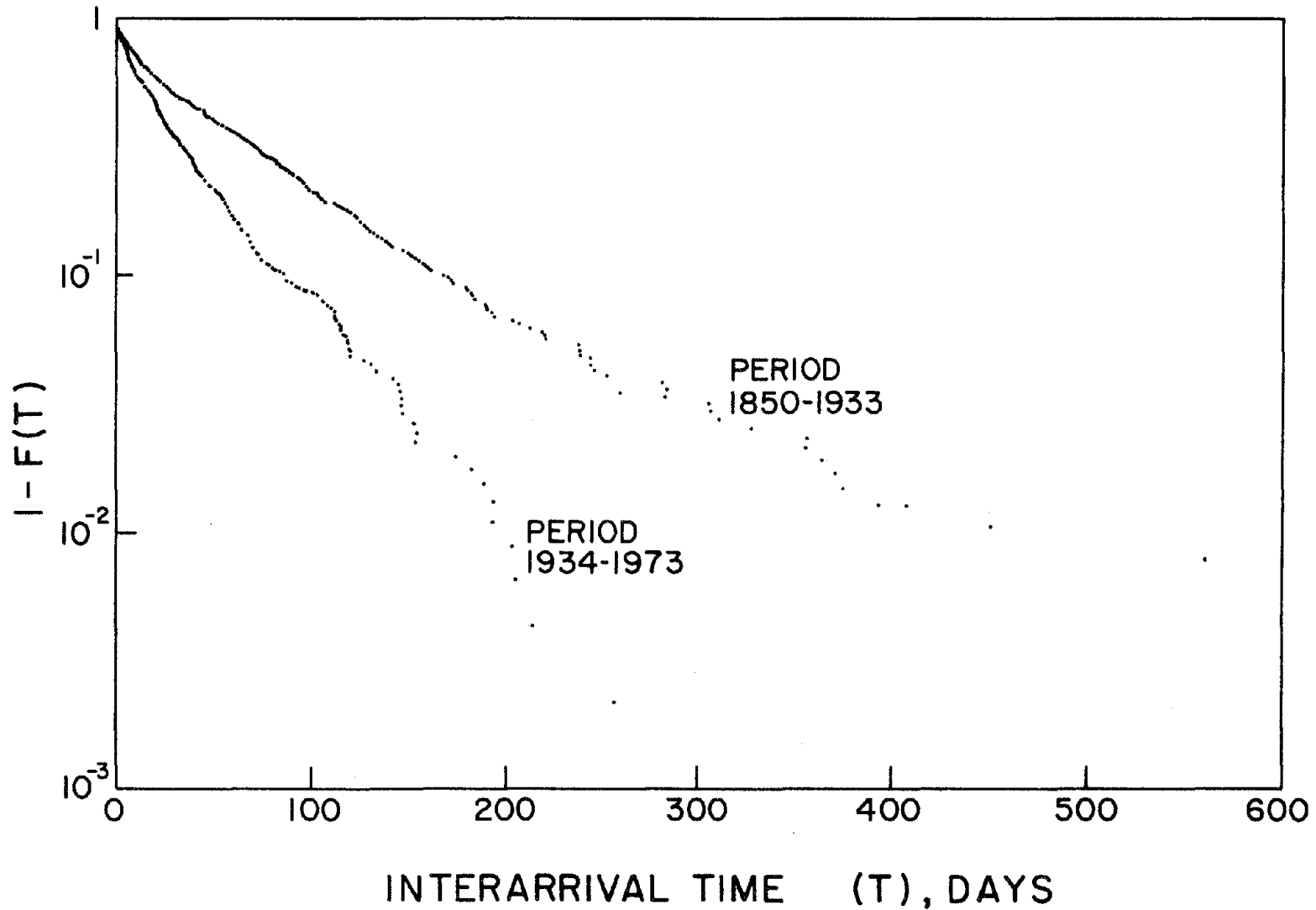


FIGURE 16 TESTING THE TIME INTERVAL BETWEEN CONSECUTIVE EVENTS FOR THE PERIODS 1934-1973 AND 1850-1933

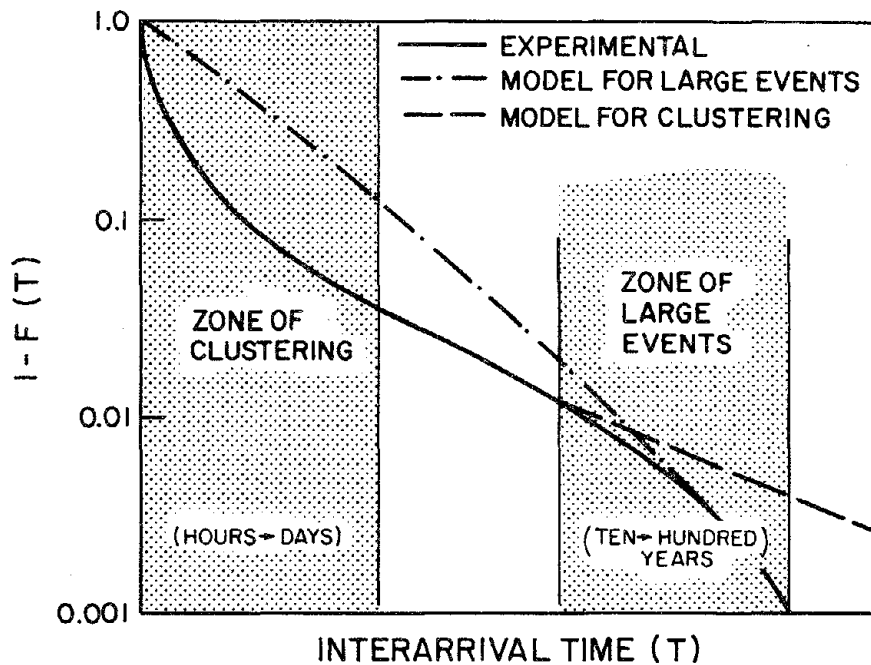


FIGURE 17 INTERPRETATION FOR THE TIME INTERVAL BETWEEN CONSECUTIVE EVENTS

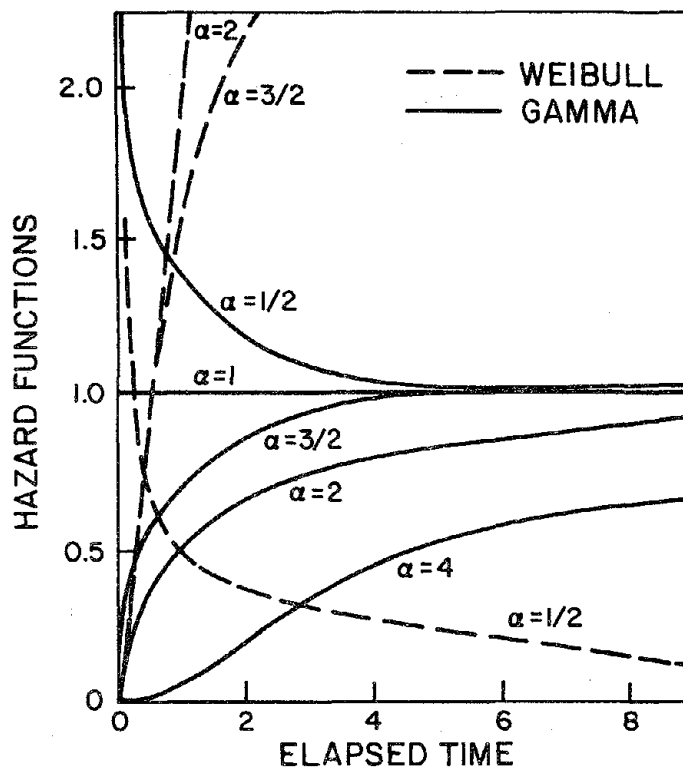


FIGURE 18 HAZARD FUNCTION FOR THE GAMMA AND WEIBULL DISTRIBUTIONS ($\lambda = 1$)

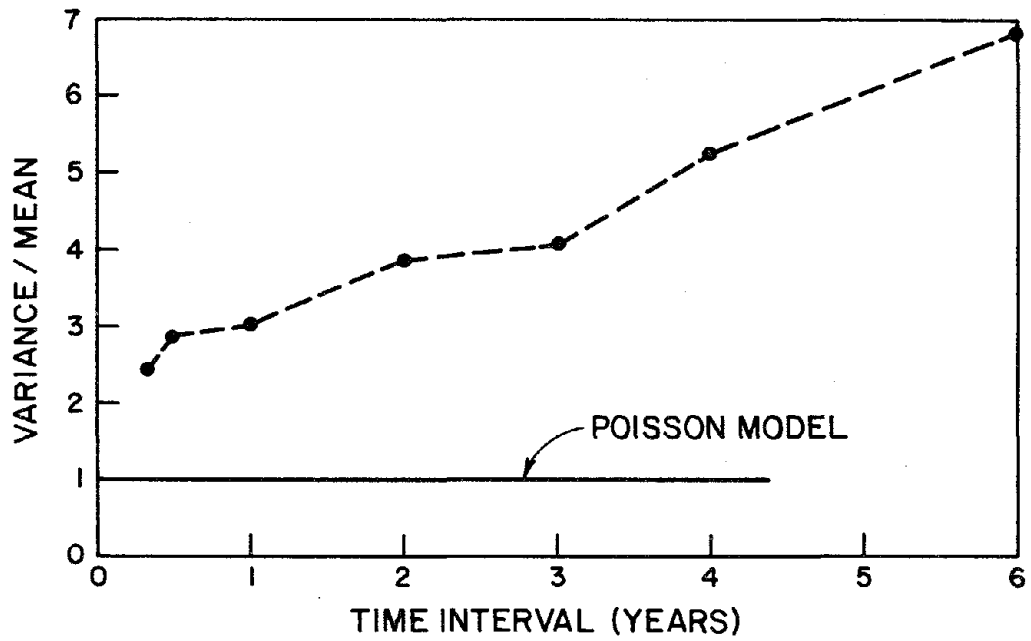


FIGURE 19 VALUES OF THE POISSON DISPERSION COEFFICIENT (VARIANCE/MEAN) AS A FUNCTION OF INCREASING TIME INTERVAL

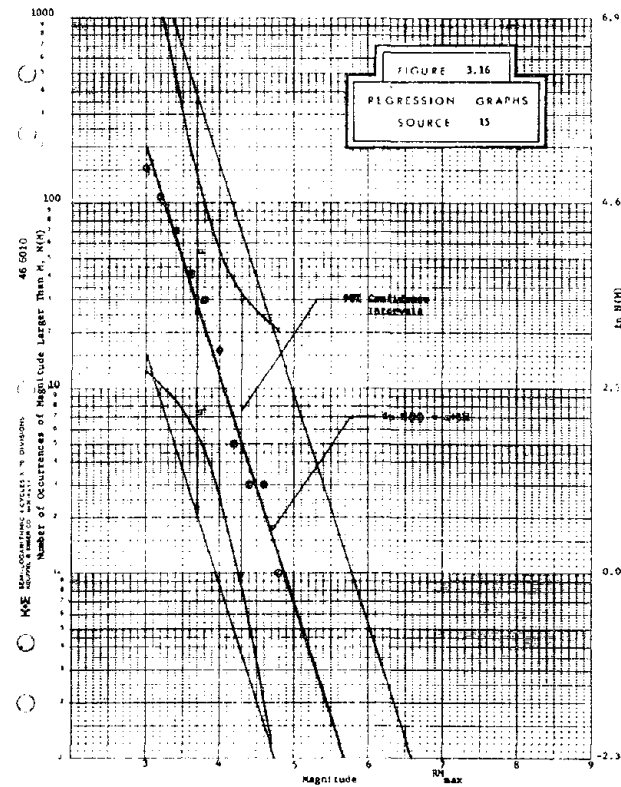
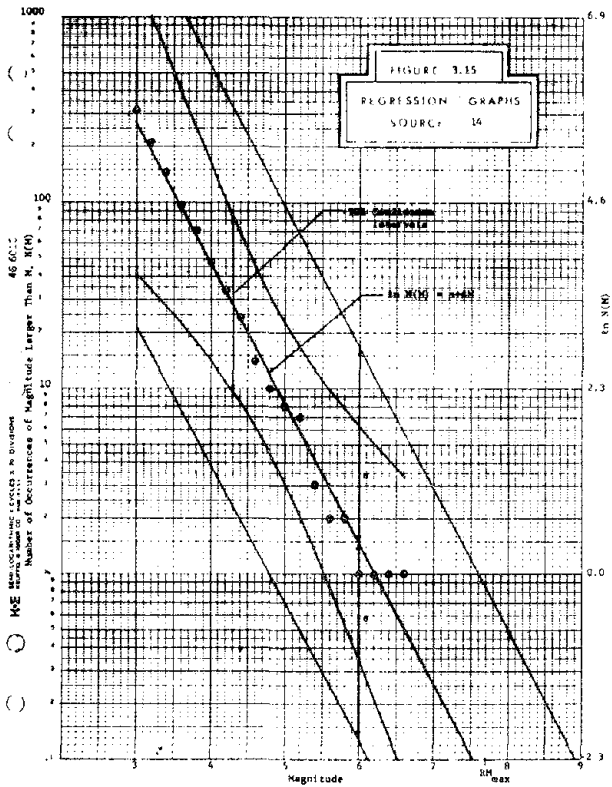
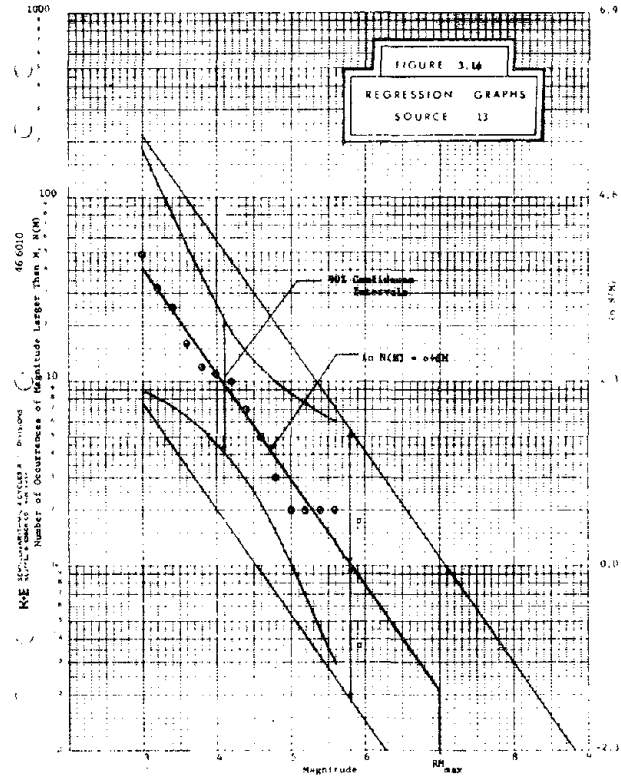
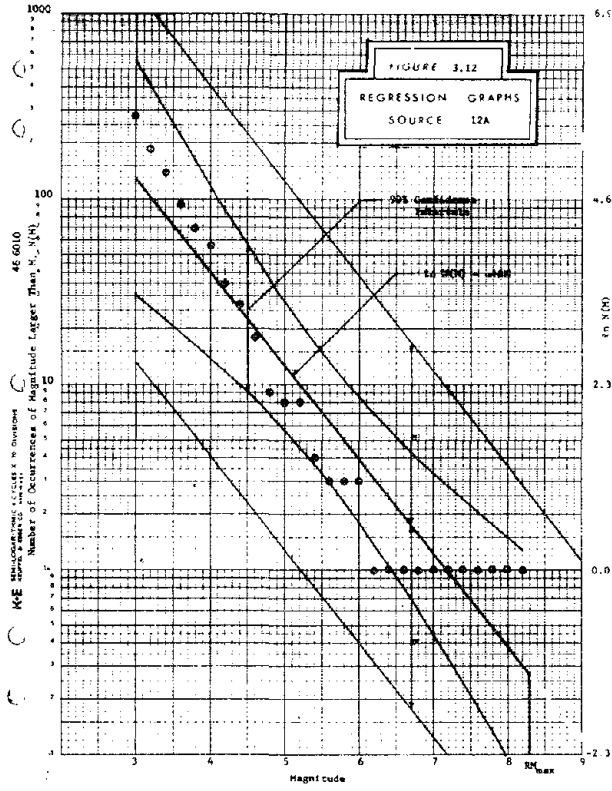
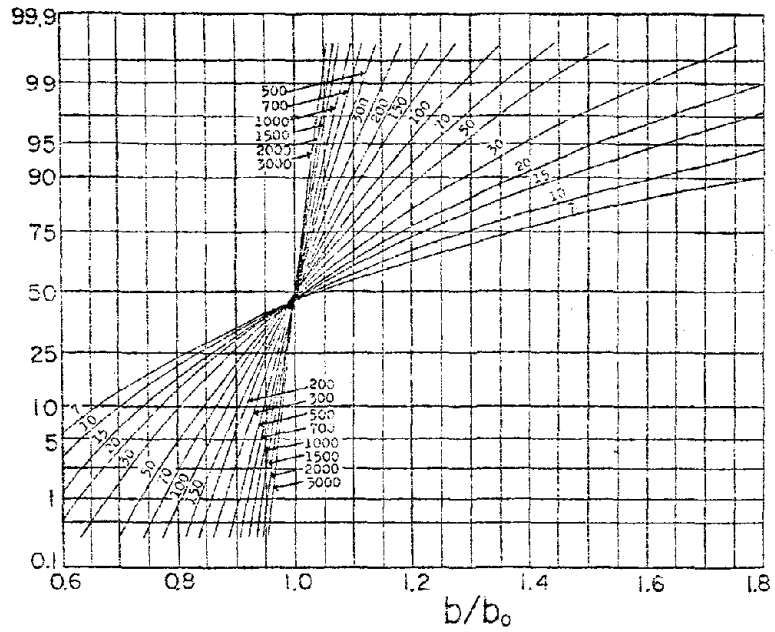


FIGURE 20 PROBABILITY DISTRIBUTIONS OF MAGNITUDE FOR THE SOURCE AREAS SHOWN IN FIGURE 13(a)

After Kiremidjian and Shah (1975)



After Utsu (1966)

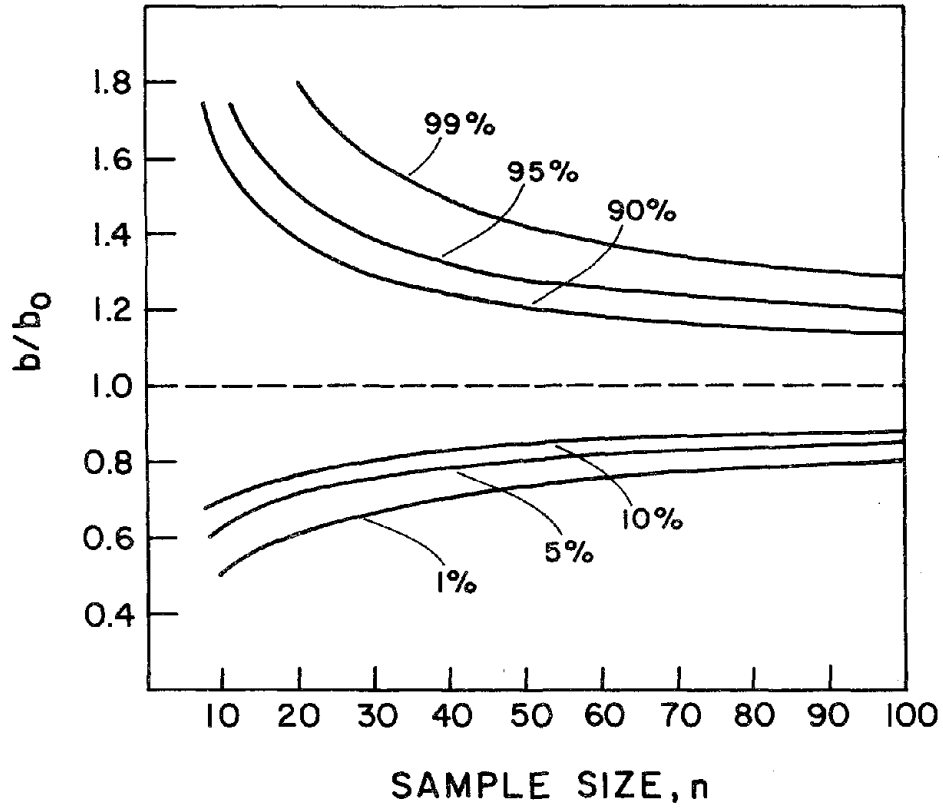
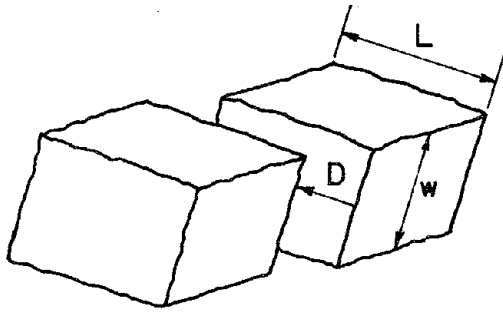
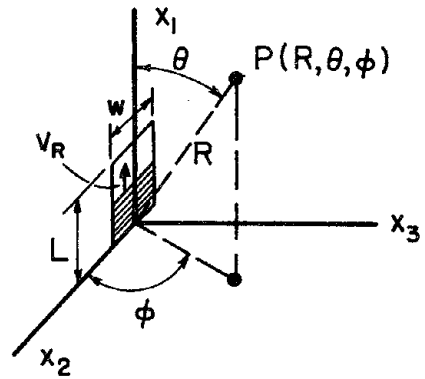


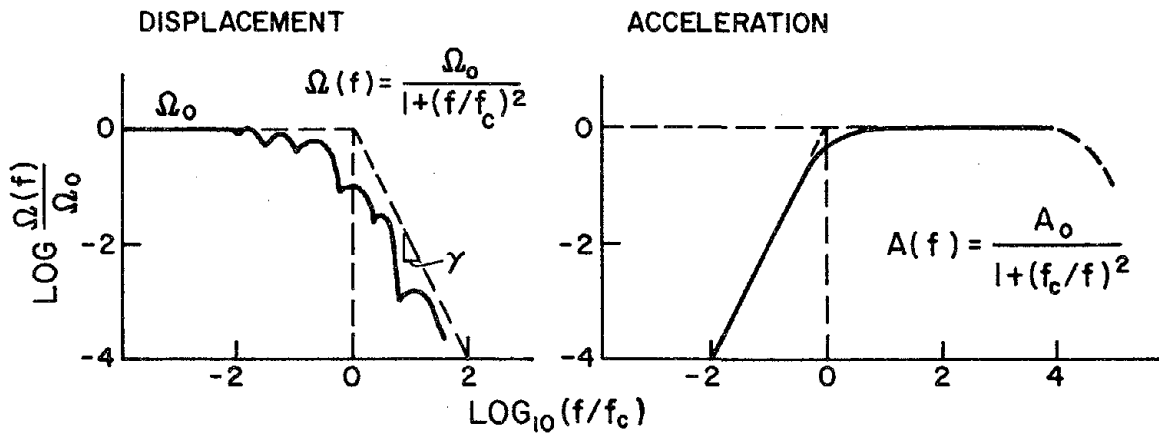
FIGURE 21 PROBABILITY DISTRIBUTION OF b/b_0



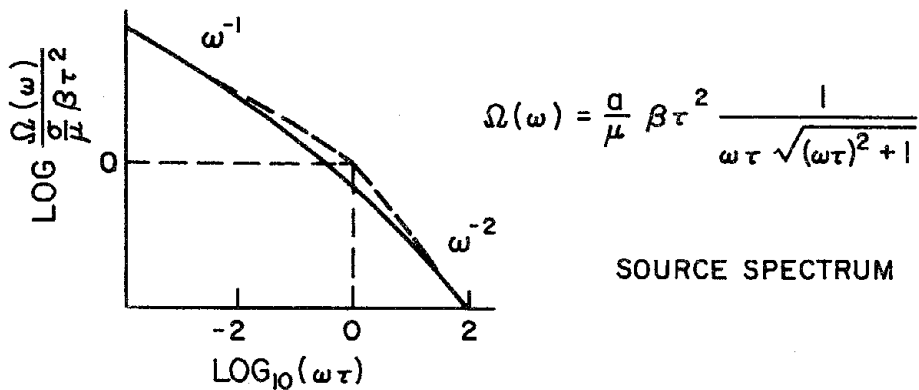
(a) FAULT MODEL



(b) SPHERICAL COORDINATE SYSTEM



(c) FOURIER AMPLITUDE SPECTRUM OF THE FAR-FIELD



(d) FOURIER AMPLITUDE SPECTRUM OF THE NEAR-FIELD

FIGURE 22 EARTHQUAKE ELASTODYNAMIC MODEL OF FAULT MECHANISM

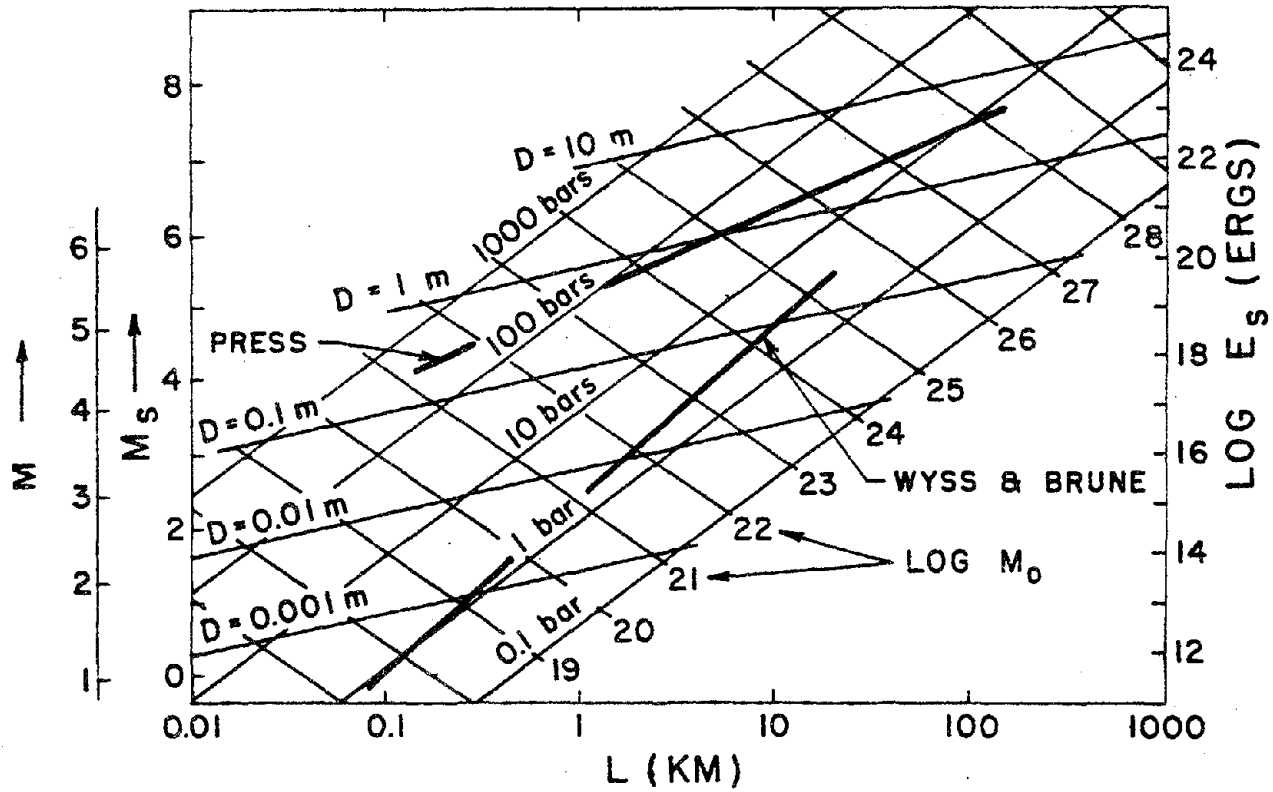
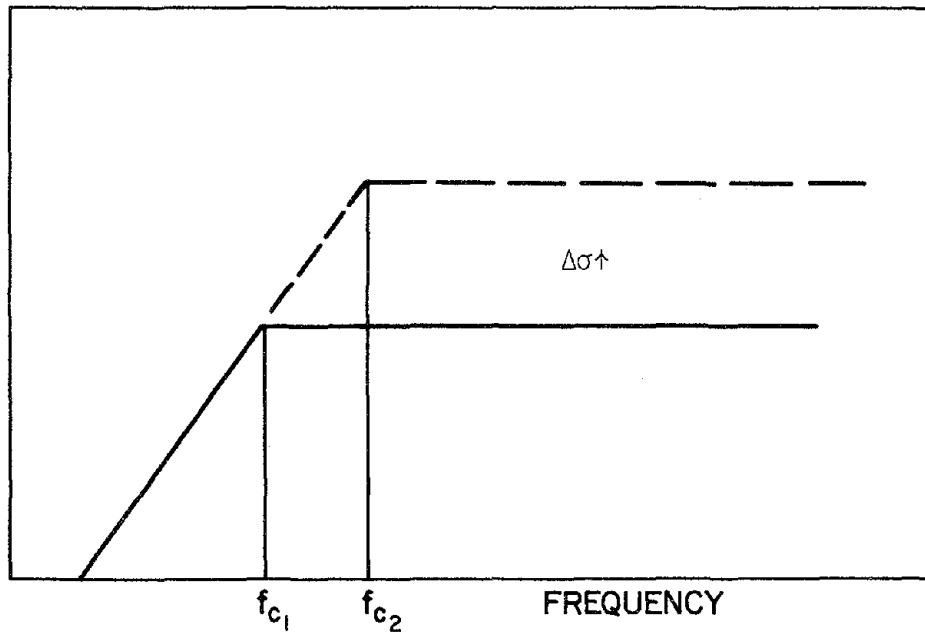


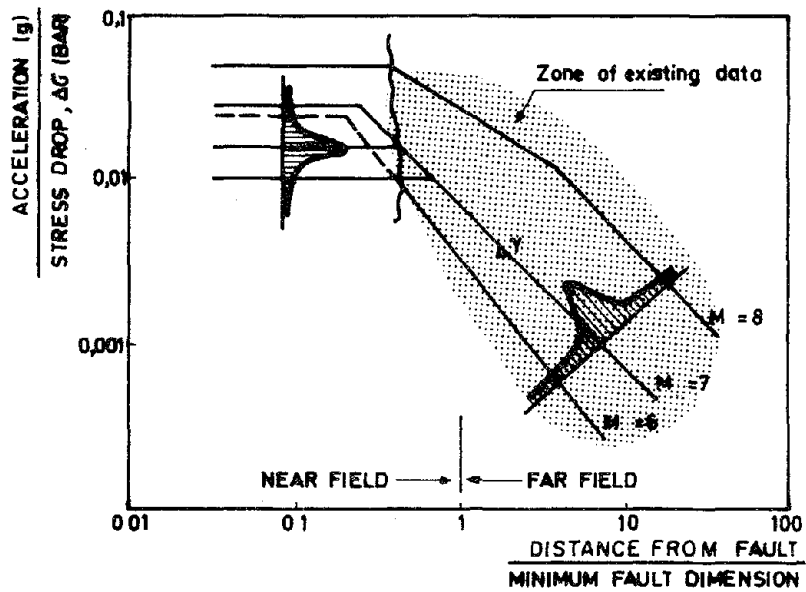
FIGURE 23 INTERRELATIONS AMONG THE FIVE MOST IMPORTANT PARAMETERS CHARACTERIZING THE ELASTODYNAMICS OF EARTHQUAKE GENERATION

After Dieterich (1973)

FOURIER AMPLITUDE SPECTRUM



(a) FOURIER AMPLITUDE SPECTRUM



(b) GROUND MOTION PARAMETERS

FIGURE 24 TWO PARAMETER MODEL FOR THE MECHANISM OF EARTHQUAKE GENERATION AT THE SOURCE

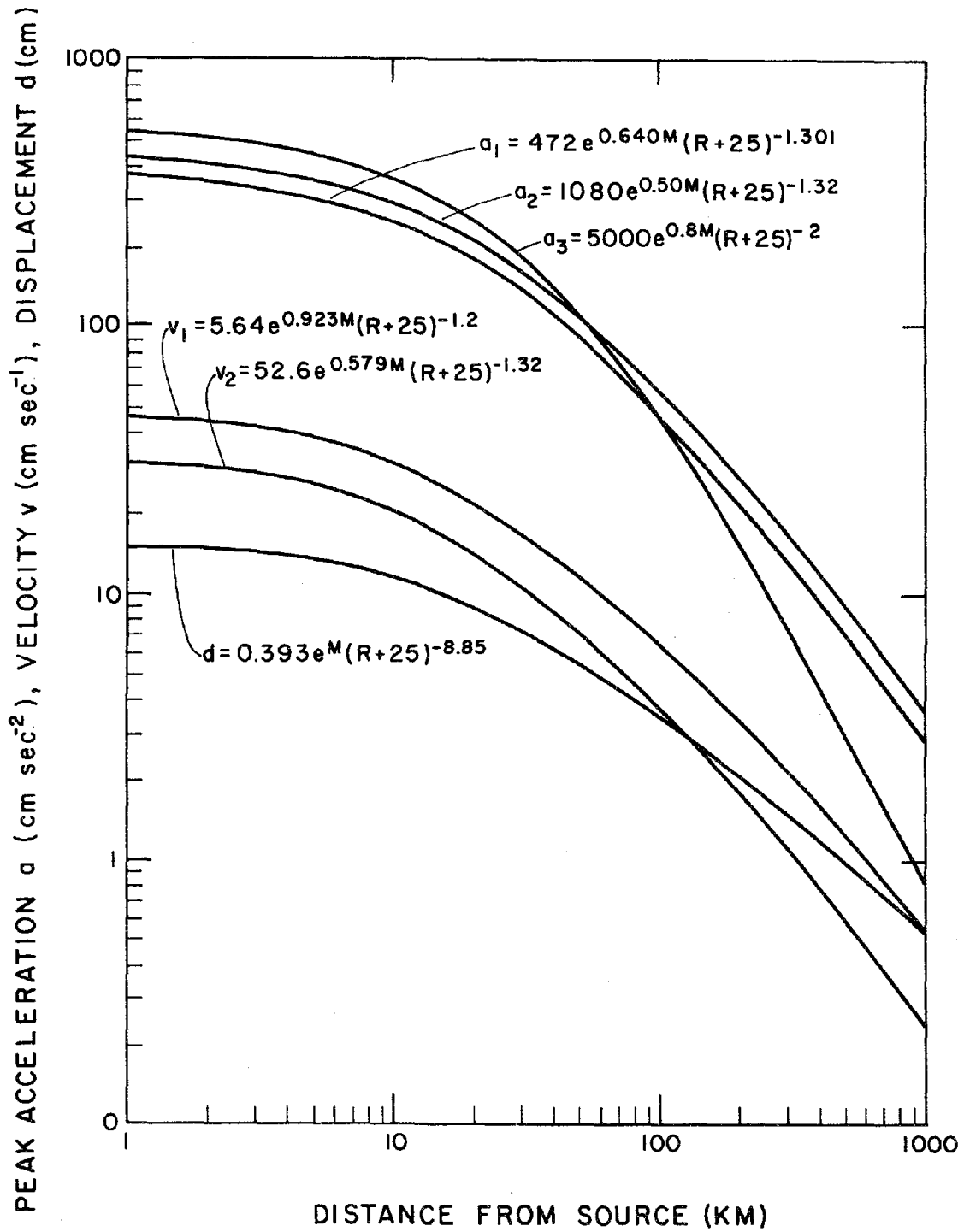


FIGURE 25 COMPARISON BETWEEN DIFFERENT ATTENUATION FORMULAE

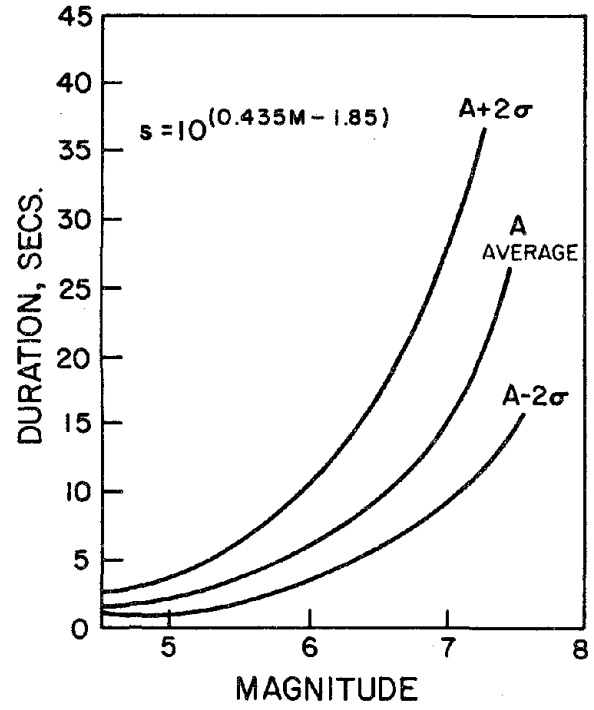
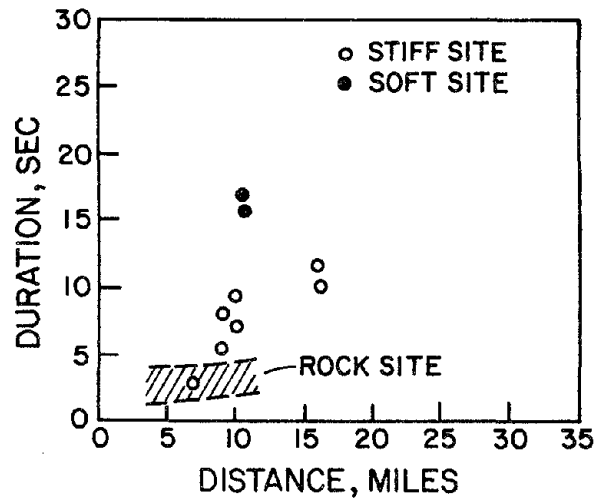


FIGURE 26 SIGNIFICANT DURATION OF GROUND MOTION AS A FUNCTION OF DISTANCE TO SOURCE, SITE CONDITIONS AND MAGNITUDE FOR THE BAY AREA

4. COMPUTER MODELLING FOR RISK ANALYSES

From the probability distributions of the three-dimensional space-time-energy continuum and the form of wave attenuation, it is possible to determine the probability distribution function, pdf, of a ground motion parameter for a site. This probability distribution provides the basic information for preparation of seismic zoning maps. Its development is known as seismic hazard analysis, SHA (Cornell, 1976). Modifications of such zones to reflect local soil conditions are referred to as micro-zoning. If, as well as the seismic hazard analysis, it is of interest to estimate global losses that could be inflicted on a community because of future earthquakes, it is necessary to consider the interaction between the seismic threat and the geographical distribution of population and property. This is referred to as seismic risk analysis, SRA.

4.1 Seismic Hazard Analysis (SHA)

Usually seismic zoning maps are prepared on the basis of peak ground accelerations. Attenuation laws, however, are different for peak ground acceleration, velocity and displacement and, since the design of different types of structures may be governed by one of these, it is meaningful to prepare separate zoning maps for each of these parameters. Further, in order to have a full description of the response spectra, seismic zoning maps could be developed directly in terms of response spectra, taking into account the changes in spectral ordinates due to magnitude and distance. For soil structures duration of motion might be very important justifying the preparation of a map of duration of strong motion. It might also be useful to develop joint probability distributions of two or more parameters.

To obtain the probability density function for extreme values of one of the parameters defined in the formula

$$y = b_1 e^{b_2 m} [f(R)]^{-b_3}$$

as the result of uncertainty in time, space and intensity, there are two main methods of analysis: (i) The analytical method considers different earthquake source areas characterized by the parameters β_i , λ_i , m_{oi} and m_{1i} and uses standard techniques of transformation of variables to transform the 3-dimensional space-time-energy into a 1-dimensional y-space; and (ii) the experimental or empirical method considers the simple family of earthquakes that have occurred, and transforms it using the attenuation law into a parameter y at the site. Only then can a statistical analysis of the extreme value be made.

Consider first the analytical method.

Assuming that the time process is Poisson with mean value λ , the magnitude is a doubly truncated negative exponential random variable, the attenuation law is given by Eq.(23) with $\ln \epsilon$ as a normal random variable where $\ln \epsilon$ has zero mean value and variance σ , then for a point-source mechanism the extreme probability density function in a period t for a given hypocentral location R is, according to Merz and Cornell (1973),

$$G_Y(y) = \text{Prob} [y_{\max} > y] \approx 1 - \exp(-P_Y \lambda t) \quad (26)$$

where

$$P_Y = (1 - K_{m1}) \left[\Phi^* \left(\frac{z}{\sigma} \right) - \Phi^* \left(\frac{z'}{\sigma} \right) \right] + \sigma^* \left(\frac{z'}{\sigma} \right) + K_{m1} \left[\Phi^* \left(\frac{z}{\sigma} - \frac{\beta\sigma}{b_2} \right) - \Phi^* \left(\frac{z'}{\sigma} - \frac{\beta\sigma}{b_2} \right) \right] e^{\beta^2 \sigma^2 / 2b_2^2} e^{\beta m_0} R^{-\beta b_3 / b_2} \left(\frac{y}{b_1} \right)^{-\beta / b_2}$$

where

$$K_{m_1} = \left[1 - e^{-\beta(m_1 - m_0)} \right]^{-1}, \quad \beta = b \ln 10$$

$$z = \ln y - \ln(b_1 e^{b_2 m_1} R^{-b_3})$$

$$z' = \ln y - \ln(b_1 e^{b_2 m_0} R^{-b_3})$$

$\Phi^*(\cdot)$ = complementary cumulative distribution function
of the standardized Gaussian distribution

The above function should be integrated over the entire earthquake source area so that all possible locations of earthquakes are considered. In the case of several independent source areas the distribution of probability is given by

$$G_Y(y) = \prod_{j=1}^n G_{Y_j}(y) \quad (27)$$

The integration over the area is done numerically. Quadrilateral area elements with parabolic sides were used in the development of the computer program needed to perform the integration. (For details see Oliveira, 1977.)

As was seen in Chapters 2 and 3, statistical data as well as the mechanics of generation indicate that the above-mentioned model should be implemented, so that uncertainties in the final probability distribution function of y are reduced.

To these uncertainties should be added those contained in the historical data arising from the location of epicenters, the evaluation of magnitude, and the incompleteness of the earthquake catalogue. As was pointed out in Chapter 2, errors affecting the determination of L_i , M_i and λ have been reduced considerably with the increase of the seismographic network. Up to 1959 the uncertainty was large and needed to be taken into

account.

Kiremidjian and Shah (1975) studied numerically the influence of a hypothetical 5% uncertainty assumed independently for each parameter over the final probability distribution function; Table VII presents their results. They concluded that the larger uncertainty in the final result of approximately 20% is due primarily to large errors caused by variations in the regression constants α and β . Another source of uncertainty comes from the value of the upper magnitude m_1 . Apparently, however, from Table VII the results are less sensitive to the attenuation constant, and almost insensitive to focal depth and location. These results differ significantly from the ones obtained in this study, as shown in Chapter 5.

TABLE VII

Sensitivity of Peak Ground Acceleration (PGA) for 10%
Chance of Exceedence

Parameter	5% Increase	5% Decrease
Name	% Change in PGA	% Change in PGA
1. Regression		
(a) α	+7%	-6.5%
(b) $ \beta $	-18%	+23%
(c) α and β	+10%	+15%
2. Attenuation		
(a) b_1	+5%	-5%
(b) b_4 ($f(R) = R + b_4$)	-5%	+6.5%
3. Focal Depth	-2%	+2%
4. Fault Location	-1%	+2%
5. m_1	+6.5%	-10%

The experimental method of analysis, which will be used frequently herein is based on extreme value distributions. It can be shown that order statistics from an exponential parent distribution are in the domain of attraction of an extreme value distribution (Hasofar, 1973). Therefore, an equivalence between the cumulative distribution based on a complete earthquake catalogue and the distribution of annual extremes has been suggested. The analysis of annual extremes, which will lead to upper bounds of the whole process, is very simple to apply. To estimate the parameters of the distribution based on the parent distribution referring to n years, the strongest event in each year is selected, the n values are ordered in increasing size and plotted according to the rule

$$P(j) = \frac{j}{n+1}$$

where j stands for the position in the ordered sample.

Extreme value type I and type II paper has been used to plot experimental distributions. When events are subjected to an upper limit on their size, an extreme type III distribution may better fit the data. A parabolic fitting may as well take into consideration the curvature shown in the plots. The techniques for parameter estimation are given in an earlier report (Oliveira, 1974).

The experimental method can be applied to any seismic hazard parameter, directly observed or transformed using the available techniques. In general the event L_i , M_i , T_i , that has taken place is transformed into the site parameter y , using the source-model and the attenuation curves and then annual extremes are plotted. Extrapolation for return periods far beyond the period covered by the data should be exercised with caution.

4.1.1 Definition of source models

The first correction applied to the model is of great importance to hazard analysis in the San Francisco Bay Area; it concerns the two-fold mechanism of rupture in the fault. For sites located near fault zones, a point-source assumption is not realistic because, due to fault rupture, the actual hypocentral distance might be smaller than the one based on the initial origin. This is equivalent to saying that the isoseismals near the fault zone are elongated in the direction of the fault trace. Secondly, the two parameter source model (M and $\Delta\sigma$) will scale the law of attenuation with distance. Both Kiureghian and Ang (1975) and Douglas and Ryall (1975, 1977), have dealt with a line-source model. An extension of Cornell's point-source model (1976) is obtained here by modifying the probability density function of epicentral locations.

Suppose that (i) the fault location is known and (ii) the fault rupture is, from Eq. (16),

$$L = a_1 \exp(a_2 M - a_3).$$

According to Fig. 27 the actual hypocentral distance R_c can be expressed as

$$R_c^2 = d^2 + \text{corr}^2 + h^2 \quad (28)$$

where

$$\text{corr} = \begin{cases} | \text{Proj} | - L & \text{if } | \text{Proj} | - L > 0 \\ 0 & \text{if } | \text{Proj} | - L < 0 \end{cases}$$

Figure 27 can be interpreted as if an epicentral location at point 1 is transferred to point 2 to take into account the line-source mechanism. When the epicentral locations are uniformly distributed along the fault, the corresponding corrected locations are distributed as shown in Fig. 28.

This algorithm does not increase the central processing unit of computations. For other types of source zones the process can be similarly implemented.

The two-parameter source model could be developed using the considerations presented in Sections 3.3.4 and 3.3.5 and briefly summarized in Fig. 24(b). For any given combination of magnitude and stress drop the site of interest is identified as in either the near field or the far field, and this determines the applicable propagation formulae. The magnitude and the stress drop can be considered as two independent random variables.

While the pdf of M is known a probability density function has to be assigned for $\Delta\sigma$. In this formulation the probability of Y cannot be expressed without the magnitude law. This leads to an additional integration which obviously increases considerably the computational time. Simulation techniques are particularly recommended in this type of problem.

4.1.2 Further Studies on Uncertainties

As seen in Table VII uncertainties in α and β are very important. One way to take into consideration these uncertainties would be estimation of confidence limits for α and β on the basis of any given probability.

$$(\alpha) \rightarrow (\alpha + \Delta\alpha), (\beta) \rightarrow (\beta - \Delta\beta).$$

This would lead to conservative estimates of SHA. Since α and β are dependent with quite large coefficients of variation, the inclusion of these two uncertainties directly into the mathematical model can be made in the following way

$$P_Y = \int_{\alpha} \int_{\beta} P(Y|\alpha, \beta) f(\alpha, \beta) d\alpha d\beta \quad (29)$$

where $f(\alpha, \beta)$ is the joint density function of α and β . α and β can be considered as bivariate normal r.v.'s (Barlow and Proschan, 1975). The marginal distribution of β can be obtained from Eq. (9), Section 3.3.3, and approximately represented by the normal density; the distribution of α , usually taken as a gamma distribution, should consider the incompleteness and reliability of the data; $cov(\alpha, \beta)$ is given by Eq. (11). It should be emphasized that the estimates of α and β are strongly dependent upon the selection of the earthquake source areas.

One way to see the influence of α in the problem (McGuire, 1976) is to assume that α has a gamma 1 distribution; then, from Eq. (7),

$$f_{k+1, \tau}(\alpha) = \frac{\tau}{k!} (\alpha\tau)^k e^{-\alpha\tau} \quad k, \alpha, \tau \geq 0, \quad (30)$$

and in the case of a Poisson distribution for the number of events with magnitude within a given range

$$P_n(t_p | \alpha) = \frac{(\alpha t_p)^n}{n!} e^{-\alpha t_p} \quad (31)$$

The total probability of $P_n(f)$ is, from Feller (1971),

$$\begin{aligned} P_n(t) &= \int_0^{\infty} P(N|\alpha) f_k(\alpha) d\alpha \\ &= C_n^{n+k} \left(\frac{\tau}{\tau+t_p} \right)^{k+1} \left(\frac{t_p}{\tau+t_p} \right)^n \end{aligned} \quad (32)$$

which is the limiting form of the Polya distribution. For $n = 0$

$$1 - F = 1 - \left(\frac{\tau}{\tau + t_p} \right)^{k+1} . \quad (33)$$

Comparing the model with a deterministic α , then

$$\frac{1 - \frac{k/\alpha}{k/\alpha + t_p}}{1 - \exp(-\lambda t_p)} \approx 1 + 1/k .$$

Since the coefficient of variation of α is $1/\sqrt{k}$, for values less than 0.4, k is greater than 6 leading to a final error smaller than 16%.

Assignment of the upper limit of magnitude for each earthquake zone constitutes another important problem. McGuire (1976) included in his model a r.v. with uniform distribution for the upper intensity between the maximum observed intensity and XII. For California, authors seem to agree that the uncertainty in m_1 is small

The effect of focal depth uncertainty can be introduced into the model. Basu and Nigam (1977) developed such a procedure for the study of Indian seismic risk. For California, however, the focal depth has little variation, as seen in Section 3.3.1, so here the average value $h = 8$ km has been used.

The last point to be discussed relates to earthquake generation in time, for which two items are considered. The first refers to the validity of the Poisson model in a zone of known elastic rebound mechanism and has already been analyzed in Section 3.3.4. The second is the comparison of the Poisson, gamma and Markov chain models in terms of final probability distribution. For an interoccurrence time interval the gamma-1 distribution gives

$$P[N(t)=n] = \exp(-\alpha t) \sum_{i=0}^{k-1} \frac{(\alpha t)^{kn+i}}{(kn+i)!} \quad (34)$$

For $k = 1$ this reduces to the Poisson model and

$$P[Y > y] = 1 - e^{-\alpha t}.$$

For $k = 2$

$$P[N(t)=n] = e^{-\alpha t} \left(\frac{(\alpha t)^{2n}}{(2n)!} + \frac{(\alpha t)^{2n+1}}{(2n+1)!} \right)$$

and

$$P[Y > y] = 1 - e^{-\alpha t} (1 + \alpha t).$$

For the Poisson model, the probability of at least one occurrence is

$$1 - e^{-\nu t}$$

where ν is the mean number of events per year.

According to the Markov model, the probability of no occurrence in the interval of T_r years is given by

$$\prod_{i=1}^{T_r} \Phi_{22}(i) = \prod_{i=1}^{T_r} \frac{1}{a+b} [a + (1-a-b)^i b] \quad (35)$$

and the probability of at least one occurrence is

$$1 - \prod_{i=1}^{T_r} \Phi_{22}(i).$$

Figure 29 compares the Poisson, gamma ($k = 2$) and the Markov models of time generation for the next 100 years. The values used to derive this figure are the ones referred to in Section 3.3.2. While the Poisson model does not depend on the initial considerations, the Markov model does.

As can be seen from Fig. 29 the Markov and the Poisson models present approximately the same results. This is due to the fact that the Markov

memory dies out after a few intervals (years), and the process rapidly approaches the Poisson model. In comparison, the gamma model presents slight differences. For small elapsed times the probability of exceedence is smaller, but for large elapsed times the probability of exceedence is larger. In fact in the latter case while the probability of exceedence for the Poisson model is of the order of νt , for the gamma with $k = 2$ it is $(\alpha t)^2/2$. In the figure both processes were scaled to the same mean value, i.e., $\alpha = 2\nu$.

The time t to the next event T_1 on fault 1 has some degree of dependence in relation to the time to the next event on fault 2 because of the fact that energy accumulation is a slow process occurring continuously for all the faults. If there is a rupture in one fault, the probability of ruptures in other faults has necessarily decreased, showing statistical dependence of fault events. Hence for this model the computation given by Eq. (28) should be corrected suitably.

4.1.3 Joint Densities of Peak Acceleration and Duration

As pointed out before, the knowledge of the joint densities of two ground motion parameters could be very important. In studies of liquefaction, usually the duration is introduced through an empirically estimated parameter, namely N_{eq} , which measures the equivalent number of significant cycles.

Since liquefaction of sands is a result of the combined action of acceleration and number of cycles, the following simple method of analysis is proposed based on the Miner criterion (Penzien and Tseng, 1977): Accumulative damage (AD) for a narrow band response as normally produced by earthquakes can be expressed in the approximate form

$$AD \approx \nu s \int_0^{\infty} \frac{p(z)}{N(z)} dz \quad (36)$$

where ν is the mean rate of occurrence of zero crossings with positive slope, s the duration of response $z(t)$, z represents the individual single amplitude of response (stress or acceleration) present in the process $z(t)$, $p(z)$ the pdf of the r.v. z , and $N(z)$ the relationship expressing number of cycles to failure (N) versus amplitude of response z . For a narrow-band process, $p(z)$ can be approximated by the Rayleigh distribution

$$p(z) = \frac{z}{\sigma_z^2} \exp\left(-\frac{z^2}{2\sigma_z^2}\right) \quad (37)$$

where σ is the variance of z .

Assuming the relation given by Yegian (1976, p.184)

$$N(z) = z_1^b N_1 e^{bz} \quad (38)$$

where N_1 and z_1 represent a convenient point on the Z-N curve and b is constant, and substituting from Eq. (37), then integration of Eq. (36) yields

$$AD = \left\{ \frac{\sigma^2}{2} + \frac{\sigma^2 b}{4} \sqrt{2\sigma^2 \Pi} e^{\frac{b^2 \sigma^2}{2}} \left[1 - \Phi\left(-\frac{b\sigma}{\sqrt{2}}\right) \right] \right\} \frac{\nu s}{z_1^b N_1} \quad (39)$$

(see Gradshteyn and Ryzhik, 1965).

To estimate the total accumulative damage during one earthquake it is necessary to establish the joint probability density function of duration and acceleration (directly related to ν and σ). This can only be done from data evaluations (Fig. 30). According to Miner's linear accumulative damage criterion, liquifaction will occur when

$$AD \text{ (total)} \geq 1.$$

Hence the joint densities of two ground-motion parameters would be invaluable for further studies of low cycle fatigue.

4.1.4 Comparison of Different Methods of Analysis of Seismic Hazard

Comparison between the analytical and the experimental methods show that the former is more consistent because it is based on the statistical characteristics of the source areas allowing the calculation of the pdf of the site parameter for its entire range. The experimental technique uses just one realization of the process and consequently does not consider the probability of its occurrence. For low probabilities extrapolations have to be made. Furthermore, it is difficult to introduce into the experimental method the effects of uncertainties derived from the generation of earthquakes. However, the experimental distribution resulting from the known history of earthquakes can be used as an initial distribution in a Bayesian model, as in the following.

Uncertainties in the modelling of earthquake sources could introduce additional uncertainty in the estimated risk. Decisions such as the type, the average recurrence rate, and the geometric parameters of each potential source may not be obvious; alternative assumptions for this purpose may have to be considered.

The following procedure of Cornell and Merz (1975) based on Bayesian estimates can be used

- i) Alternative recurrence lines, upper magnitudes and source model geometries may be assumed.
- ii) To each alternative set of parameters a weighting factor is assigned on a subjective basis. The weighting factors represent the relative likelihoods that the assumed alternatives will be the correct ones.

iii) Using the theorem of total probability,

$$P_r(Y_a > y) = \sum_{i=1}^n P_r(Y_a > y | A_i) w_i \quad (40)$$

where A_i = the i^{th} set of alternatives

w_i = the weighting factor for the i^{th} set of alternatives

and n = the number of possible sets of alternatives

This method could be called semi-analytic.

Now the discussion of distributions in terms of response spectrum has not included the effect of randomness of the response for a fixed intensity of seismic action. Actually, for low risks ($<10^{-3}$) the final distribution of maximum response of a one degree-of-freedom system considering both the randomness of intensity and the randomness of response, has to be computed using the two distributions and it is no longer valid to consider only the distribution of intensity and the mean value of maximum response (Oliveira, 1975).

In fact, the above problem is directly connected with the general philosophy of definition of probability levels of safety. The low risk levels ($<10^{-8}$) require extrapolation to a period of time that extends as far into the future as the Early Tertiary goes back into the past. This is to say that it is necessary to jump into the unknown a higher order of steps. Extrapolation based only on extreme value statistics for return periods beyond the period covered by the data set, was criticized by Knopoff and Kagan (1977). The geotectonics of the past million years may add information about the possible evolution of our present state.

Furthermore, to compute the safety levels it is necessary to know the interval of time for which the structure should be designed. It appears that the estimation of this reference interval of time is

settled quite arbitrarily. This point is analyzed briefly as follows.

Assume first that the reference interval of time T_r , is fixed with a certain uncertainty expressed as a

$$f_{T_r}(t) = \nu e^{-\nu t},$$

and the time generation is Poisson with mean value equal to

$$P_N(n) = \int_0^{\infty} P_N(n|t) f(t) dt = \left(\frac{\nu}{\nu+\lambda}\right) \left(\frac{\nu}{\nu+\lambda}\right)^n, \quad (41)$$

which is a geometric distribution (Feller, 1971). The ratio of $P_N(n)$ obtained from the above to $E[T_r] = 50$ years is approximately one. But if the distribution of T is different, the ratio could be important, depending on the coefficient of variation of T_r . For one case that was studied of the gamma-1 distribution with $k = 2$ the final distribution would change from 0.999 to a 0.996.

4.2 Risk Analysis

4.2.1 Generalities

As previously stated, the seismic risk over a region cannot be given simply by a single parameter such as maximum acceleration, velocity or displacement measured at one site because of the spatial correlation existing among performances at different sites for the same earthquake (Oliveira, 1975). In terms of total losses over an area it means that, when summing up local losses from different sites, dependent r.v.'s are involved.

This section is included in the report to make sure that this concept is not overlooked when characterizing risk for a zone, and the San Francisco Bay Area is one of the places where this type of analysis should be applied.

4.2.2 How to Handle the Problem

There are several ways to attack the problem of spatial correlation, depending on the objectives under analysis. For instance, Oliveira (1975) developed an overall methodology which takes care of the variation of damage with distance for a given earthquake in terms of mean and variance, and integrates that information over the metropolitan area. Taleb-Agha (1975) developed a technique of analysis of discrete and continuous systems such as pipe-lines, power stations, where it is necessary to obtain the probability of exceeding given levels of excitation simultaneously for a set of k objects. It is evident that the simultaneous failure of two, three, or more elements of a chain would have consequences that are not two, three, or more times the consequences of a single failure. Caputo et al. (1973), however, developed a technique of analysis for both discrete and continuous systems in which they consider the perceptibility area for given intensity and study the statistics of the possible occurrence of earthquakes striking the given object.

In short, the way to study the risk problem depends on the objectives, and the objectives can vary from consideration of the number of times a given area is struck by earthquake intensities larger than I_0 , to an estimation of the total losses that could be inflicted on an entire region. Authors usually consider that the transformation between ground motion and damage requires another random step (Whitman and Cornell, 1977). What really ought to be known is the direct relation between the earthquake characterized by at least M and R and the corresponding impact on the region affected, economic, social, or whatever output is of interest.

Bearing in mind the application of Taleb-Agha's model to study the

exposure of people to seismic threat, the principles of his model are developed as follows.

Consider a group of point objects each one defined by a damage threshold $r_1, r_2 \dots r_n$. Assume that r is directly related to ground motion parameters. Using the attenuation formula of Eq. (23)

$$a = b_1 e^{b_2 m} (f(R))^{-b_3},$$

the probability of exceeding the threshold r_i at point i is

$$P \left[r_i \leq a(m, R) \right]$$

or

$$P \left[\frac{r_i R_i^{b_3}}{b_1} \leq e^{b_2 m} \right].$$

Let $\bar{R}_i = r_i R_i^{b_3}$ then

$$P \left[\frac{\bar{R}_i (1.0)^{b_3}}{b_1} \leq e^{b_2 m} \right]$$

or

$$P \left[m \geq \frac{1}{b_2} \ln \left(\frac{\bar{R}_i}{b_1} \right) \right].$$

If $F_M(m)$ is known, then the probability of exceeding r_i is

$$1 - F_M \left[\frac{1}{b_2} \ln \left(\frac{\bar{R}_i}{b_1} \right) \right] \quad (42)$$

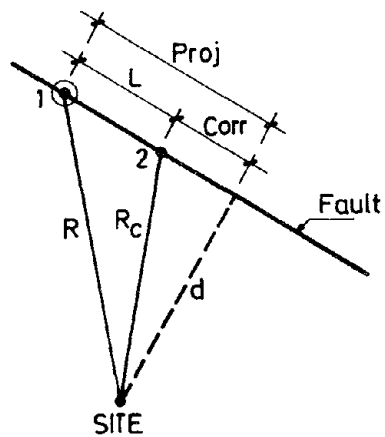
If the attenuation parameters are constant for the entire region, to obtain the probability of simultaneously exceeding r_i at j points the R_i are ordered in increasing size

$$\bar{R}_{i1} < \bar{R}_{ij} < \dots < \bar{R}_{in}$$

and

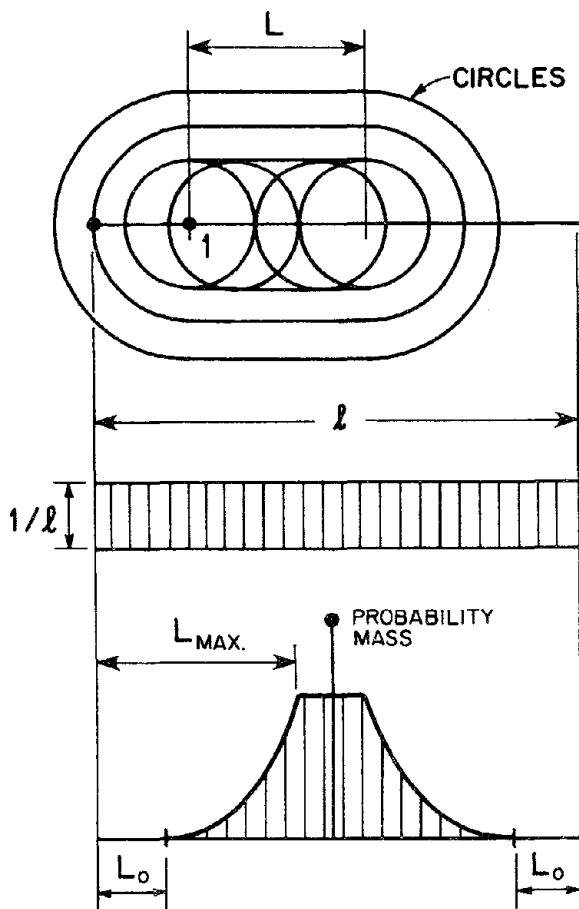
$$1 - F_M \left[\frac{1}{b_2} \ln \left(\frac{\bar{R}_{ij}}{b_1} \right) \right]$$

is computed. If the model of earthquake occurrence is Poisson, then Eq. (26) should be used.



1 - Initial point for rupture
 2 - Final point of rupture

FIGURE 27 SKETCH FOR LINE-SOURCE MODEL



ISOSEISMALS FOR EARTHQUAKE ORIGIN AT POINT 1 AND RUPTURE LENGTH L

UNIFORM DISTRIBUTION OF EPICENTRAL LOCATIONS ALONG THE LINEAR SOURCE ZONE OF LENGTH l

CORRECTED DISTRIBUTION TAKING INTO ACCOUNT THE RUPTURE LENGTH AND THE pdf OF MAGNITUDE

FIGURE 28 LINEAR EARTHQUAKE SOURCE ZONE. CORRECTION TO ACCOUNT FOR THE LINE-SOURCE MODEL

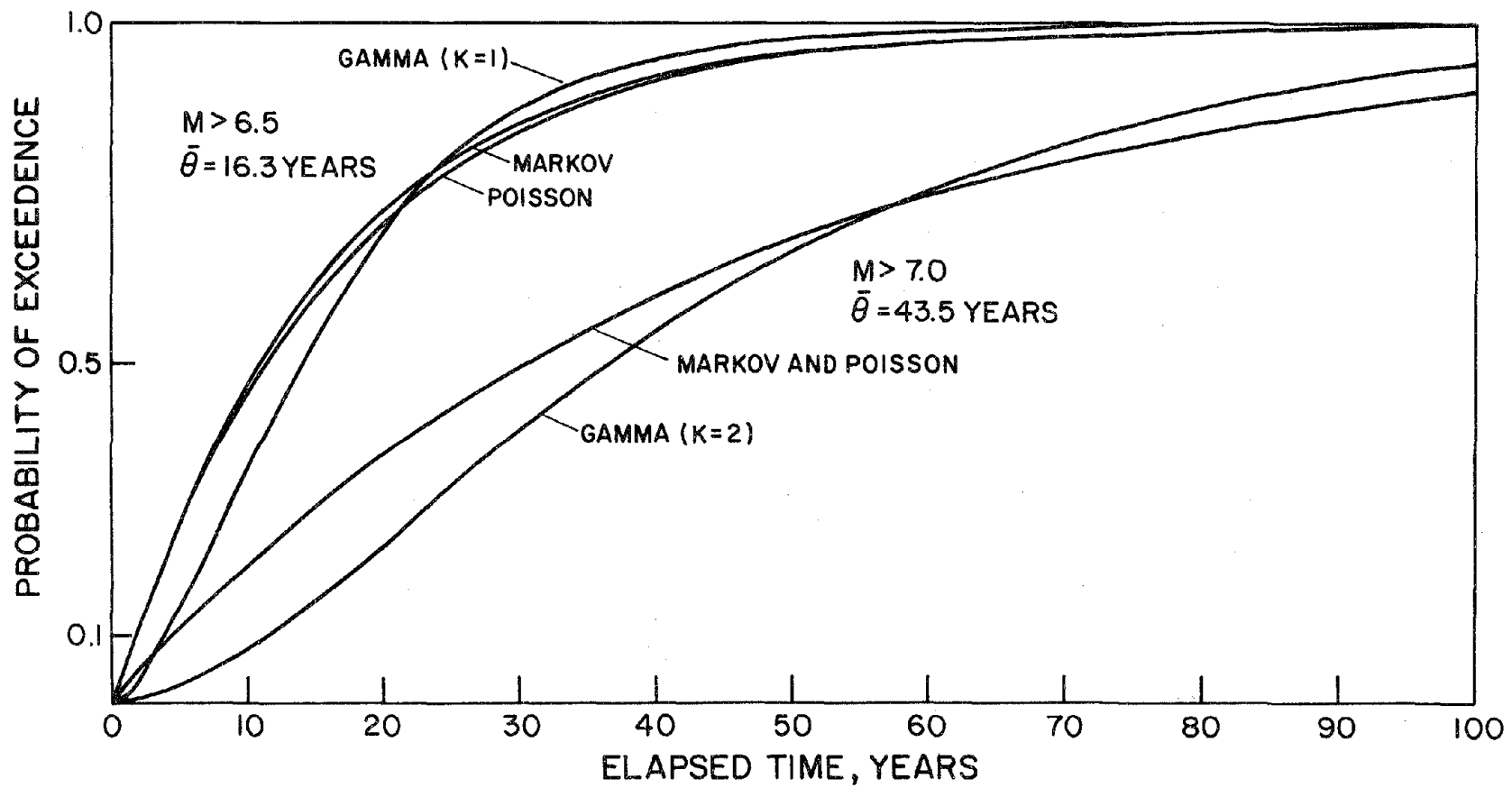


FIGURE 29 COMPARISON BETWEEN THE MARKOV, POISSON AND GAMMA MODELS OF TIME GENERATION

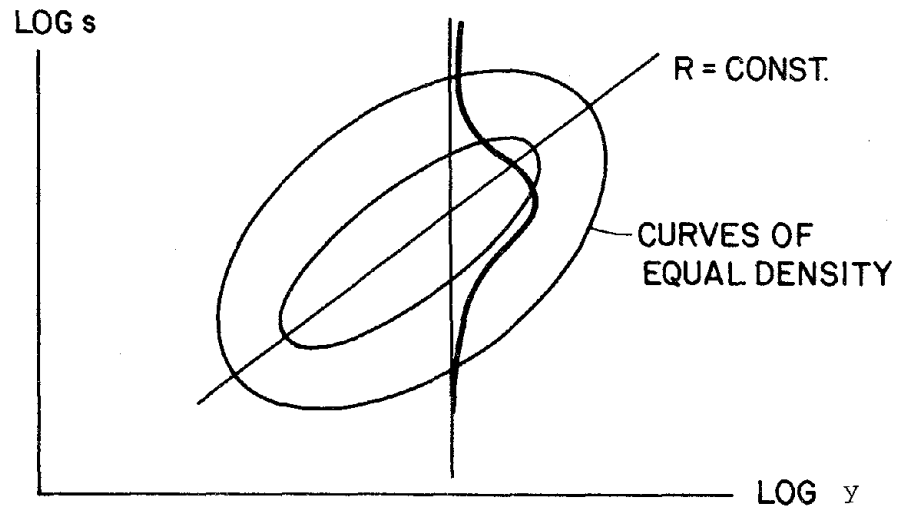


FIGURE 30 CORRELATION BETWEEN PEAK GROUND ACCELERATION AND DURATION OF MOTION

5. SEISMIC HAZARD ANALYSIS FOR A SITE IN DOWNTOWN SAN FRANCISCO

5.1 Main Results

As shown by the data presented in Chapter 3 and the mathematical models reviewed in Chapter 4, a variety of hypotheses have been studied, and both analytic and experimental techniques have been considered.

The effect of the geometry of earthquake source areas is examined next, using three different models as shown in Fig. 13. The first case corresponds to the idealization of three source lines or three main faults, San Andreas, Calaveras-Hayward and Middland. The second idealization corresponds to three area sources with uniform epicentral distribution from a model of Algermissen and Perkins (1976). The third idealization corresponds to a single rectangular source area having as longer axis the San Andreas trace and with a bell-shaped epicentral distribution in the transverse direction, as in Fig. 31. The seismic characteristics of each earthquake source area corresponding to each of these three models are given in Table V. Wave attenuation formulae used in this work are given in Table VI. Maximum values of acceleration, velocity, displacement, as well as spectral pseudo-velocities and duration of strong motion were analyzed. The influence of some uncertainties in the parameters was thoroughly studied.

In the experimental case extrapolation for intermediate risk ($< 10^{-2}$) was made by parabolic fitting of the following: $\ln(-\ln G_y(y))$ versus $\ln(y)$. Straight-line fitting is not realistic for large extrapolations, because it does not consider the upper truncation of magnitudes.

In the following, results of the analyses are presented.

Figure 32 shows the annual probability distribution for maximum accelerations, velocities, displacements and duration using the

experimental method. Differences up to 30% can be found. The line-source mechanism increases the parameter estimates based on point source models by at most 80%. The results are very sensitive to the period of time in the study (see Fig. 33). Indeed for the period 1934-1973, which corresponds to the full instrumental recording, the seismicity is moderate and the extreme value type II plot is very linear. The 1880-1907 period, however, shows a much greater seismicity and the plot reflects the incompleteness of the records for small magnitude events, expressed by its parabolic form. A comparison of the full period 1800-1973 with the period 1800-1907 shows that the assigned San Francisco seismicity is mainly due to activity during the 19th century. If maximum values in a 10-year period are used instead of the yearly period used before, the results are approximately the same*.

A comparison between analytic and experimental techniques is illustrated in Fig. 34 (on semi-log paper) for both line-source and point-source mechanisms. The experimental technique yields 40% to 50% higher estimates.

Figure 35 compares the influence of uncertainties on the attenuation curves, on the value of β and on the geometry of earthquake source areas. The uncertainty in attenuation curves has been directly incorporated in the mathematical formulation.

Figure 36 shows the probabilistic distribution function for response spectrum according to the McGuire and Lynch expressions using the experimental method. The plotted distribution refers to the case of a one

* Larger intervals of sampling are desirable for better analysis of large earthquake activity. However, increasing the sampling interval reduces the number of intervals to be used in estimation and extrapolation. For the algorithm to transform T-year intervals into yearly intervals see Oliveira (1974).

degree-of-freedom system with a 5% damping ratio. Both linear and parabolic fitting are presented for the experimental case. Consistent response spectra were drawn in Fig. 37 for 10, 100 and 1000 year mean return periods. A comparison made with the values determined for ground motion parameters shows discrepancies of two types: first, the technique of analysis for maximum acceleration, velocity and displacement was more sophisticated than the one used for the response spectra; secondly, the curves proposed by McGuire and Lynch were obtained from data referring to few earthquakes. No studies of uncertainty were made.

All the above studies were conducted for a site in downtown San Francisco, or more precisely located at 37.75°N and 122.45°W . For other sites located along a transverse profile to the San Andreas fault see Fig. 38. Along profiles parallel to the San Andreas fault there is not too much change.

It should be emphasized once more that the geology has not been taken into account; the amplification factors defined in Section 2.5 could be used to do so.

The annual probability distribution functions of peak ground acceleration, discussed previously, are presented in Fig. 39. As can be seen, there are upper and lower distribution bounds which correspond to the results obtained throughout this study. The shaded area that represents the uncertainty estimation increases towards the zone of larger return periods. The middle distribution is the best estimate of hazard distribution in downtown San Francisco for bedrock formations. Table VIII shows the values proposed for accelerations, velocity, displacement and duration for different return periods. The values of v/a , d/a and ad/v^2 are also presented.

TABLE VIII

Proposed Values for Seismic Hazard Parameters in
San Francisco (for Bedrock)

Return Periods (years)	10	20	50	100	200	500	1000
Acceleration (% g)	0.10	0.18	0.32	0.46	0.62	0.85	1.02
Velocity (cm sec ⁻¹)	12	20	30	40	50	60	120
Displacement (cm)	7	-	-	25	-	-	70
Duration (sec)	8	-	-	20	-	-	50
v/a (sec)	0.12	-	-	0.09	-	-	0.12
d/a (sec ²)	0.07	-	-	0.05	-	-	0.07
ad/v ²	4.86	-	-	7.19	-	-	4.96

These values characterize adequately the seismic parameters needed for code purposes, cost-benefit analysis, etc. To obtain design values with probability of occurrence far beyond 10^{-3} , however, as is the case of nuclear power plants, the extrapolations cannot be done without introducing

large uncertainties. For these cases it is necessary to look at the geological evolution of the plate tectonics, in order to trace the seismic activity of faults. As far as the San Francisco area is concerned, the strike-slip evolution over the past 20×10^6 years seems to be taking place without any drastic changes. Based on these assertions (see Chapter 2), and on physical insight into the mechanism of generation, there should be a definite upper bound on the strong motion parameters, and therefore the hazard curve should be upper truncated at a convenient level.

5.2 Comparison with Previous Studies

Greensfelder (1972) prepared a map for the State of California which indicates for the San Francisco Bay Area, a maximum acceleration slightly above 0.5 g. The approach followed by Greensfelder does not consider the probability of exceedence of that value. According to Culver et al. (1975) the maximum hard rock velocity to be expected for a 100-year mean return period is 18 cm sec^{-1} . Dalal (1972) proposes a maximum acceleration equal to 0.2 g for the 100-year period whereas Kiremidjian and Shah (1975) propose 0.3 g; Algermissen and Perkins propose 0.45 g and 34.3 cm sec^{-1} , respectively, for maximum acceleration and velocity; Kiureghian and Ang (1975) propose 0.47 g, 72 cm sec^{-1} and 37 cm, respectively, for maximum acceleration, velocity and displacement.

The largest values proposed in previous studies agree with the ones obtained herein as far as acceleration is concerned even though for the small return periods the estimates in this work are smaller. This may be explained by the emphasis given in this study to the nonstationary process of earthquake occurrence in the San Andreas system in the vicinity of San Francisco. The values obtained here for maximum velocity and displacement are, respectively, half and 2/3 of the largest presented in previous studies.

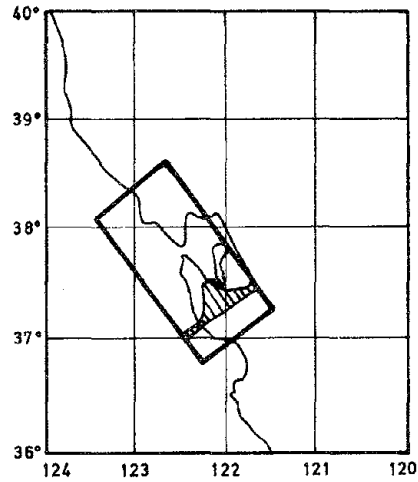


FIGURE 31 LOCATION OF A SINGLE RECTANGULAR SOURCE REPRESENTING BAY AREA CONDITIONS WITH NORMAL DISTRIBUTION OF EPICENTERS IN THE TRANSVERSE DIRECTION

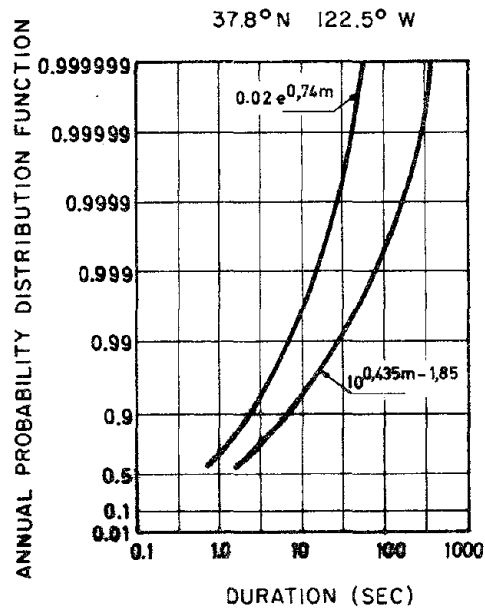


FIGURE 32(a) ANNUAL PROBABILITY DISTRIBUTION OF DURATION USING THE EXPERIMENTAL METHOD WITH A POINT-SOURCE GENERATING PROCESS

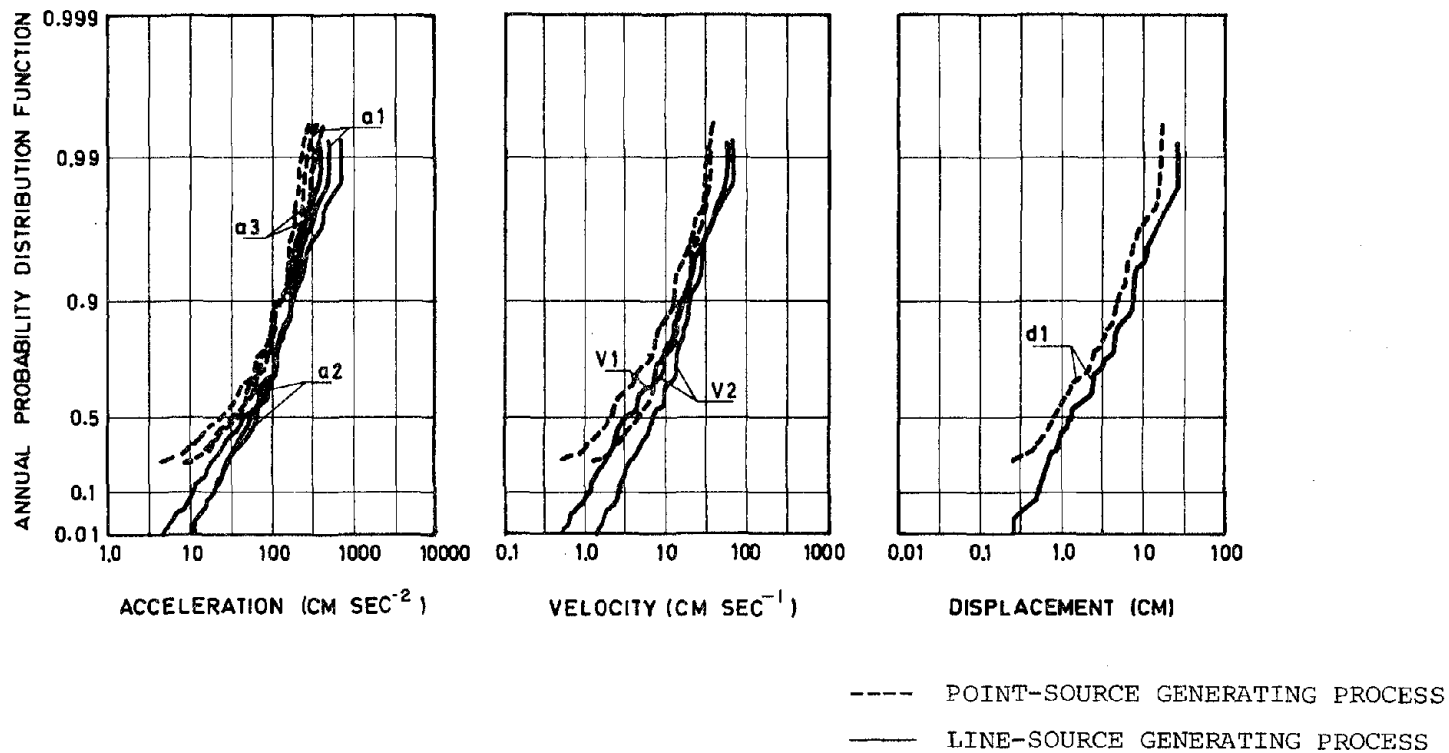


FIGURE 32 (b) ANNUAL PROBABILITY DISTRIBUTIONS OF GROUND MOTION PARAMETERS USING THE EXPERIMENTAL METHOD FOR THE PERIOD 1800 - 1973, WITH THE ATTENUATION FORMULAE OF TABLE V

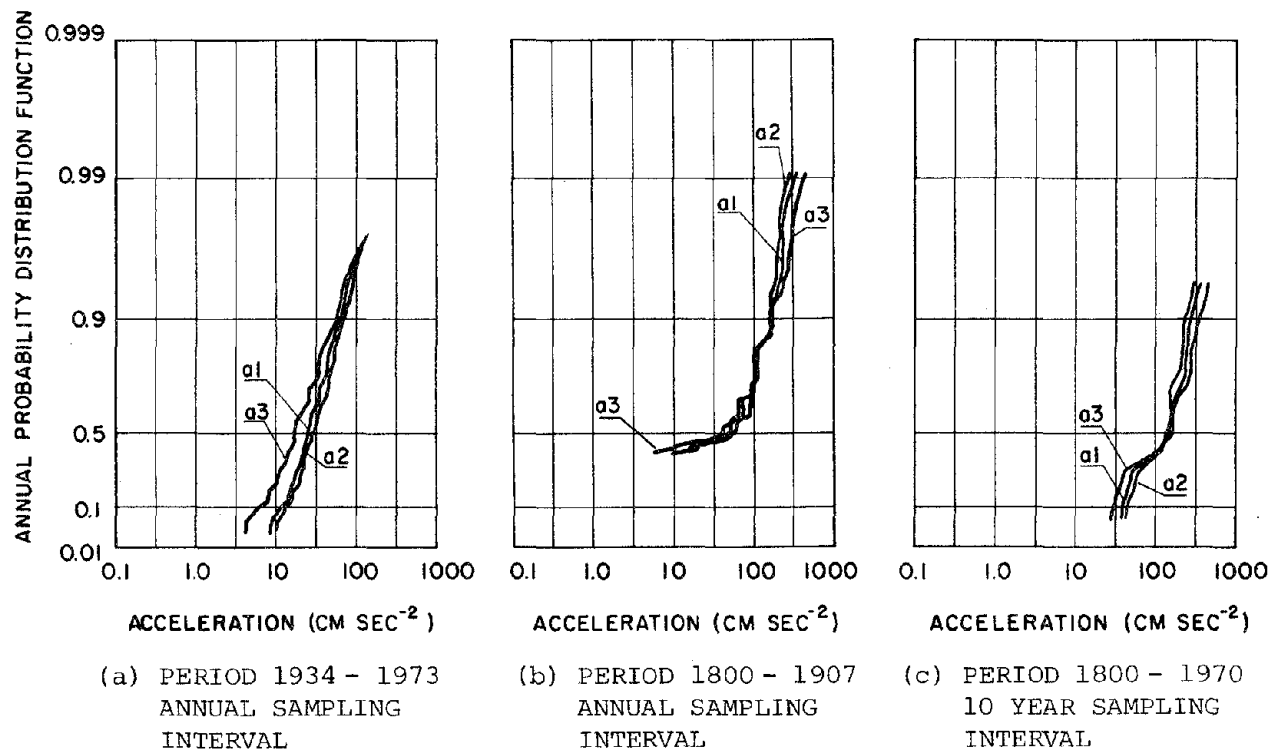
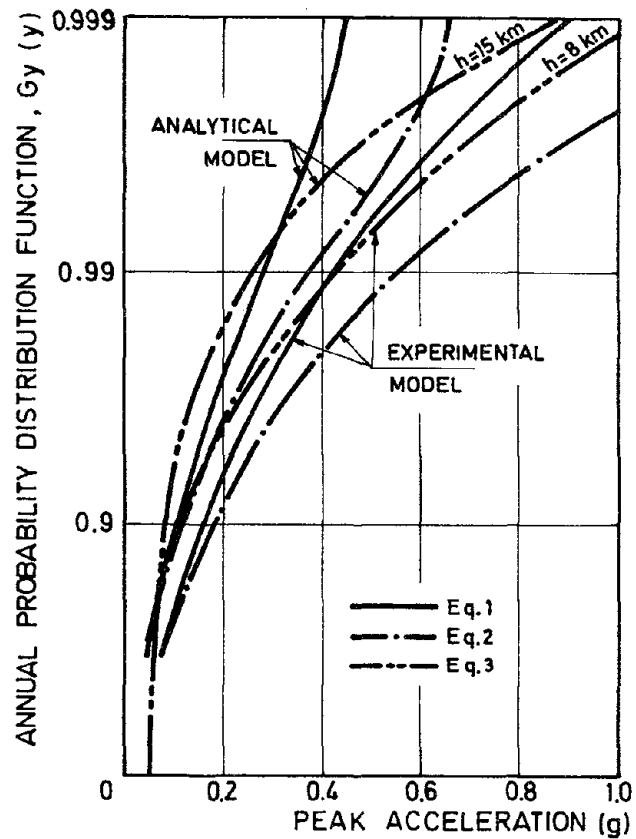


FIGURE 33 INFLUENCE OF SAMPLING INTERVAL FOR THE POINT-SOURCE MODEL USING THE EXPERIMENTAL METHOD



Eq. 1 (TABLE V) : LINE-SOURCE GENERATION PROCESS
 Eq. 2 (TABLE V) : LINE-SOURCE GENERATION PROCESS
 Eq. 3 (TABLE V) : POINT-SOURCE GENERATION PROCESS

FIGURE 34 COMPARISON BETWEEN EXPERIMENTAL AND ANALYTICAL MODELS

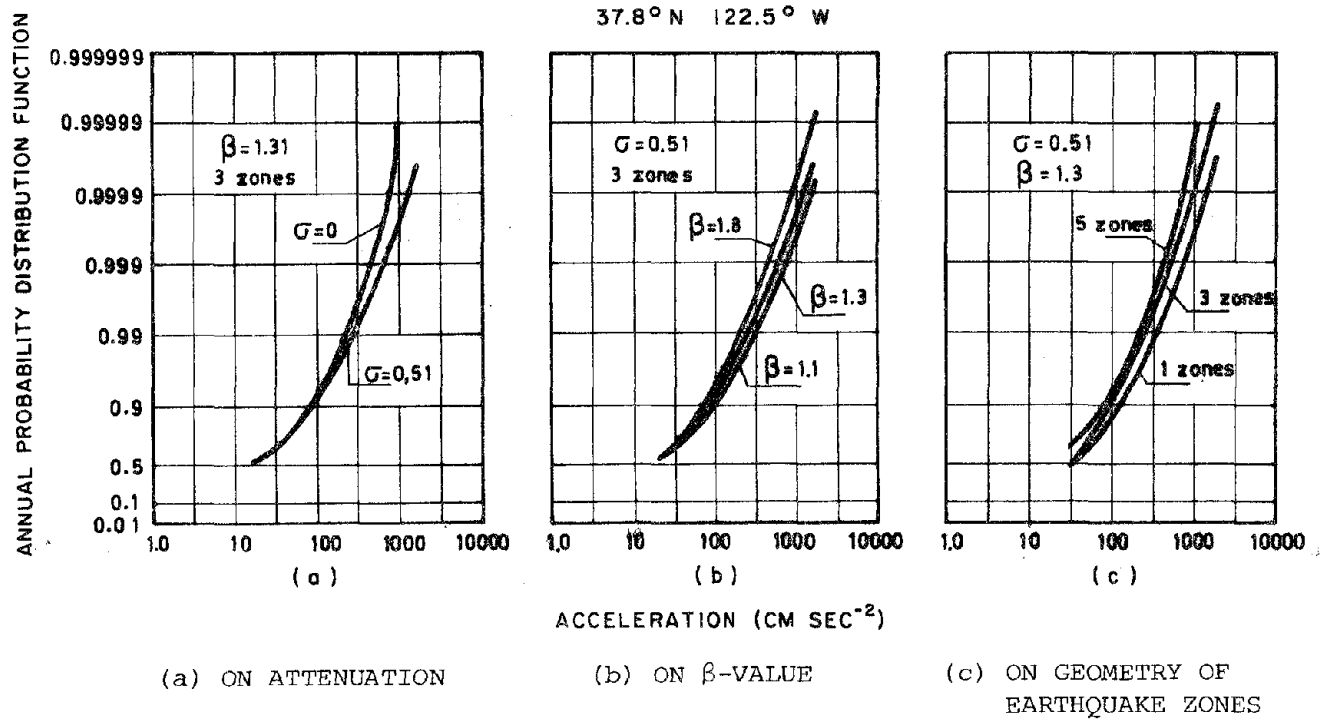


FIGURE 35 SENSITIVITY STUDIES OF THE INFLUENCE OF UNCERTAINTIES

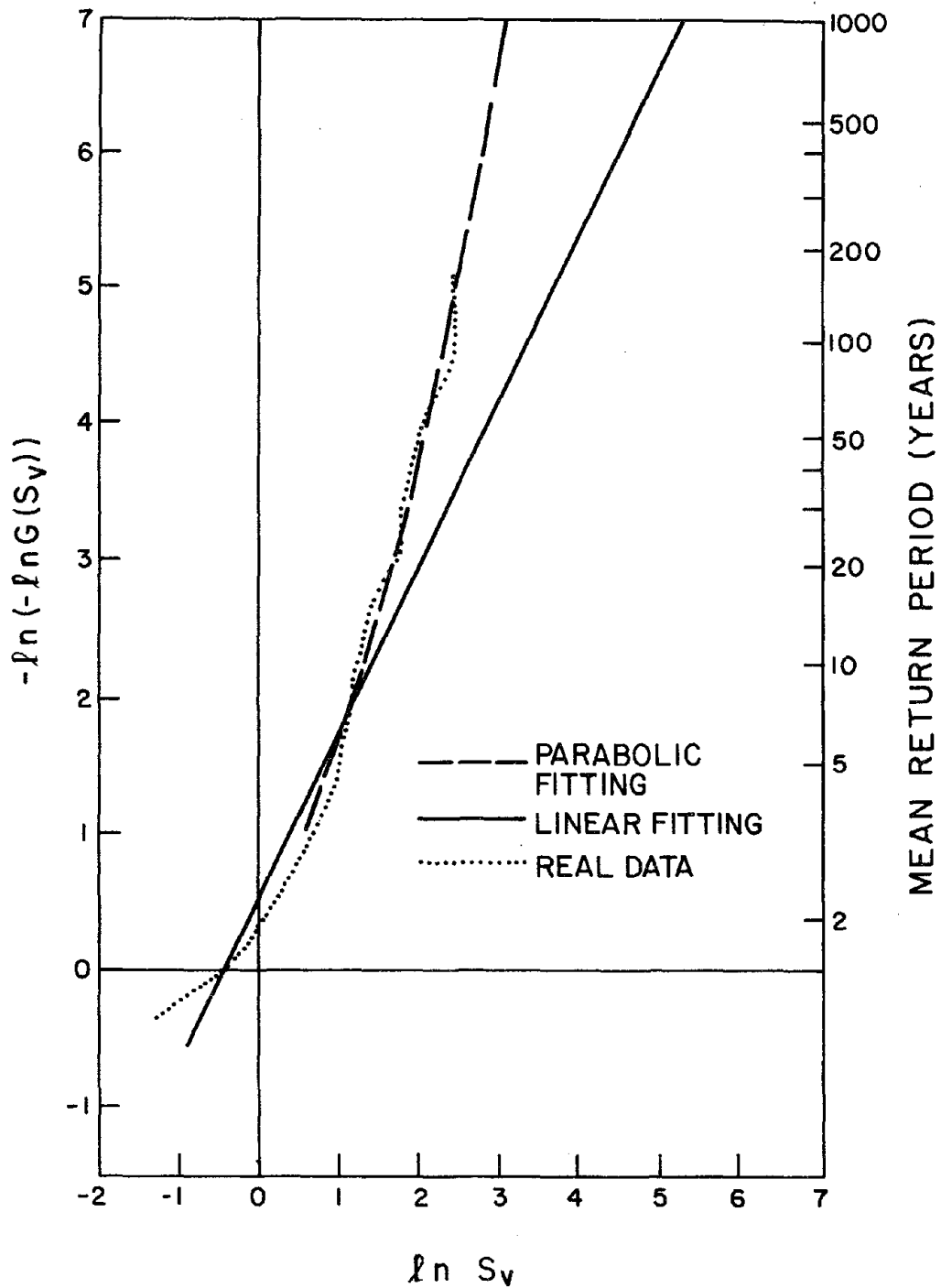


FIGURE 36 ANNUAL PROBABILITY DISTRIBUTION FUNCTION FOR RESPONSE SPECTRA ($T_0 = 0.1$ sec, $\eta = 5\%$)

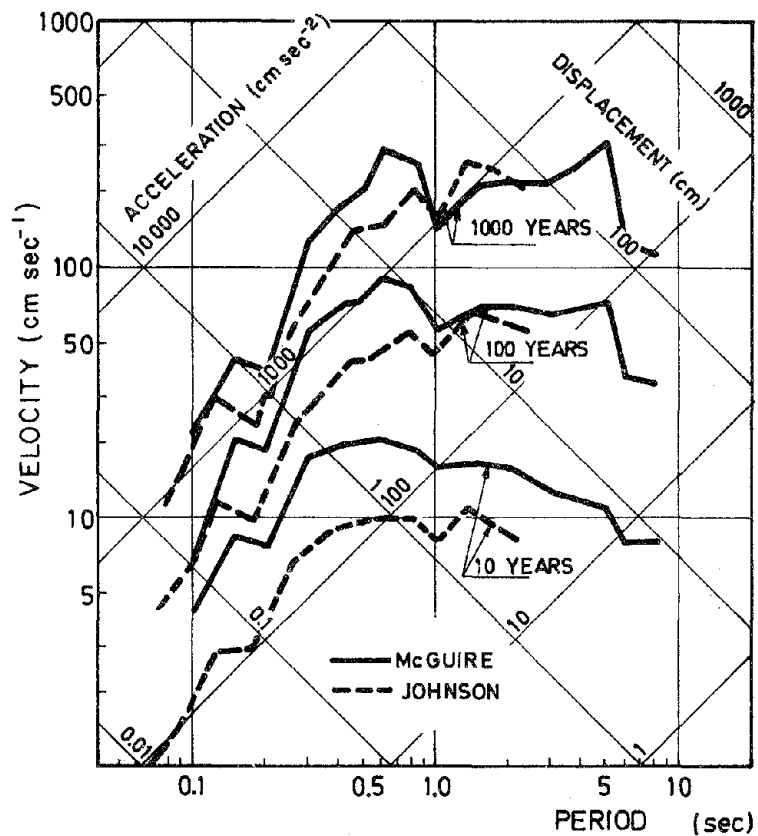


FIGURE 37 SEISMIC HAZARD ANALYSIS IN TERMS OF RESPONSE SPECTRA FOR 10, 100 AND 1000 YEAR MEAN RETURN PERIODS (5% DAMPING)

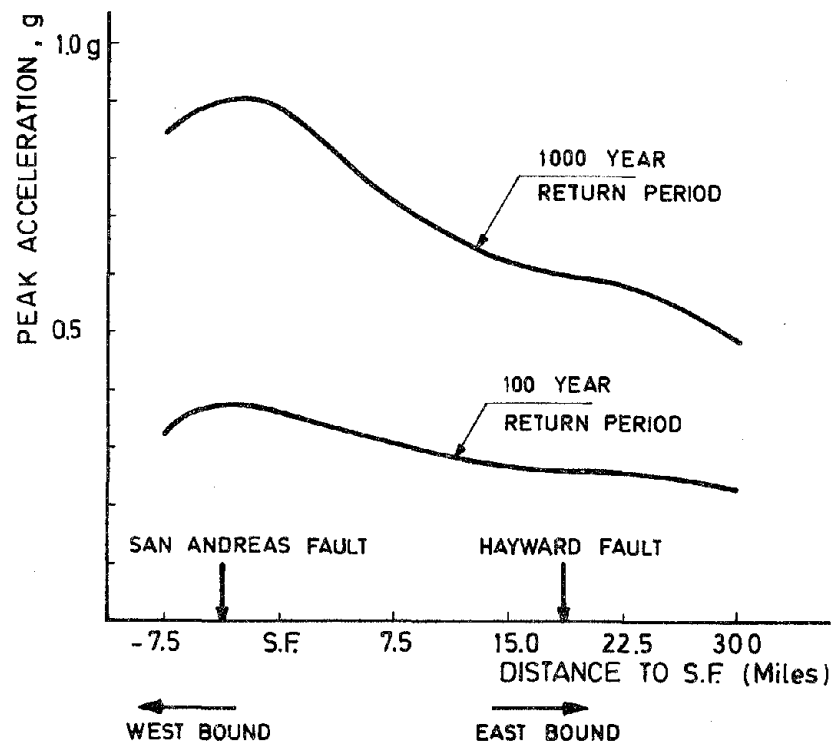


FIGURE 38 MAXIMUM ACCELERATIONS EXPECTED ALONG TRANSVERSE PROFILE TO THE SAN ANDREAS FAULT, FOR 100 AND 1000 YEAR MEAN RETURN PERIODS

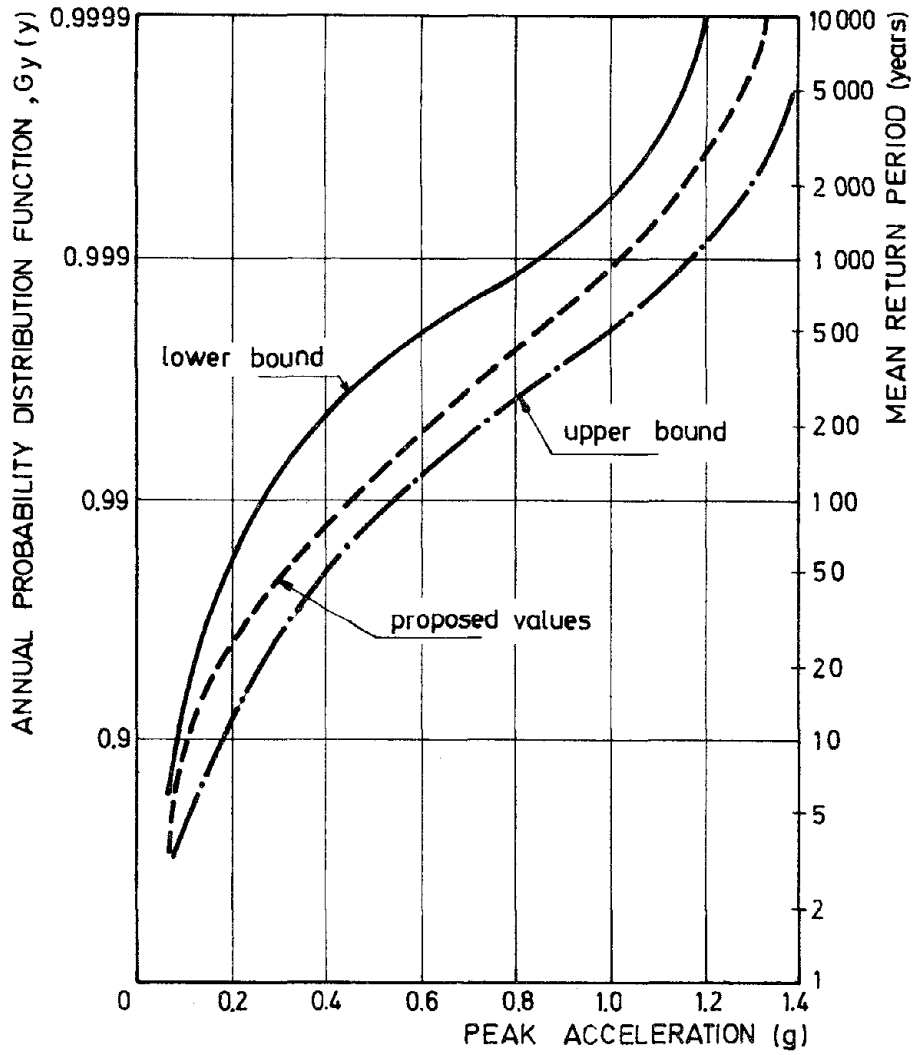


FIGURE 39 PROPOSED ANNUAL PROBABILITY DISTRIBUTION FUNCTION OF PEAK ACCELERATION FOR SAN FRANCISCO

6. POPULATION EXPOSURE TO SEISMIC HAZARD IN THE GREATER SAN FRANCISCO BAY AREA

A few studies of overall damage in this region have already been made (OPE, 1972; Friedman, 1975); but in these studies spatial correlation was not considered.

The study area covered in this chapter is defined as being limited to the nine Bay Area counties shown in Figure 40. The geographical location of the population was determined using the 1970 United States Census, and 95 cities and towns were considered. A computer program was developed to study population exposure according to the model of Section 4.2.2. To introduce the data into the program, a set of 145 points, each one representing 25,000 people in a total of 3.6 million, was reformulated to take into account the geographical distribution of population. Each new point corresponds approximately to the centers of mass of the populations they represent.

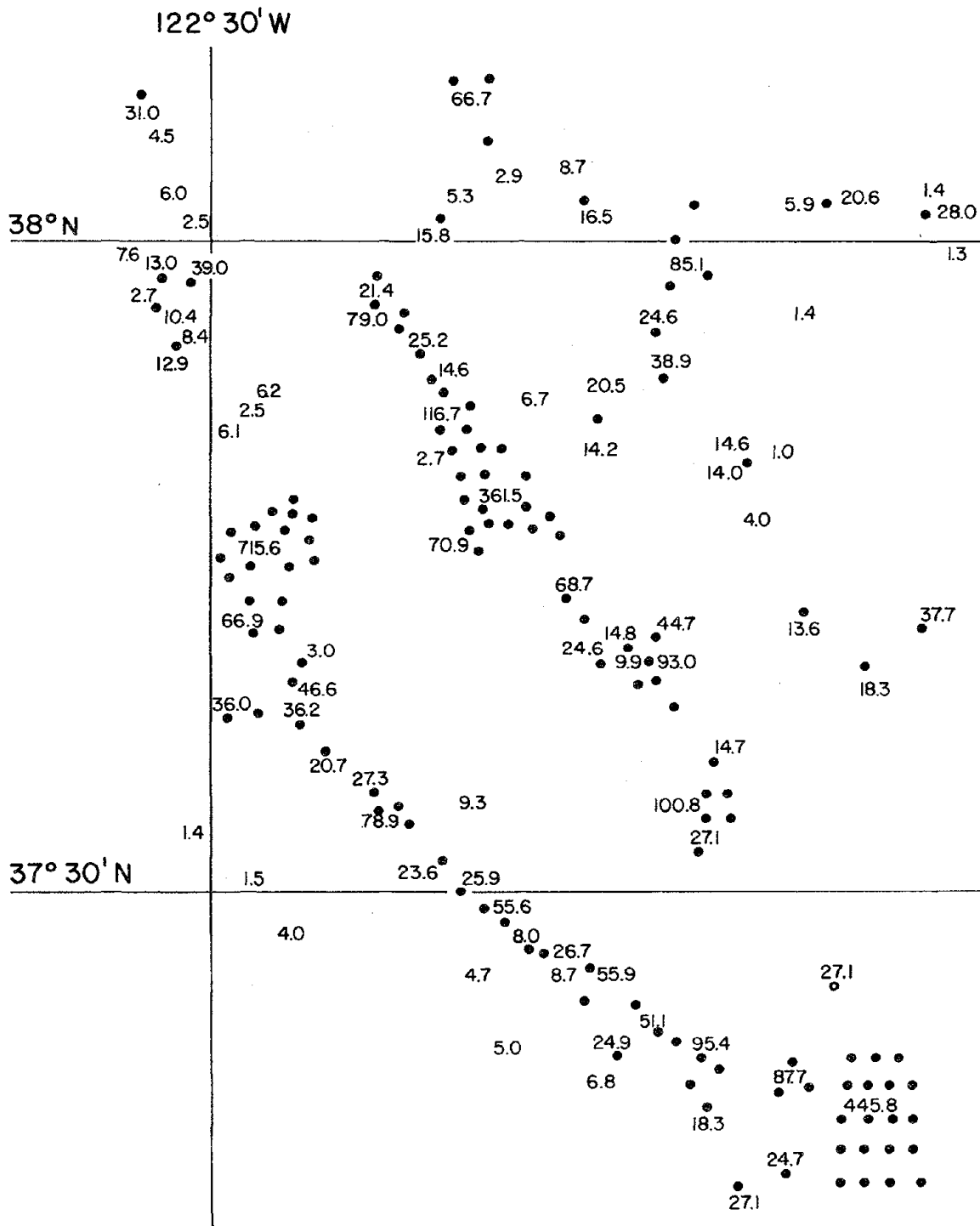
For generation source areas, the hypothesis of a point-source methodology was considered. Figure 41 presents the results of the present study in terms of the number of people exposed to accelerations of 100, 200 and 500 cm/sec^2 during an interval of time of 10 years.

This example is a simple illustration of the spatial correlation problem. It should be considered as a tentative case.

In other studies the same technique could be used to obtain the effects of changes in population at the town level. For instance, the population of San Francisco decreased from 775×10^3 in 1950 to 714×10^3 in 1970, whereas the population of California increased from 10.5 million to 19.9 million in the same interval of time. Geology of the Bay Area is another parameter of great interest that could be considered in the

analysis. For this purpose use could be made of data as shown in Figure 7.

Another factor which could be considered in the analysis is the variation in the geographical distribution of population throughout a day.



NUMBERS REPRESENT POPULATION PER TOWN ($\times 10^3$)
 DOTS REPRESENT DISCRETIZATION USED IN MODEL

FIGURE 40(b) POPULATION DISTRIBUTION FOR THE STUDY CASE

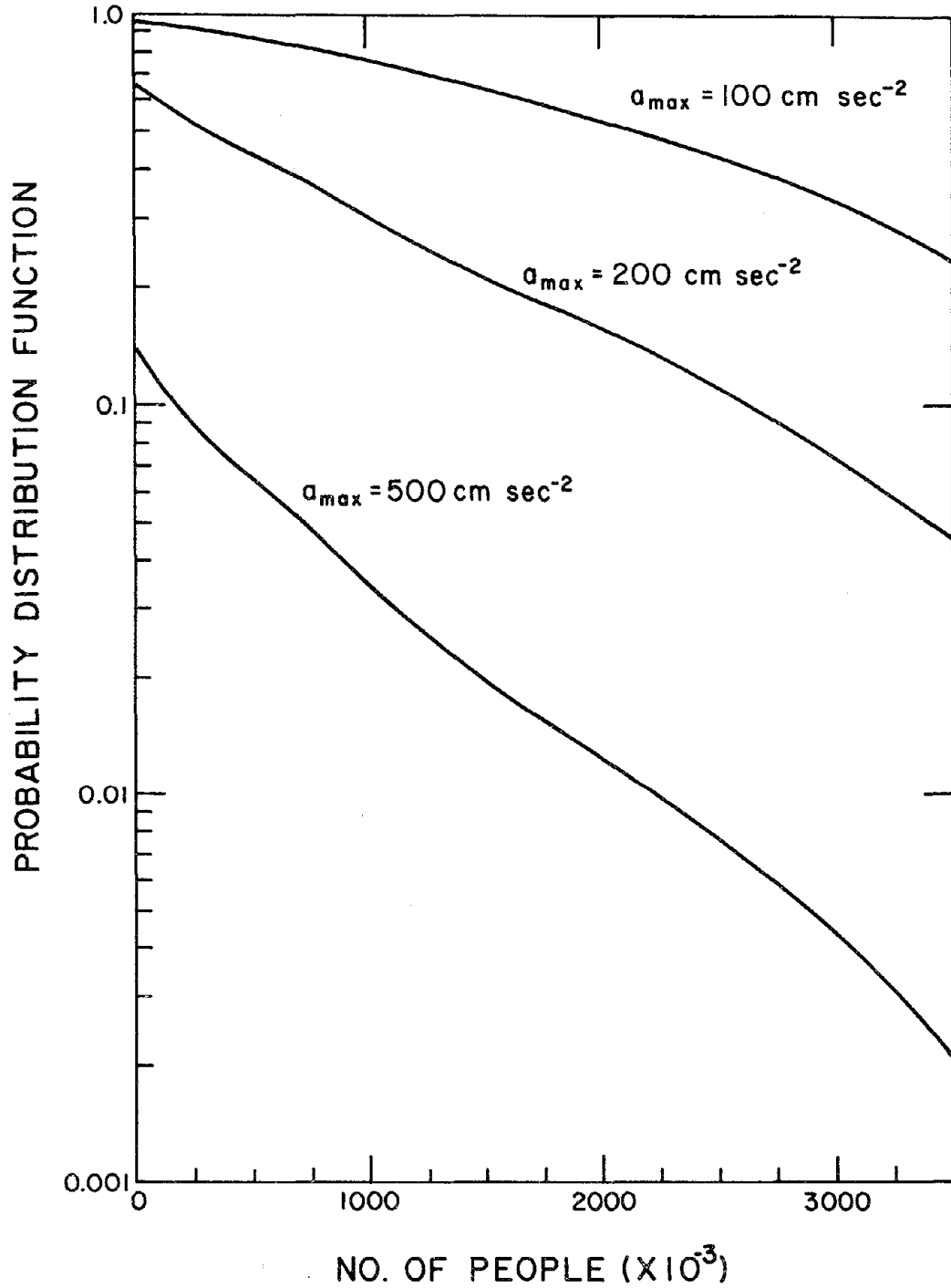


FIGURE 41 POPULATION EXPOSURE IN THE GREATER SAN FRANCISCO BAY AREA. PROBABILITY DISTRIBUTION FUNCTION OF PEOPLE EXPERIENCING THE THREAT OF PEAK ACCELERATIONS GREATER THAN a_{max} DURING A REFERENCE TIME INTERVAL $T_r = 10$ YEARS

TABLE IX

Résumé of Sensitivity Studies Analysed

TYPE	DESCRIPTION	
Geotectonics	Tectonic evolution; surveillance; correlation with observed seismicity	
Geology	Bay Area geology; influence on earthquake ground motion	
Recorded data	Reliability, completeness	
Earthquake zones	Four different geometries were analyzed; line and area sources; constant depth	
Occurrence times	Poisson, gamma and Markov models; stationarity	
Size of earthquakes	Source-mechanism: Point-source, line-source, magnitude, stress-drop Intensity distribution: α , β , m_1	
Attenuation of ground motion	Three acceleration models Two velocity One displacement Two spectral ordinates Two duration	Uncertainty on data
Methods of analysis	Site (SHA)	Experimental technique
		Analytical technique
	Global (SRA)	Population exposure

7. CONCLUSIONS

The main conclusions to be drawn from this review study on methods of hazard and risk analysis for the greater San Francisco Bay Area are as follows:

- a. The historical record of seismicity (about 170 years) is not long enough to allow the acceptance or rejection of the Poisson model of generation of earthquakes.
- b. Line-source models of generation are very important when the site is near the fault zone. This geometrical consideration should always be considered.
- c. Results obtained from experimental and analytical techniques should always be compared. Experimental data fit approximately an extreme value type III distribution or a truncated type II.
- d. Extrapolation to the zone of very low risk ($< 10^{-3}$) can only be based on geotectonic evolution of the fault system in the last 20×10^6 years. Indications are that this evolution took place without drastic changes.
- e. Uncertainties in the mathematical model, on source mechanism, attenuation features and on the definition of earthquake zones are most critical in the evaluation of final probability distributions.
- f. Spatial correlation of earthquake action cannot be neglected in global risk studies for San Francisco.

Table IX presents a résumé of the sensitivity studies analyzed.

The first steps towards the implementation of risk analysis studies are as follows:

- (i) Definition of response spectra or power spectral density functions based on a two-parameter mechanism of generation, i.e., magnitude and stress drop.
- (ii) Derivation of a joint probability density function of two ground motion parameters, such as acceleration and duration.

Further investigations should be made on the effects of uncertainties, particularly those derived from the correlation between α and β , and on models of earthquake generation taking into account the spatial dependence of times of occurrence. Global seismic risk studies for the San Francisco Bay Area following the guidelines presented can easily be extended to other types of exposure.

REFERENCES

- Aki, K. (1965) "Maximum Likelihood Estimate of b in the formula $\log N = a - bM$ and its Confidence Limits", Bulletin Earthquake Research Institute, Tokyo University (43).
- Algermissen, S.T. and Perkins D.M. (1976) "A Probabilistic Estimate of Maximum Acceleration in Rock in the Contiguous United States", U.S. Dept. of the Interior, Geol. Survey, Open File Report 76-416.
- Atwater, T. (1970) "Implications of Plate Tectonics for the Cenozoic Tectonic Evolution of Western North America", Bulletin Geol. Soc. of America (81).
- Barlow, R.E. and Proschan F. (1975) "STATISTICAL THEORY OF RELIABILITY AND LIFE TESTING", International Series in Decision Processes, Holt, Rinehart and Winston, Inc.
- Basu, S. and Nigam N.C. (1977) "Seismic Risk of the Indian Peninsula", Proc. of 6th World Conference on Earthquake Engineering, India.
- Berrill, J.B. (1975) "A Study of High Frequency Strong Ground Motion from the San Fernando Earthquake", PhD Thesis, California Institute of Technology.
- Bolt, B.A., Lomnitz C. and McEvelly T.V. (1968) "Seismological Evidence on The Tectonics of Central and Northern California and the Mendocino Escarpment", Bulletin Seism. Soc. of America, (58), 6.
- Bolt, B.A. and Miller, R.D. (1971) "Seismicity of Northern and Central California 1965-1969", Bulletin Seism. Soc. of America, (61), 6.
- Bolt, B.A. and Miller, R.D. (1975) "Catalogue of Earthquakes in Northern California and Adjoining Areas, 1 January 1910 - 31 December 1972", Seismographic Stations, University of California, Berkeley, California.
- Borcherdt, R.D. (1975) Editor, "Studies for Seismic Zonation of the San Francisco Bay Region", U.S. Dept. of the Interior, Geological Survey Paper 941-A.
- Borcherdt, R.D. and Gibbs, J.F. (1976) "Effects of Local Geological Conditions in the San Francisco Bay Region on Ground Motions and the Intensities of the 1906 Earthquake", Bulletin Seism. Soc. of America, (66), 2.
- Brazee, R.J. (1976) "Final Report of Earthquake Intensities with Respect to Attenuation, Magnitude and Rate of Recurrence", Revised Editions, National Geophysical and Solar Terrestrial Data Center, Boulder, Colorado.
- Brune, J.N. (1977) "The Physics of Earthquake Strong Motion", SEISMIC RISK AND ENGINEERING DECISIONS, Ch. 5, C. Lomnitz and E. Rosenblueth (Editors), Developments in Geotechnical Engineering, 15, Elsevier.
- Caputo, M., Keilis-Borok, V., Kronrod, T., Molchan, G., Panza, G.F., Piva, A., Podgajzskaya, V. and Postpischl, D. (1973) "Models of Earthquake Occurrence and Isoleismals in Italy", Annali di Geofisica (XXVI), (2-3).

- Cornell, C.A. and Merz, H.A., (1975) "Seismic Risk Analysis of Boston", Journal of the Structural Division, ASCE, Vol. 101, No. ST10.
- Cornell, C.A. (1976) "Seismic Risk Analysis", Lecture notes from Course 'Recent Advances in Earthquake Resistant Design of Structures' University Extension, University of California, Berkeley.
- Culver, C.G., Lew, H.S., Hart, G.C. and Pinkham, C.W. (1975) "National Hazards Evaluation of Existing Buildings" U.S. Dept. of Commerce, National Bureau of Standards Building Science Series 61.
- Dalal, J.S. (1972) "Probabilistic Seismic Exposure and Structural Risk Evaluation", PhD Thesis, Stanford University.
- Degenkolb, H.J. (1975) "Guest Editorial", Earthquake Engineering Research Institute, Newsletter (9), 2.
- Dieterich, J.H. (1973) "A Deterministic Near-Field Source Model" Proceedings of 5th World Conference on Earthquake Engineering, Italy.
- Dobry R., Idriss, I.M., Chang C.-Y and Ng, E. (1977) "Influence of Magnitude, Site Conditions and Distance on Significant Duration of Earthquakes", Proceedings of 6th World Conference of Earthquake Engineering, India.
- Douglas, B.M. and Ryall, A. (1975) "Return Periods for Rock Acceleration in Western Nevada", Bulletin Seism. Soc. of America, (65), 6.
- Douglas, B.M. and Ryall, A. (1977) "Seismic Risk in Linear Source Regions with Application to the San Andreas Fault", Bulletin Seism. Soc. of America (67), 1.
- Esteva, L. (1975) "Geology and Probability in the Assessment of Seismic Risk", Report EL3, Universidad Nacional Autonoma de Mexico.
- Esteva, L. (1977) "Seismicity", SEISMIC RISK AND ENGINEERING DECISIONS. Ch. 6, Lomnitz and E. Rosenblueth (Editors), Developments in Geotechnical Engineering, 15, Elsevier.
- Feller, W. (1971) "AN INTRODUCTION TO PROBABILITY THEORY AND ITS APPLICATIONS", Vol. II, John Wiley & Sons, New York.
- Friedman, D.G. (1975) "Computer Simulation in Natural Hazard Assessment", Institute of Behavioral Science, University of Colorado.
- Galanopoulos, A.G. (1968) "On Quantitative Determination of Earthquake Risk", Annali di Geofisica, Vol. XXI, No. 2.
- Gardner, J.K. and Knopoff, L. (1974) "Is the Sequence of Earthquakes in Southern California with Aftershocks Removed, Poissonian", Bulletin Seism. Soc. of America, (64), 5.
- Gradshteyn, I.S. and Ryzhik, I.M. (1965) "TABLE OF INTEGRALS SERIES, AND PRODUCTS", Academic Press.
- Greensfelder, R. (1972) "Maximum Expected Bedrock Acceleration from Earthquakes in California", Unpublished California Division of Mines and Geology Map.

- Hasofar, A.M. (1973) "Contributions to Probabilistic Methods in Civil Engineering", MIT Dept. of C.E. Report R73-33., Order No. 369, Massachusetts Institute of Technology.
- Herd, D.G. (1978) "Neotectonic Framework of Central Coastal California and the Implications to Microzonation of the San Francisco Bay Region" Proceedings of 2nd Int. Conf. on Microzonation (1), San Francisco, California .
- Hofman, R.B. (1968) "Geodimeter Fault Movement Investigations in California", Dept. of Water Resources Bulletin No. 116-6.
- Idriss, I.M. and Seed, H.B. (1968) "An Analysis of Ground Motions During the 1957 San Francisco Earthquake", Bulletin Seism. Soc. of America, (58), 6.
- Johnson, L. and McEvelly, T.V. (1974) "Near-Field Observations and Source Parameters of Central California Earthquakes", Bulletin Seism. Soc. of America, (64), 6.
- Johnson, R.A. (1973) "An Earthquake Spectrum Prediction Technique", Bulletin Seism. Soc. of America, (63), 4.
- Kelleher, J., Sykes, L. and Oliver, J. (1973) "Possible Criteria for Predicting Earthquake Locations and Their Application to Major Plate Boundaries of the Pacific and the Caribbean", Journal Geophys. Research, 78, (14).
- Kiremidjian, A. and Shah, H.C. (1975) "Seismic Hazard Mapping of California", Technical Report No. 21. The John A. Blume Earthquake Engineering Center, Dept. of C.E., Stanford University.
- Kiureghian, A.D. and Ang., H-S. (1975) "A Line Source Model for Seismic Risk Analysis", Report UILU-ENG-75-2023 Structural Research Series No. 419, University of Illinois.
- Knopoff, L. (1964) "The Statistics of Earthquakes in Southern California", Bulletin Seism. Soc. of America, (54), 6.
- Knopoff, L. (1971) "A Stochastic Model for the Occurrence of Main Sequence Earthquakes", Review of Geophysics (9).
- Knopoff, L. and Kagan, Y. (1977) "Analysis of the Theory of Extremes as Applied in Earthquake Problems", Journal of Geophys. Research (82).
- Lomnitz, C. (1974) "GLOBAL TECTONICS AND EARTHQUAKE RISK", Development in Geotectonics 5, Elsevier, Amsterdam, London, N.Y.
- Lynch, R.D. (1969) "Response Spectra for Pahute Mesa Nuclear Events", Bulletin Seism. Soc. of America (59), 6.
- McEvelly, T.V. and Simla, G.W. (1972) "Earthquake Ground Motion Study", Lawrence Berkeley Laboratory Report UCID-3575, University of California, Berkeley.
- McGuire, R.K. (1974) "Seismic Structural Response Analysis Incorporating Peak Response Regressions on Earthquake Magnitude and Distance", MIT Dept. of C.E. R74-51, Order No. 399, Massachusetts Institute of Technology.

- McGuire, R.K. (1976) "Methodology for Incorporating Parameter Uncertainties into Seismic Hazard Analysis for Low Risk Design Intensities", Symposium on Earthquake Structural Engineering, St. Louis.
- McNally, K.C. (1976) "Spatial, Temporal and Mechanistic Character in Earthquake Occurrence: A Segment of the San Andreas Fault in Central California", PhD Thesis, University of California, Berkeley.
- Merz, H.A. and Cornell, A.C. (1973) "Seismic Risk Analysis Based on a Quadratic Magnitude-Frequency Law", Bulletin Seism. Soc. of America, (63), 6.
- Newmark, N.M. and Rosenblueth, E. (1971) "FUNDAMENTALS OF EARTHQUAKE ENGINEERING", Prentice Hall, Inc.
- O.E.P. (1972) "A Study of Earthquake Losses in the San Francisco Bay Area", Report prepared by National Oceanic and Atmospheric Administration for the Office of Emergency Preparedness.
- Oliveira, C.S. (1974) "Seismic Risk Analysis", EERC 74-1, Earthquake Engineering Research Center, University of California, Berkeley.
- Oliveira, C.S. (1975) "Seismic Risk Analysis for a Site and a Metropolitan Region", EERC 75-3, Earthquake Engineering Research Center, University of California, Berkeley.
- Oliveira, C.S. (1977) "Sismologia, Sismicidade e Risco Sismico. Aplicacoes em Portugal", Relatorio, Laboratorio Nacional de Engenharia Civil, Lisboa.
- Page, R.A., Boore, D.M., Dieterich, J.H. (1975) "Estimation of Bedrock Motion at the Ground Surface" in Studies for Seismic Zonation of the San Francisco Bay Region, R.D. Borcherdt (Editor), Geological Survey Paper No. 941-A.
- Penzien, J. and Tseng, W.S. (1977) "Three Dimensional Dynamic Analysis of Fixed Offshore Platforms", Proceedings International Symposium on Numerical Methods, Offshore Engineering, Swansea.
- Pereira, J., Oliveira, C.S. and Duarte, R.T. (1977) "Direct and Inverse Conversion from Power Spectra to Response Spectra", Proceedings of 6th. World Conference of Earthquake Engineering, India.
- Richter, C.F. (1955) "ELEMENTARY SEISMOLOGY", W.H. Freeman & Co., San Francisco, Calif.
- Steward, I.C.F. (1974) "On the Use of Maximum Likelihood Estimator for Recurrence Curves", Earthquake Notes (45), 3.
- Taleb-Agha, G. (1975) "Seismic Risk Analysis of Discrete Systems", MIT, Dept. of C.E. Report No. R75-48, Order No. 523, Massachusetts Institute of Technology.
- Tocher, D. (1959) "Seismic History of the San Francisco Region", in San Francisco Earthquake of March 1957, Special Report 57, California Division of Mines and Geology.

Tocher, D., Patwardhan, A.S. and Cluff, L.S. (1977) "Estimation of Near-Field Characteristics of Earthquake Motion", Proceedings of 6th World Conference on Earthquake Engineering, India.

Udias, A. and Rice, J. (1975) "Statistical Analysis of Microearthquake Activity near San Andreas Geophysical Observatory, Hollister, California", Bulletin Seism. Soc. of America, (6), 4.

Utsu, T. (1966) "A Statistical Significance Test of the Difference in b-value between two Earthquake Groups", Journal of Physics of the Earth (14), 2.

Vagliente, V.N. (1973) "Forecasting the Risk Inherent in Earthquake Resistant Design", Dept. of Civil Engineering, Technical Report No. 174, Stanford University.

Wallace, R.E. (1970) "Earthquake Recurrence Intervals on the San Andreas Fault", Bulletin Geol. Soc. of America (81).

Wallace, R.E. (1977) "Time-history Analysis of Fault Scarps and Fault Traces a Longer View of Seismicity", Proceedings of 6th World Conference on Earthquake Engineering, India.

Whitman, R.V. and Cornell, C.A. (1977) "Design" in SEISMIC RISK AND ENGINEERING DECISIONS, Chapter 9. C. Lomnitz and E. Rosenblueth (Editors), Developments in Geotechnical Engineering 15, Elsevier.

Yegian, M.K. (1976) "Risk Analysis for Earthquake Induced Ground Failure by Liquefaction", M.I.T. Department of Civil Engineering, R76-22, Order No. 542, Massachusetts Inst. of Technology.

EARTHQUAKE ENGINEERING RESEARCH CENTER REPORTS

NOTE: Numbers in parenthesis are Accession Numbers assigned by the National Technical Information Service; these are followed by a price code. Copies of the reports may be ordered from the National Technical Information Service, 5285 Port Royal Road, Springfield, Virginia, 22161. Accession Numbers should be quoted on orders for reports (PB --- ---) and remittance must accompany each order. Reports without this information were not available at time of printing. Upon request, EERC will mail inquirers this information when it becomes available.

- EERC 67-1 "Feasibility Study Large-Scale Earthquake Simulator Facility," by J. Penzien, J.G. Bouwkamp, R.W. Clough and D. Rea - 1967 (PB 187 905)A07
- EERC 68-1 Unassigned
- EERC 68-2 "Inelastic Behavior of Beam-to-Column Subassemblages Under Repeated Loading," by V.V. Bertero - 1968 (PB 184 888)A05
- EERC 68-3 "A Graphical Method for Solving the Wave Reflection-Refraction Problem," by H.D. McNiver and Y. Mengi - 1968 (PB 187 943)A03
- EERC 68-4 "Dynamic Properties of McKinley School Buildings," by D. Rea, J.G. Bouwkamp and R.W. Clough - 1968 (PB 187 902)A07
- EERC 68-5 "Characteristics of Rock Motions During Earthquakes," by H.B. Seed, I.M. Idriss and F.W. Kiefer - 1968 (PB 188 338)A03
- EERC 69-1 "Earthquake Engineering Research at Berkeley," - 1969 (PB 187 906)A11
- EERC 69-2 "Nonlinear Seismic Response of Earth Structures," by M. Dibaj and J. Penzien - 1969 (PB 187 904)A08
- EERC 69-3 "Probabilistic Study of the Behavior of Structures During Earthquakes," by R. Ruiz and J. Penzien - 1969 (PB 187 886)A06
- EERC 69-4 "Numerical Solution of Boundary Value Problems in Structural Mechanics by Reduction to an Initial Value Formulation," by N. Distefano and J. Schujman - 1969 (PB 187 942)A02
- EERC 69-5 "Dynamic Programming and the Solution of the Biharmonic Equation," by N. Distefano - 1969 (PB 187 941)A03
- EERC 69-6 "Stochastic Analysis of Offshore Tower Structures," by A.K. Malhotra and J. Penzien - 1969 (PB 187 903)A09
- EERC 69-7 "Rock Motion Accelerograms for High Magnitude Earthquakes," by H.B. Seed and I.M. Idriss - 1969 (PB 187 940)A02
- EERC 69-8 "Structural Dynamics Testing Facilities at the University of California, Berkeley," by R.M. Stephen, J.G. Bouwkamp, R.W. Clough and J. Penzien - 1969 (PB 189 111)A04
- EERC 69-9 "Seismic Response of Soil Deposits Underlain by Sloping Rock Boundaries," by H. Dezfulian and H.B. Seed - 1969 (PB 189 114)A03
- EERC 69-10 "Dynamic Stress Analysis of Axisymmetric Structures Under Arbitrary Loading," by S. Ghosh and E.L. Wilson - 1969 (PB 189 026)A10
- EERC 69-11 "Seismic Behavior of Multistory Frames Designed by Different Philosophies," by J.C. Anderson and V. V. Bertero - 1969 (PB 190 662)A10
- EERC 69-12 "Stiffness Degradation of Reinforcing Concrete Members Subjected to Cyclic Flexural Moments," by V.V. Bertero, B. Bresler and H. Ming Liao - 1969 (PB 202 942)A07
- EERC 69-13 "Response of Non-Uniform Soil Deposits to Travelling Seismic Waves," by H. Dezfulian and H.B. Seed - 1969 (PB 191 023)A03
- EERC 69-14 "Damping Capacity of a Model Steel Structure," by D. Rea, R.W. Clough and J.G. Bouwkamp - 1969 (PB 190 663)A06
- EERC 69-15 "Influence of Local Soil Conditions on Building Damage Potential during Earthquakes," by H.B. Seed and I.M. Idriss - 1969 (PB 191 036)A03
- EERC 69-16 "The Behavior of Sands Under Seismic Loading Conditions," by M.L. Silver and H.B. Seed - 1969 (AD 714 982)A07
- EERC 70-1 "Earthquake Response of Gravity Dams," by A.K. Chopra - 1970 (AD 709 640)A03
- EERC 70-2 "Relationships between Soil Conditions and Building Damage in the Caracas Earthquake of July 29, 1967," by H.B. Seed, I.M. Idriss and H. Dezfulian - 1970 (PB 195 762)A05
- EERC 70-3 "Cyclic Loading of Full Size Steel Connections," by E.P. Popov and R.M. Stephen - 1970 (PB 213 545)A04
- EERC 70-4 "Seismic Analysis of the Charaima Building, Caraballeda, Venezuela," by Subcommittee of the SEAONC Research Committee: V.V. Bertero, P.F. Fratessa, S.A. Mahin, J.H. Sexton, A.C. Scordelis, E.L. Wilson, L.A. Wyllie, H.B. Seed and J. Penzien, Chairman - 1970 (PB 201 455)A06

- EERC 70-5 "A Computer Program for Earthquake Analysis of Dams," by A.K. Chopra and P. Chakrabarti - 1970 (AD 723 994)A05
- EERC 70-6 "The Propagation of Love Waves Across Non-Horizontally Layered Structures," by J. Lysmer and L.A. Drake 1970 (PB 197 896)A03
- EERC 70-7 "Influence of Base Rock Characteristics on Ground Response," by J. Lysmer, H.B. Seed and P.B. Schnabel 1970 (PB 197 897)A03
- EERC 70-8 "Applicability of Laboratory Test Procedures for Measuring Soil Liquefaction Characteristics under Cyclic Loading," by H.B. Seed and W.H. Peacock - 1970 (PB 198 016)A03
- EERC 70-9 "A Simplified Procedure for Evaluating Soil Liquefaction Potential," by H.B. Seed and I.M. Idriss - 1970 (PB 198 009)A03
- EERC 70-10 "Soil Moduli and Damping Factors for Dynamic Response Analysis," by H.B. Seed and I.M. Idriss - 1970 (PB 197 869)A03
- EERC 71-1 "Koyna Earthquake of December 11, 1967 and the Performance of Koyna Dam," by A.K. Chopra and P. Chakrabarti 1971 (AD 731 496)A06
- EERC 71-2 "Preliminary In-Situ Measurements of Anelastic Absorption in Soils Using a Prototype Earthquake Simulator," by R.D. Borcherdt and P.W. Rodgers - 1971 (PB 201 454)A03
- EERC 71-3 "Static and Dynamic Analysis of Inelastic Frame Structures," by F.L. Porter and G.H. Powell - 1971 (PB 210 135)A06
- EERC 71-4 "Research Needs in Limit Design of Reinforced Concrete Structures," by V.V. Bertero - 1971 (PB 202 943)A04
- EERC 71-5 "Dynamic Behavior of a High-Rise Diagonally Braced Steel Building," by D. Rea, A.A. Shah and J.G. Bouwkamp 1971 (PB 203 584)A06
- EERC 71-6 "Dynamic Stress Analysis of Porous Elastic Solids Saturated with Compressible Fluids," by J. Ghaboussi and E. L. Wilson - 1971 (PB 211 396)A06
- EERC 71-7 "Inelastic Behavior of Steel Beam-to-Column Subassemblies," by H. Krawinkler, V.V. Bertero and E.P. Popov 1971 (PB 211 335)A14
- EERC 71-8 "Modification of Seismograph Records for Effects of Local Soil Conditions," by P. Schnabel, H.B. Seed and J. Lysmer - 1971 (PB 214 450)A03
- EERC 72-1 "Static and Earthquake Analysis of Three Dimensional Frame and Shear Wall Buildings," by E.L. Wilson and H.H. Dovey - 1972 (PB 212 904)A05
- EERC 72-2 "Accelerations in Rock for Earthquakes in the Western United States," by P.B. Schnabel and H.B. Seed - 1972 (PB 213 100)A03
- EERC 72-3 "Elastic-Plastic Earthquake Response of Soil-Building Systems," by T. Minami - 1972 (PB 214 868)A08
- EERC 72-4 "Stochastic Inelastic Response of Offshore Towers to Strong Motion Earthquakes," by M.K. Kaul - 1972 (PB 215 713)A05
- EERC 72-5 "Cyclic Behavior of Three Reinforced Concrete Flexural Members with High Shear," by E.P. Popov, V.V. Bertero and H. Krawinkler - 1972 (PB 214 555)A05
- EERC 72-6 "Earthquake Response of Gravity Dams Including Reservoir Interaction Effects," by P. Chakrabarti and A.K. Chopra - 1972 (AD 762 330)A08
- EERC 72-7 "Dynamic Properties of Pine Flat Dam," by D. Rea, C.Y. Liaw and A.K. Chopra - 1972 (AD 763 928)A05
- EERC 72-8 "Three Dimensional Analysis of Building Systems," by E.L. Wilson and H.H. Dovey - 1972 (PB 222 438)A06
- EERC 72-9 "Rate of Loading Effects on Uncracked and Repaired Reinforced Concrete Members," by S. Mahin, V.V. Bertero, D. Rea and M. Atalay - 1972 (PB 224 520)A08
- EERC 72-10 "Computer Program for Static and Dynamic Analysis of Linear Structural Systems," by E.L. Wilson, K.-J. Bathe, J.E. Peterson and H.H. Dovey - 1972 (PB 220 437)A04
- EERC 72-11 "Literature Survey - Seismic Effects on Highway Bridges," by T. Iwasaki, J. Penzien and R.W. Clough - 1972 (PB 215 613)A19
- EERC 72-12 "SHAKE-A Computer Program for Earthquake Response Analysis of Horizontally Layered Sites," by P.B. Schnabel and J. Lysmer - 1972 (PB 220 207)A06
- EERC 73-1 "Optimal Seismic Design of Multistory Frames," by V.V. Bertero and H. Kamil - 1973
- EERC 73-2 "Analysis of the Slides in the San Fernando Dams During the Earthquake of February 9, 1971," by H.B. Seed, K.L. Lee, I.M. Idriss and F. Makdisi - 1973 (PB 223 402)A14

- EERC 73-3 "Computer Aided Ultimate Load Design of Unbraced Multistory Steel Frames," by M.B. El-Hafez and G.H. Powell 1973 (PB 248 315)A09
- EERC 73-4 "Experimental Investigation into the Seismic Behavior of Critical Regions of Reinforced Concrete Components as Influenced by Moment and Shear," by M. Celebi and J. Penzien - 1973 (PB 215 884)A09
- EERC 73-5 "Hysteretic Behavior of Epoxy-Repaired Reinforced Concrete Beams," by M. Celebi and J. Penzien - 1973 (PB 239 568)A03
- EERC 73-6 "General Purpose Computer Program for Inelastic Dynamic Response of Plane Structures," by A. Kanaan and G.H. Powell - 1973 (PB 221 260)A08
- EERC 73-7 "A Computer Program for Earthquake Analysis of Gravity Dams Including Reservoir Interaction," by P. Chakrabarti and A.K. Chopra - 1973 (AD 766 271)A04
- EERC 73-8 "Behavior of Reinforced Concrete Deep Beam-Column Subassemblages Under Cyclic Loads," by O. Küstü and J.G. Bouwkamp - 1973 (PB 246 117)A12
- EERC 73-9 "Earthquake Analysis of Structure-Foundation Systems," by A.K. Vaish and A.K. Chopra - 1973 (AD 766 272)A07
- EERC 73-10 "Deconvolution of Seismic Response for Linear Systems," by R.B. Reimer - 1973 (PB 227 179)A08
- EERC 73-11 "SAP IV: A Structural Analysis Program for Static and Dynamic Response of Linear Systems," by K.-J. Bathe, E.L. Wilson and F.E. Peterson - 1973 (PB 221 967)A09
- EERC 73-12 "Analytical Investigations of the Seismic Response of Long, Multiple Span Highway Bridges," by W.S. Tseng and J. Penzien - 1973 (PB 227 816)A10
- EERC 73-13 "Earthquake Analysis of Multi-Story Buildings Including Foundation Interaction," by A.K. Chopra and J.A. Gutierrez - 1973 (PB 222 970)A03
- EERC 73-14 "ADAP: A Computer Program for Static and Dynamic Analysis of Arch Dams," by R.W. Clough, J.M. Raphael and S. Mojtahedi - 1973 (PB 223 763)A09
- EERC 73-15 "Cyclic Plastic Analysis of Structural Steel Joints," by R.B. Pinkney and R.W. Clough - 1973 (PB 226 843)A08
- EERC 73-16 "QUAD-4: A Computer Program for Evaluating the Seismic Response of Soil Structures by Variable Damping Finite Element Procedures," by I.M. Idriss, J. Lysmer, R. Hwang and H.B. Seed - 1973 (PB 229 424)A05
- EERC 73-17 "Dynamic behavior of a Multi-Story Pyramid Shaped Building," by R.M. Stephen, J.P. Hollings and J.G. Bouwkamp - 1973 (PB 240 718)A06
- EERC 73-18 "Effect of Different Types of Reinforcing on Seismic Behavior of Short Concrete Columns," by V.V. Bertero, J. Hollings, O. Küstü, R.M. Stephen and J.G. Bouwkamp - 1973
- EERC 73-19 "Olive View Medical Center Materials Studies, Phase I," by B. Bresler and V.V. Bertero - 1973 (PB 235 986)A06
- EERC 73-20 "Linear and Nonlinear Seismic Analysis Computer Programs for Long Multiple-Span Highway Bridges," by W.S. Tseng and J. Penzien - 1973
- EERC 73-21 "Constitutive Models for Cyclic Plastic Deformation of Engineering Materials," by J.M. Kelly and P.P. Gillis 1973 (PB 226 024)A03
- EERC 73-22 "DRAIN - 2D User's Guide," by G.H. Powell - 1973 (PB 227 016)A05
- EERC 73-23 "Earthquake Engineering at Berkeley - 1973," (PB 226 033)A11
- EERC 73-24 Unassigned
- EERC 73-25 "Earthquake Response of Axisymmetric Tower Structures Surrounded by Water," by C.Y. Liaw and A.K. Chopra 1973 (AD 773 052)A09
- EERC 73-26 "Investigation of the Failures of the Olive View Stairtowers During the San Fernando Earthquake and Their Implications on Seismic Design," by V.V. Bertero and R.G. Collins - 1973 (PB 235 106)A13
- EERC 73-27 "Further Studies on Seismic Behavior of Steel Beam-Column Subassemblages," by V.V. Bertero, H. Krawinkler and E.P. Popov - 1973 (PB 234 172)A06
- EERC 74-1 "Seismic Risk Analysis," by C.S. Oliveira - 1974 (PB 235 920)A06
- EERC 74-2 "Settlement and Liquefaction of Sands Under Multi-Directional Shaking," by R. Pyke, C.K. Chan and H.B. Seed 1974
- EERC 74-3 "Optimum Design of Earthquake Resistant Shear Buildings," by D. Ray, K.S. Pister and A.K. Chopra - 1974 (PB 231 172)A06
- EERC 74-4 "IUSH - A Computer Program for Complex Response Analysis of Soil-Structure Systems," by J. Lysmer, T. Udaka, H.B. Seed and R. Hwang - 1974 (PB 236 796)A05

- EERC 74-5 "Sensitivity Analysis for Hysteretic Dynamic Systems: Applications to Earthquake Engineering," by D. Ray 1974 (PB 233 213)A06
- EERC 74-6 "Soil Structure Interaction Analyses for Evaluating Seismic Response," by H.B. Seed, J. Lysmer and R. Hwang 1974 (PB 236 519)A04
- EERC 74-7 Unassigned
- EERC 74-8 "Shaking Table Tests of a Steel Frame - A Progress Report," by R.W. Clough and D. Tang - 1974 (PB 240 869)A03
- EERC 74-9 "Hysteretic Behavior of Reinforced Concrete Flexural Members with Special Web Reinforcement," by V.V. Bertero, E.P. Popov and T.Y. Wang - 1974 (PB 236 797)A07
- EERC 74-10 "Applications of Reliability-Based, Global Cost Optimization to Design of Earthquake Resistant Structures," by E. Vitiello and K.S. Pister - 1974 (PB 237 231)A06
- EERC 74-11 "Liquefaction of Gravelly Soils Under Cyclic Loading Conditions," by R.T. Wong, H.B. Seed and C.K. Chan 1974 (PB 242 042)A03
- EERC 74-12 "Site-Dependent Spectra for Earthquake-Resistant Design," by H.B. Seed, C. Ugas and J. Lysmer - 1974 (PB 240 953)A03
- EERC 74-13 "Earthquake Simulator Study of a Reinforced Concrete Frame," by P. Hidalgo and R.W. Clough - 1974 (PB 241 944)A13
- EERC 74-14 "Nonlinear Earthquake Response of Concrete Gravity Dams," by N. Pal - 1974 (AD/A 006 583)A06
- EERC 74-15 "Modeling and Identification in Nonlinear Structural Dynamics - I. One Degree of Freedom Models," by N. Distefano and A. Rath - 1974 (PB 241 548)A06
- EERC 75-1 "Determination of Seismic Design Criteria for the Dumbarton Bridge Replacement Structure, Vol. I: Description, Theory and Analytical Modeling of Bridge and Parameters," by F. Baron and S.-H. Pang - 1975 (PB 259 407)A15
- EERC 75-2 "Determination of Seismic Design Criteria for the Dumbarton Bridge Replacement Structure, Vol. II: Numerical Studies and Establishment of Seismic Design Criteria," by F. Baron and S.-H. Pang - 1975 (PB 259 408)A11 (For set of EERC 75-1 and 75-2 (PB 259 406))
- EERC 75-3 "Seismic Risk Analysis for a Site and a Metropolitan Area," by C.S. Oliveira - 1975 (PB 248 134)A09
- EERC 75-4 "Analytical Investigations of Seismic Response of Short, Single or Multiple-Span Highway Bridges," by M.-C. Chen and J. Penzien - 1975 (PB 241 454)A09
- EERC 75-5 "An Evaluation of Some Methods for Predicting Seismic Behavior of Reinforced Concrete Buildings," by S.A. Mahin and V.V. Bertero - 1975 (PB 246 306)A16
- EERC 75-6 "Earthquake Simulator Study of a Steel Frame Structure, Vol. I: Experimental Results," by R.W. Clough and D.T. Tang - 1975 (PB 243 981)A13
- EERC 75-7 "Dynamic Properties of San Bernardino Intake Tower," by D. Rea, C.-Y. Liaw and A.K. Chopra - 1975 (AD/A008 406) A05
- EERC 75-8 "Seismic Studies of the Articulation for the Dumbarton Bridge Replacement Structure, Vol. I: Description, Theory and Analytical Modeling of Bridge Components," by F. Baron and R.E. Hamati - 1975 (PB 251 539)A07
- EERC 75-9 "Seismic Studies of the Articulation for the Dumbarton Bridge Replacement Structure, Vol. 2: Numerical Studies of Steel and Concrete Girder Alternates," by F. Baron and R.E. Hamati - 1975 (PB 251 540)A10
- EERC 75-10 "Static and Dynamic Analysis of Nonlinear Structures," by D.P. Mondkar and G.H. Powell - 1975 (PB 242 434)A08
- EERC 75-11 "Hysteretic Behavior of Steel Columns," by E.P. Popov, V.V. Bertero and S. Chandramouli - 1975 (PB 252 365)A11
- EERC 75-12 "Earthquake Engineering Research Center Library Printed Catalog," - 1975 (PB 243 711)A26
- EERC 75-13 "Three Dimensional Analysis of Building Systems (Extended Version)," by E.L. Wilson, J.P. Hollings and H.H. Dovey - 1975 (PB 243 989)A07
- EERC 75-14 "Determination of Soil Liquefaction Characteristics by Large-Scale Laboratory Tests," by P. De Alba, C.K. Chan and H.B. Seed - 1975 (NUREG 0027)A08
- EERC 75-15 "A Literature Survey - Compressive, Tensile, Bond and Shear Strength of Masonry," by R.L. Mayes and R.W. Clough - 1975 (PB 246 292)A10
- EERC 75-16 "Hysteretic Behavior of Ductile Moment Resisting Reinforced Concrete Frame Components," by V.V. Bertero and E.P. Popov - 1975 (PB 246 388)A05
- EERC 75-17 "Relationships Between Maximum Acceleration, Maximum Velocity, Distance from Source, Local Site Conditions for Moderately Strong Earthquakes," by H.B. Seed, R. Murarka, J. Lysmer and I.M. Idriss - 1975 (PB 248 172)A03
- EERC 75-18 "The Effects of Method of Sample Preparation on the Cyclic Stress-Strain Behavior of Sands," by J. Mullis, C.K. Chan and H.B. Seed - 1975 (Summarized in EERC 75-28)

- EERC 75-19 "The Seismic Behavior of Critical Regions of Reinforced Concrete Components as Influenced by Moment, Shear and Axial Force," by M.B. Atalay and J. Penzien - 1975 (PB 258 842)A11
- EERC 75-20 "Dynamic Properties of an Eleven Story Masonry Building," by R.M. Stephen, J.P. Hollings, J.G. Bouwkamp and D. Jurukovski - 1975 (PB 246 945)A04
- EERC 75-21 "State-of-the-Art in Seismic Strength of Masonry - An Evaluation and Review," by R.L. Mayes and R.W. Clough - 1975 (PB 249 040)A07
- EERC 75-22 "Frequency Dependent Stiffness Matrices for Viscoelastic Half-Plane Foundations," by A.K. Chopra, P. Chakrabarti and G. Dasgupta - 1975 (PB 248 121)A07
- EERC 75-23 "Hysteretic Behavior of Reinforced Concrete Framed Walls," by T.Y. Wong, V.V. Bertero and E.P. Popov - 1975
- EERC 75-24 "Testing Facility for Subassemblages of Frame-Wall Structural Systems," by V.V. Bertero, E.P. Popov and T. Endo - 1975
- EERC 75-25 "Influence of Seismic History on the Liquefaction Characteristics of Sands," by H.B. Seed, K. Mori and C.K. Chan - 1975 (Summarized in EERC 75-28)
- EERC 75-26 "The Generation and Dissipation of Pore Water Pressures during Soil Liquefaction," by H.B. Seed, P.P. Martin and J. Lysmer - 1975 (PB 252 648)A03
- EERC 75-27 "Identification of Research Needs for Improving Aseismic Design of Building Structures," by V.V. Bertero - 1975 (PB 248 136)A05
- EERC 75-28 "Evaluation of Soil Liquefaction Potential during Earthquakes," by H.B. Seed, I. Arango and C.K. Chan - 1975 (NUREG 0026)A13
- EERC 75-29 "Representation of Irregular Stress Time Histories by Equivalent Uniform Stress Series in Liquefaction Analyses," by H.B. Seed, I.M. Idriss, F. Makdisi and N. Banerjee - 1975 (PB 252 635)A03
- EERC 75-30 "FLUSH - A Computer Program for Approximate 3-D Analysis of Soil-Structure Interaction Problems," by J. Lysmer, T. Udaka, C.-F. Tsai and H.B. Seed - 1975 (PB 259 332)A07
- EERC 75-31 "ALUSH - A Computer Program for Seismic Response Analysis of Axisymmetric Soil-Structure Systems," by E. Berger, J. Lysmer and H.B. Seed - 1975
- EERC 75-32 "TRIP and TRAVEL - Computer Programs for Soil-Structure Interaction Analysis with Horizontally Travelling Waves," by T. Udaka, J. Lysmer and H.B. Seed - 1975
- EERC 75-33 "Predicting the Performance of Structures in Regions of High Seismicity," by J. Penzien - 1975 (PB 248 130)A03
- EERC 75-34 "Efficient Finite Element Analysis of Seismic Structure - Soil - Direction," by J. Lysmer, H.B. Seed, T. Udaka, R.N. Hwang and C.-F. Tsai - 1975 (PB 253 570)A03
- EERC 75-35 "The Dynamic Behavior of a First Story Girder of a Three-Story Steel Frame Subjected to Earthquake Loading," by R.W. Clough and L.-Y. Li - 1975 (PB 248 841)A05
- EERC 75-36 "Earthquake Simulator Study of a Steel Frame Structure, Volume II - Analytical Results," by D.T. Tang - 1975 (PB 252 926)A10
- EERC 75-37 "ANSR-I General Purpose Computer Program for Analysis of Non-Linear Structural Response," by D.P. Mondkar and G.H. Powell - 1975 (PB 252 386)A08
- EERC 75-38 "Nonlinear Response Spectra for Probabilistic Seismic Design and Damage Assessment of Reinforced Concrete Structures," by M. Murakami and J. Penzien - 1975 (PB 259 530)A05
- EERC 75-39 "Study of a Method of Feasible Directions for Optimal Elastic Design of Frame Structures Subjected to Earthquake Loading," by N.D. Walker and K.S. Pister - 1975 (PB 257 781)A06
- EERC 75-40 "An Alternative Representation of the Elastic-Viscoelastic Analogy," by G. Dasgupta and J.L. Sackman - 1975 (PB 252 173)A03
- EERC 75-41 "Effect of Multi-Directional Shaking on Liquefaction of Sands," by H.B. Seed, R. Pyke and G.R. Martin - 1975 (PB 258 781)A03
- EERC 76-1 "Strength and Ductility Evaluation of Existing Low-Rise Reinforced Concrete Buildings - Screening Method," by T. Okada and B. Bresler - 1976 (PB 257 906)A11
- EERC 76-2 "Experimental and Analytical Studies on the Hysteretic Behavior of Reinforced Concrete Rectangular and T-Beams," by S.-Y.M. Ma, E.P. Popov and V.V. Bertero - 1976 (PB 260 843)A12
- EERC 76-3 "Dynamic Behavior of a Multistory Triangular-Shaped Building," by J. Petrovski, R.M. Stephen, E. Gartenbaum and J.G. Bouwkamp - 1976 (PB 273 279)A07
- EERC 76-4 "Earthquake Induced Deformations of Earth Dams," by N. Serff, H.B. Seed, F.I. Makdisi & C.-Y. Chang - 1976 (PB 292 065)A08

- EERC 76-5 "Analysis and Design of Tube-Type Tall Building Structures," by H. de Clercq and G.H. Powell - 1976 (PB 252 220) A10
- EERC 76-6 "Time and Frequency Domain Analysis of Three-Dimensional Ground Motions, San Fernando Earthquake," by T. Kubo and J. Penzien (PB 260 556)A11
- EERC 76-7 "Expected Performance of Uniform Building Code Design Masonry Structures," by R.L. Mayes, Y. Omote, S.W. Chen and R.W. Clough - 1976 (PB 270 098)A05
- EERC 76-8 "Cyclic Shear Tests of Masonry Piers, Volume 1 - Test Results," by R.L. Mayes, Y. Omote, R.W. Clough - 1976 (PB 264 424)A06
- EERC 76-9 "A Substructure Method for Earthquake Analysis of Structure - Soil Interaction," by J.A. Gutierrez and A.K. Chopra - 1976 (PB 257 783)A08
- EERC 76-10 "Stabilization of Potentially Liquefiable Sand Deposits using Gravel Drain Systems," by H.B. Seed and J.R. Booker - 1976 (PB 258 820)A04
- EERC 76-11 "Influence of Design and Analysis Assumptions on Computed Inelastic Response of Moderately Tall Frames," by G.H. Powell and D.G. Row - 1976 (PB 271 409)A06
- EERC 76-12 "Sensitivity Analysis for Hysteretic Dynamic Systems: Theory and Applications," by D. Ray, K.S. Pister and E. Polak - 1976 (PB 262 859)A04
- EERC 76-13 "Coupled Lateral Torsional Response of Buildings to Ground Shaking," by C.L. Kan and A.K. Chopra - 1976 (PB 257 907)A09
- EERC 76-14 "Seismic Analyses of the Banco de America," by V.V. Bertero, S.A. Mahin and J.A. Hollings - 1976
- EERC 76-15 "Reinforced Concrete Frame 2: Seismic Testing and Analytical Correlation," by R.W. Clough and J. Gidwani - 1976 (PB 261 323)A08
- EERC 76-16 "Cyclic Shear Tests of Masonry Piers, Volume 2 - Analysis of Test Results," by R.L. Mayes, Y. Omote and R.W. Clough - 1976
- EERC 76-17 "Structural Steel Bracing Systems: Behavior Under Cyclic Loading," by E.P. Popov, K. Takanashi and C.W. Roeder - 1976 (PB 260 715)A05
- EERC 76-18 "Experimental Model Studies on Seismic Response of High Curved Overcrossings," by D. Williams and W.G. Godden - 1976 (PB 269 548)A08
- EERC 76-19 "Effects of Non-Uniform Seismic Disturbances on the Dumbarton Bridge Replacement Structure," by F. Baron and R.E. Hamati - 1976 (PB 282 981)A16
- EERC 76-20 "Investigation of the Inelastic Characteristics of a Single Story Steel Structure Using System Identification and Shaking Table Experiments," by V.C. Matzen and H.D. McNiven - 1976 (PB 258 453)A07
- EERC 76-21 "Capacity of Columns with Splice Imperfections," by E.P. Popov, R.M. Stephen and R. Philbrick - 1976 (PB 260 378)A04
- EERC 76-22 "Response of the Olive View Hospital Main Building during the San Fernando Earthquake," by S. A. Mahin, V.V. Bertero, A.K. Chopra and R. Collins - 1976 (PB 271 425)A14
- EERC 76-23 "A Study on the Major Factors Influencing the Strength of Masonry Prisms," by N.M. Mostaghel, R.L. Mayes, R. W. Clough and S.W. Chen - 1976 (Not published)
- EERC 76-24 "GADPLEA - A Computer Program for the Analysis of Pore Pressure Generation and Dissipation during Cyclic or Earthquake Loading," by J.R. Booker, M.S. Rahman and H.B. Seed - 1976 (PB 263 947)A04
- EERC 76-25 "Seismic Safety Evaluation of a R/C School Building," by B. Bresler and J. Axley - 1976
- EERC 76-26 "Correlative Investigations on Theoretical and Experimental Dynamic Behavior of a Model Bridge Structure," by K. Kawashima and J. Penzien - 1976 (PB 263 388)A11
- EERC 76-27 "Earthquake Response of Coupled Shear Wall Buildings," by T. Srichatrapimuk - 1976 (PB 265 157)A07
- EERC 76-28 "Tensile Capacity of Partial Penetration Welds," by E.P. Popov and R.M. Stephen - 1976 (PB 262 899)A03
- EERC 76-29 "Analysis and Design of Numerical Integration Methods in Structural Dynamics," by H.M. Hilber - 1976 (PB 264 410)A06
- EERC 76-30 "Contribution of a Floor System to the Dynamic Characteristics of Reinforced Concrete Buildings," by L.E. Malik and V.V. Bertero - 1976 (PB 272 247)A13
- EERC 76-31 "The Effects of Seismic Disturbances on the Golden Gate Bridge," by F. Baron, M. Arikan and R.E. Hamati - 1976 (PB 272 279)A09
- EERC 76-32 "Infilled Frames in Earthquake Resistant Construction," by R.E. Klingner and V.V. Bertero - 1976 (PB 265 892)A13

- UCB/EERC-77/01 "PLUSH - A Computer Program for Probabilistic Finite Element Analysis of Seismic Soil-Structure Interaction," by M.P. Romo Organista, J. Lysmer and H.B. Seed - 1977.
- UCB/EERC-77/02 "Soil-Structure Interaction Effects at the Humboldt Bay Power Plant in the Ferndale Earthquake of June 7, 1975," by J.E. Valera, H.B. Seed, C.F. Tsai and J. Lysmer - 1977 (PB 265 795)A04
- UCB/EERC-77/03 "Influence of Sample Disturbance on Sand Response to Cyclic Loading," by K. Mori, H.B. Seed and C.K. Chan - 1977 (PB 267 352)A04
- UCB/EERC-77/04 "Seismological Studies of Strong Motion Records," by J. Shoja-Taheri - 1977 (PB 269 655)A10
- UCB/EERC-77/05 "Testing Facility for Coupled-Shear Walls," by L. Li-Hyung, V.V. Bertero and E.P. Popov - 1977
- UCB/EERC-77/06 "Developing Methodologies for Evaluating the Earthquake Safety of Existing Buildings," by No. 1 - B. Bresler; No. 2 - B. Bresler, T. Okada and D. Zisling; No. 3 - T. Okada and B. Bresler; No. 4 - V.V. Bertero and B. Bresler - 1977 (PB 267 354)A08
- UCB/EERC-77/07 "A Literature Survey - Transverse Strength of Masonry Walls," by Y. Omote, R.L. Mayes, S.W. Chen and R.W. Clough - 1977 (PB 277 933)A07
- UCB/EERC-77/08 "DRAIN-TABS: A Computer Program for Inelastic Earthquake Response of Three Dimensional Buildings," by R. Guendelman-Israel and G.H. Powell - 1977 (PB 270 693)A07
- UCB/EERC-77/09 "SUBWALL: A Special Purpose Finite Element Computer Program for Practical Elastic Analysis and Design of Structural Walls with Substructure Option," by D.Q. Le, H. Peterson and E.P. Popov - 1977 (PB 270 567)A05
- UCB/EERC-77/10 "Experimental Evaluation of Seismic Design Methods for Broad Cylindrical Tanks," by D.P. Clough (PB 272 280)A13
- UCB/EERC-77/11 "Earthquake Engineering Research at Berkeley - 1976," - 1977 (PB 273 507)A09
- UCB/EERC-77/12 "Automated Design of Earthquake Resistant Multistory Steel Building Frames," by N.D. Walker, Jr. - 1977 (PB 276 526)A09
- UCB/EERC-77/13 "Concrete Confined by Rectangular Hoops Subjected to Axial Loads," by J. Vallenias, V.V. Bertero and E.P. Popov - 1977 (PB 275 165)A06
- UCB/EERC-77/14 "Seismic Strain Induced in the Ground During Earthquakes," by Y. Sugimura - 1977 (PB 284 201)A04
- UCB/EERC-77/15 "Bond Deterioration under Generalized Loading," by V.V. Bertero, E.P. Popov and S. Viathanatepa - 1977
- UCB/EERC-77/16 "Computer Aided Optimum Design of Ductile Reinforced Concrete Moment Resisting Frames," by S.W. Zagajeski and V.V. Bertero - 1977 (PB 280 137)A07
- UCB/EERC-77/17 "Earthquake Simulation Testing of a Stepping Frame with Energy-Absorbing Devices," by J.M. Kelly and D.F. Tsztoo - 1977 (PB 273 506)A04
- UCB/EERC-77/18 "Inelastic Behavior of Eccentrically Braced Steel Frames under Cyclic Loadings," by C.W. Roeder and E.P. Popov - 1977 (PB 275 526)A15
- UCB/EERC-77/19 "A Simplified Procedure for Estimating Earthquake-Induced Deformations in Dams and Embankments," by F.I. Makdisi and H.B. Seed - 1977 (PB 276 820)A04
- UCB/EERC-77/20 "The Performance of Earth Dams during Earthquakes," by H.B. Seed, F.I. Makdisi and P. de Alba - 1977 (PB 276 821)A04
- UCB/EERC-77/21 "Dynamic Plastic Analysis Using Stress Resultant Finite Element Formulation," by P. Lukkunapvasit and J.M. Kelly - 1977 (PB 275 453)A04
- UCB/EERC-77/22 "Preliminary Experimental Study of Seismic Uplift of a Steel Frame," by R.W. Clough and A.A. Huckelbridge 1977 (PB 278 769)A08
- UCB/EERC-77/23 "Earthquake Simulator Tests of a Nine-Story Steel Frame with Columns Allowed to Uplift," by A.A. Huckelbridge - 1977 (PB 277 944)A09
- UCB/EERC-77/24 "Nonlinear Soil-Structure Interaction of Skew Highway Bridges," by M.-C. Chen and J. Penzien - 1977 (PB 276 176)A07
- UCB/EERC-77/25 "Seismic Analysis of an Offshore Structure Supported on Pile Foundations," by D.D.-N. Liou and J. Penzien 1977 (PB 283 180)A06
- UCB/EERC-77/26 "Dynamic Stiffness Matrices for Homogeneous Viscoelastic Half-Planes," by G. Dasgupta and A.K. Chopra - 1977 (PB 279 654)A06
- UCB/EERC-77/27 "A Practical Soft Story Earthquake Isolation System," by J.M. Kelly, J.M. Eidinger and C.J. Derham - 1977 (PB 276 814)A07
- UCB/EERC-77/28 "Seismic Safety of Existing Buildings and Incentives for Hazard Mitigation in San Francisco: An Exploratory Study," by A.J. Meltsner - 1977 (PB 281 970)A05
- UCB/EERC-77/29 "Dynamic Analysis of Electrohydraulic Shaking Tables," by D. Rea, S. Abedi-Hayati and Y. Takahashi 1977 (PB 282 569)A04
- UCB/EERC-77/30 "An Approach for Improving Seismic - Resistant Behavior of Reinforced Concrete Interior Joints," by B. Galunic, V.V. Bertero and E.P. Popov - 1977 (PB 290 870)A06

- UCB/EERC-78/01 "The Development of Energy-Absorbing Devices for Aseismic Base Isolation Systems," by J.M. Kelly and D.F. Tsztoo - 1978 (PB 284 978)A04
- UCB/EERC-78/02 "Effect of Tensile Prestrain on the Cyclic Response of Structural Steel Connections, by J.G. Bouwkamp and A. Mukhopadhyay - 1978
- UCB/EERC-78/03 "Experimental Results of an Earthquake Isolation System using Natural Rubber Bearings," by J.M. Eiding and J.M. Kelly - 1978 (PB 281 686)A04
- UCB/EERC-78/04 "Seismic Behavior of Tall Liquid Storage Tanks," by A. Niwa - 1978 (PB 284 017)A14
- UCB/EERC-78/05 "Hysteretic Behavior of Reinforced Concrete Columns Subjected to High Axial and Cyclic Shear Forces," by S.W. Zagajeski, V.V. Bertero and J.G. Bouwkamp - 1978 (PB 283 858)A13
- UCB/EERC-78/06 "Inelastic Beam-Column Elements for the ANSR-I Program," by A. Riahi, D.G. Row and G.H. Powell - 1978
- UCB/EERC-78/07 "Studies of Structural Response to Earthquake Ground Motion," by O.A. Lopez and A.K. Chopra - 1978 (PB 282 790)A05
- UCB/EERC-78/08 "A Laboratory Study of the Fluid-Structure Interaction of Submerged Tanks and Caissons in Earthquakes," by R.C. Byrd - 1978 (PB 284 957)A08
- UCB/EERC-78/09 "Model for Evaluating Damageability of Structures," by I. Sakamoto and B. Bresler - 1978
- UCB/EERC-78/10 "Seismic Performance of Nonstructural and Secondary Structural Elements," by I. Sakamoto - 1978
- UCB/EERC-78/11 "Mathematical Modelling of Hysteresis Loops for Reinforced Concrete Columns," by S. Nakata, T. Sproul and J. Penzien - 1978
- UCB/EERC-78/12 "Damageability in Existing Buildings," by T. Elejwas and B. Bresler - 1978
- UCB/EERC-78/13 "Dynamic Behavior of a Pedestal Base Multistory Building," by R.M. Stephen, E.L. Wilson, J.G. Bouwkamp and M. Button - 1978 (PB 286 650)A08
- UCB/EERC-78/14 "Seismic Response of Bridges - Case Studies," by R.A. Imbsen, V. Nutt and J. Penzien - 1978 (PB 286 503)A10
- UCB/EERC-78/15 "A Substructure Technique for Nonlinear Static and Dynamic Analysis," by D.G. Row and G.H. Powell - 1978 (PB 288 077)A10
- UCB/EERC-78/16 "Seismic Risk Studies for San Francisco and for the Greater San Francisco Bay Area," by C.S. Oliveira - 1978